

**The Popeye domain containing gene 2 (*Popdc2*).
Generation and functional characterization of a null
mutant in mice and promoter analysis.**



Dissertation

For completion of the Doctorate degree in Natural Sciences at the
Bayerische Julius-Maximilians-Universität Würzburg

Alexander Froese

from Dushanbe

Würzburg 2007

Declaration:

I hereby declare that the submitted dissertation was completed by myself and no other. I have not used any sources or materials other than those enclosed.

Moreover I declare that the following dissertation has not been submitted further in this form or any other form, and has not been used to obtain any other equivalent qualifications at any other organisation/institution.

Additionally, I have not applied for, nor will I attempt to apply for any other degree or qualification in relation to this work.

Würzburg, den 21.12.2007

Alexander Froese

The hereby submitted thesis was completed from January 2001 until April 2005 at the Cell and Molecular Biology Department, Technical University Braunschweig, Braunschweig and from May 2005 until December 2007 at the Department of Cell and Developmental Biology, University of Würzburg, under the supervision of **Professor Dr. T. Brand.**

Members of the thesis committee:

Chairman: Professor Dr. M. Müller

Examiner: Professor Dr. T. Brand

Examiner: PD Dr. S. Maier

Submitted on: 21.12.2007

Date of oral exam: 20.02.2008

Wahrlich, wahrlich, ich sage euch:
Wenn das Weizenkorn nicht in die Erde
fällt und stirbt, bleibt es allein; wenn es
aber stirbt, bringt es viel Frucht.

Johannes 12;23-25

Истинно, истинно говорю вам: если
пшеничное зерно, падши в землю, не
умрёт, то останется одно; а если
умрёт, то принесёт много плода.

Иоанн 12;23-25

ACKNOWLEDGEMENTS

I would like to address my gratitude to Prof. Thomas Brand for giving me the possibility to do my PhD in his group and for his strong scientific guidance during my study. Especially I would like to express my thanks to Prof. Thomas Brand for the idea and financial support of my participation of the Workshop on Phenotyping New Mouse Models for Heart, Lung, Blood and Sleep Disorders in the Jackson Laboratory, USA.

I thank PD Dr. Sebastian Maier for his kindness to evaluate this work as coreferee.

Here I give my thanks to Prof. Hans-Henning Arnold and Prof. Ulrich Scheer for giving me the opportunity to work in their departments.

I am very grateful to my best friends during my PhD study Dr. Marcell Lederer and Nicole Meyer. Without their scientific and moral support in critical situations my project would have never been able to be finished.

In particular I would like to thank my long-standing colleague Stephanie Breher for the numerous social and scientific events we have shared.

Many thanks also to other students past and present: Christian Brenneis for the very friendly atmosphere in the lab, Jan Schlüter for sharing his time and lots of work done for my project, Florian David, Maren Meysing, Rita Mavridou, Gabi Bartelmes and Franziska Günthner for the teamwork.

I would like to thank Iris Kautzner for her assistance beyond the call of duty, her technical expertise and enthusiasm. Many thanks to Fabiene Lütge, Reinhild Fischer, Anneliesa Striewe-Conz and Ellen Fecher for pretty much the same.

I would like to thank secretary Uli Borst for the very professional work, allowing the smooth running of things and simply for smalltalk.

I also thank Dr. Tim Krüger, PD Dr. Manfred Alsheimer and Dr. Norbert Wilken for being prepared to help with various problems.

Finally and most importantly, I thank my wife Natali and our kids Valeria and Anton who were extremely patient with me and accepted and supported my work whenever it was possible.

Table of contents

1. Summary.....	1
2. Introduction.....	2
2.1 Early heart development	2
2.2 Molecular control of early heart development	4
2.2.1 Nkx2.5.....	4
2.2.2 GATA genes.....	4
2.2.3 SRF.....	5
2.2.4 The Mef2 family	6
2.2.5 The Tbox transcription factor family.....	6
2.2.6 The HAND genes.....	8
2.2.7 The Hey genes.....	8
2.2.8 The transcriptional repressor CDP.....	9
2.3 The cardiac conduction system	10
2.4 The Popeye domain-containing gene family.....	13
2.5 Aim of the study.....	18
3. Material and methods.....	19
3.1 Chemicals.....	19
3.2 Enzymes.....	20
3.3 Eggs.....	20
3.4 Clones and vectors.....	20
3.5 Primers.....	21
3.6 Mice	23
3.7 General molecular biology techniques	23
3.8 Database analyzes of the mouse genome.....	24
3.9 Cosmid library screening	24
3.10 Site-directed mutagenesis	24
3.11 Cell culture.....	24
3.11.1 ES cell line.....	24
3.11.2 Mouse Embryo Fibroblast (MEF).....	25
3.11.3 Electroporation and selection of ES cells.....	25
3.11.4 Isolation and cryopreservation of ES cell clones.....	25
3.11.5 In vitro differentiation of ES cell.....	25
3.11.6 Isolation of primary embryonic chick cardiomyocytes.....	25
3.12 Luciferase assay.....	26
3.13 Ex ovo electroporation.....	26
3.14 DNA and RNA analysis.....	27
3.14.1 Extraction of Genomic DNA	27

Table of contents

3.14.2 Southern Blot Analysis	27
3.14.3 DNA sequencing.....	28
3.14.4 Isolation of total RNA.....	28
3.14.5 RT-PCR.....	28
3.14.6 Northern blot analysis.....	29
3.14.7 Probes and probe synthesis	30
3.15 Protein analysis	30
3.15.1 Western blot	30
3.15.2 Preparation of nuclear extract.....	30
3.15.3 Electromobility Shift Assay (EMSA).....	32
3.16 Histology.....	33
3.16.1 Paraffin sectioning	33
3.16.2 Cryostat sectioning	33
3.17 LacZ staining and Acetylcholine esterase (AChE) enzyme histochemistry.....	33
3.18 Image acquisition	34
3.19 Non-radioactive in situ hybridization on sections	34
3.20 Whole-Mount Immunostaining.....	36
3.21 Statistical analysis	36
3.22 Three-Dimensional Reconstruction	36
4. Results.....	37
4.1 Generation and characterization of a <i>Popdc2</i> knockout mouse	37
4.1.1 Isolation of a genomic clone for the <i>Popdc2</i> locus.....	37
4.1.2 Generation of a <i>Popdc2</i> null mutant in mice	37
4.1.3 Analysis of <i>Popdc2</i> gene inactivation in ES cells.....	39
4.1.4 Analysis of <i>Popdc2</i> gene inactivation in mice and genotyping strategy.....	41
4.1.5 Deletion of the neomycin selection cassette from the <i>Popdc2-LacZ</i> allele in mice.	42
4.2 Generation of a <i>Popdc2</i> null mutant ES cell line.....	43
4.2.1 Targeting strategy.....	43
4.3 Characterization of a <i>Popdc2</i> knockout mouse.....	46
4.3.1 Effect of <i>Popdc2</i> ^{LacZ/LacZ} deletion on the heart and body weight.....	46
4.3.2 <i>Popdc2-LacZ</i> expression analysis in early embryo.....	51
4.3.3 In the gastrulating mouse embryo LacZ is expressed in the heart fields and in the somato- and splanchnopleura.....	52
4.3.4 Two distinct cell populations were labeled by LacZ during EB differentiation.....	53
4.3.5 Myocardial expression pattern of <i>Popdc2-LacZ</i> and <i>Popdc2</i> in selected developmental stages	55
4.3.6 Myocardial expression of <i>Popdc2-LacZ</i> at dE12.5.....	58

Table of contents

4.3.7 Expression of <i>Popdc2</i> and <i>Popdc2-LacZ</i> in different organs at E12.5 and <i>Popdc2-LacZ</i> at E17.5.....	59
4.3.8 Expression of <i>Popdc2-LacZ</i> in skeletal muscle and absence of expression in the brain.....	61
4.3.9 Expression of <i>Popdc2-LacZ</i> in the newborn lungs	63
4.3.10 Expression of <i>Popdc2</i> and <i>Popdc2-LacZ</i> in gastrointestinal tract, kidney, bladder and skeletal muscle of newborn mouse	64
4.3.11 Myocardial expression of <i>Popdc2-LacZ</i> in 7d heart	67
4.3.12 Expression of <i>Popdc2-LacZ</i> in gastrointestinal tract, bladder, kidney, spleen, skeletal muscle and heart of 3 months old mouse.....	68
4.3.13 Expression of <i>Popdc2-LacZ</i> in conduction system	71
4.3.14 <i>Popdc2</i> null mutants display a stress-induced bradycardia	74
4.3.15 Structural alterations of sinus node cells in <i>Popdc2</i> null mutants as revealed by HCN4 whole-mount staining.....	79
4.4 <i>Popdc2</i> promoter analysis.....	82
4.4.1 Transcriptional control of <i>Popdc2</i>	82
4.4.2 The 1.7 kb promoter fragment is sufficient to recapitulate <i>Popdc2</i> gene expression in transgenic mouse embryos.....	88
5. Discussion.....	92
5.1 <i>Popdc2</i> knockout mouse.....	92
5.1.1 <i>Popdc2</i> gene inactivation	92
5.1.2 Analysis of <i>Popdc2-LacZ</i> expression in development and postnatally and comparison with <i>Popdc1-LacZ</i> expression	94
5.2 Role of <i>Popdc2</i> gene in the cardiac conduction system.....	97
5.3 Molecular control of <i>Popdc2</i> expression.....	103
6. References.....	106
7. Supplement.....	125
7.1 Abbreviations.....	125
7.2 Publications.....	127
7.3 Presentations	128
8. Zusammenfassung.....	129
Lebenslauf	130

1. Summary

In the present study a knockout mouse model of the Popeye domain containing gene 2 (*Popdc2*) was generated and functionally characterized. The *Popdc2* null mutants were viable with an apparent normal life span. β -galactosidase staining to visualize the expression of the *Popdc2-LacZ* transgene revealed the presence of the *Popdc2* in heart, bladder, smooth and skeletal muscles. In the heart *LacZ* was found to be present in cardiac myocytes with elevated levels in the myocytes of the cardiac conduction system.

Holter ECGs records of the heart function of the 8 months (but not in 3 and 6 months) old mutant and WT littermates revealed a pronounced sinus bradycardia in the mutant mice in response to three different stress regimens: isoproterenol infusion, mental stress and a physical exercise. Histological examination of the *Popdc2* null mutants SAN revealed structural alterations as was detected by HCN4 staining. Moreover, volume measurements using 3-D reconstructions of serial sections stained with HCN4 antibody revealed a volume reduction of about 30% in the mutant SAN. Taken together data presented in this study suggest that the *Popdc2* KO mouse line may serve as an animal model of human sick sinus syndrome.

In the second part of this thesis the *Popdc2* gene promoter was analyzed. Three transcription factors binding sites were predicted in the promoter region and characterized.

2. Introduction

2.1 Early heart development

The heart is the first organ, which develops in the amniote embryo. Precardiac cells are first found to be present in the anterior third of the primitive streak at HH stage 3 (Garcia-Martinez and Schoenwolf 1993). At Hamburger Hamilton (HH) stage 4 in the chick and 7dpc (primitive streak stage) in the mouse, these cells ingress through the primitive streak and migrate rostro-lateral to form paired heart-forming fields (Rosenquist and DeHaan, 1966). After reaching the splanchnic mesoderm the cells are getting specified as cardiac lineage (Gonzalez-Sanchez and Bader, 1990). At

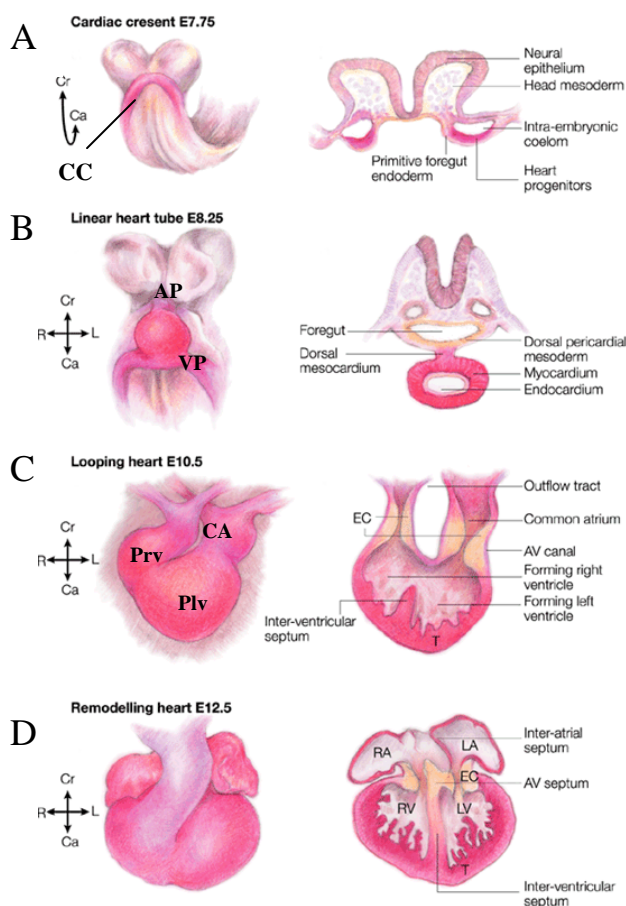


Figure 1. Schematic representation of mouse heart development. A. Anterior ventral view of a 7.75-day mouse embryo showing the cardiac crescent (CC) which is formed by the progenitors of the primary heart field. On the right, a transverse section through the posterior region of the cardiac crescent shows the location of heart progenitor cells in lateral splanchnic mesoderm. B. Anterior ventral view of 8.25-day mouse embryo showing the linear heart tube. Transverse section demonstrates that it consists of two epithelial layers: the outer myocardium and inner endocardium. C. Looping stage. View of rightward looped heart tube. In the section the atrioventricular (AV) canal with endocardial cushions which later form tricuspid and mitral valves is seen. Endocardial cushions (EC) in the outflow tract will form the aorticopulmonary septum. At this stage formation of trabeculae (T) occurs. D. Structure of a day 12.5 embryonic heart. After completion of looping, the heart shows extensive remodelling leading to the formation of four distinct heart chambers.

AP, arterial pole; VP, venous pole; CA, common atrium; Plv, primitive left ventricle; Prv, primitive right ventricle; RA, right atria; RV, right ventricle; LA, left atria; LV, left ventricle; Ca, caudal; Cr, cranial; R, right; L, left (Harvey RP. 2002).

HH stage 7 in the chick and 8dpc in mouse these cells move rostrally and medially to meet at the midline, forming the cardiac crescent and subsequently the linear heart tube. At HH stage 10 in the chick and E8.5 in mouse the tubular heart starts to contract, and at HH stage 11 in the chick and E8.5 in the mouse the heart undergoes rightward looping, the first morphological sign of the emerging left-right axis (DeHaan, 1965; Fishman and Chien, 1997). During this complex morphogenetic process,

demarcation of individual ventricular chambers occurs (Firulli *et al.*, 1998). The next steps, involved in the formation of an integrated four-chambered heart are septal division of the chambers, formation of valves and great vessels, and extensive growth and differentiation of cardiac muscle tissue. Two extracardiac cell populations, the neural crest and the epicardial cells are required to successfully accomplish these processes (Jiang *et al.*, 2000; Mu H *et al.*, 2005).

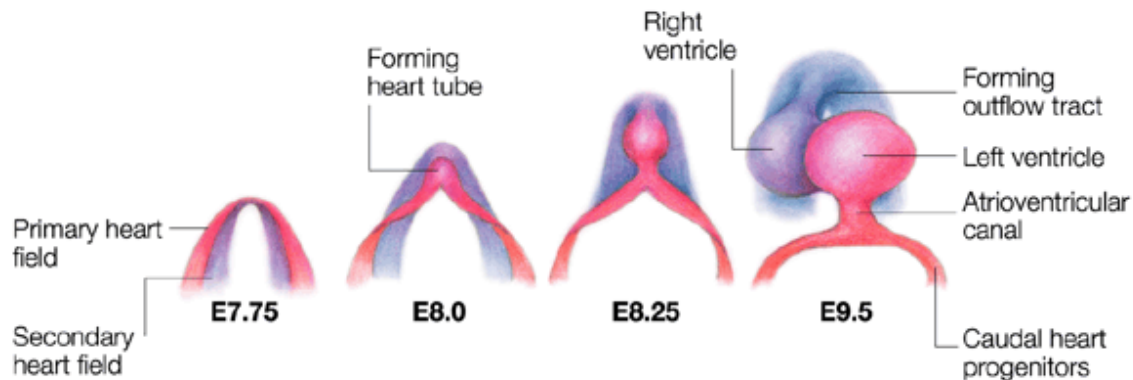


Figure 2. Position and contribution of the primary and secondary heart fields during mouse heart development. Two cardiac precursor cell lineages contribute differentially to different parts of the mammalian heart (Harvey RP. 2002).

It was recently realized, that the amniote heart is built from two myocardial precursor cell populations. Both of them have different origins and are regulated by distinct genetic programmes. One cell population is derived from the primary heart forming fields in the splanchnic mesoderm, as discussed above, and is involved in the formation of the linear heart tube. Subsequently, these cells form mainly the left ventricle and part of the atria. The second cell population is more medially positioned in gastrulating embryos (Fig. 2) and after heart tube formation compose a part of the pharyngeal mesoderm region, also known as the anterior or secondary heart field (Kelly and Buckingham, 2002, Yutzey and Kirby, 2002). This group of cells is populating the heart at the time of cardiac looping. They contribute to the outflow tract, right ventricle and atrial muscle including the sinus node (Kelly and Buckingham, 2002; Schwartz and Olson, 1999).

2.2 Molecular control of early heart development

The mechanisms regulating heart development have been extensively studied recently. Application of modern molecular techniques allowed the identification of multiple genes that are involved in various aspects of cardiogenesis. Nevertheless, the precise function and regulation of a majority of these genes remains to be defined. Among the genes, that are required for heart specification, patterning and differentiation of the heart, are those, which code for the NK homeodomain, GATA, T-box and HAND transcription factor families (Zaffran and Frasch, 2002). In addition signalling molecules such as BMP2 and FGF8 were identified to be specifically involved in the induction of the cardiac transcription program (Brand, 2003).

2.2.1 Nkx2.5

The single *Drosophila tinman* gene is an ortholog of the vertebrate cardiac NK homeodomain proteins. In *Drosophila*, the role of the heart is carried out by a contractile dorsal vessel, which pumps hemolymph through the tissues. *Tinman* is expressed in precardiac mesoderm and its targeted ablation prevents formation of the dorsal vessel and specification of all of its progenitor cells (Bodmer, 1993). Unlike *Drosophila*, vertebrates express several members of the NK gene family (*Nkx2.3*, *Nkx2.5*, *Nkx2.7*, *Nkx2.8*, *Nkx2.9*, *Nkx2.10*) and inactivation of any of these genes does not prevent heart formation. One of them, *Nkx2.5* is found in all vertebrate hearts and belongs to the group of the earliest transcription factors that specifically mark the heart precursors (Lints et al., 1993; Schultheiss et al., 1995). Mutation of *Nkx2.5* in the mouse blocks heart formation at looping stage.

2.2.2 GATA genes

Cardiac transcription factors of the GATA family are homologues of a single *Drosophila* gene *pannier* and are represented in the vertebrate heart by *Gata4*, *Gata5*, and *Gata6* (Molkentin, 2000). They belong to the zinc finger transcription factor family and are essential for vertebrate heart development. GATA proteins recognize and bind to the consensus motif A/T-G-A-T-A-A/G in the promoter region of many cardiac genes (Ko and Engel, 1993; Merika and Orkin, 1993). Similar to *Nkx2.5*, all three GATA genes are expressed in precardiac mesoderm and represent the earliest markers of the cardiac cell lineage (Harvey, 1996). *Pannier* mutant embryos lack all cardiomyocytes. *Gata4* null mutant mouse embryos develop a

cardia bifida phenotype and have a diminished number of cardiomyocytes (Kuo et al., 1997; Molkenin et al., 1997). *Gata5* null mutants are viable (Molkenin et al., 1997), whereas *Gata6* null mutants do not develop beyond the implantation step (Morrissey et al., 1998). *Gata4* and *Gata6* in mouse are expressed in the heart both prenatally and postnatally, whereas *Gata5* expression is limited to the E16.5. It is likely, that *Gata4* and *Gata6* form a pair of redundant transcription factors. Compound heterozygotes of *Gata4* and *Gata6* die at E13.5 with multiple cardiac malformations (Xin et al. 2006). In zebrafish embryos depleted of *gata5* and *gata6* are heartless (Holtzinger and Evans, 2007).

2.2.3 SRF

Serum response factor (SRF), is a 67-kDa protein which belongs to the MADS box (MCM1, Agamous, Deficiens, SRF) family. The 90-amino-acid MADS box is a conserved motif found within the DNA-binding/dimerization domain (Shore and Sharrocks, 1995). SRF binds to the CC(A/T)GG (known as a CA₂G box) motif on many cardiac genes. By using a SRF-specific antiserum the first SRF expression in mouse was detected at E6.5 in ectoderm as well as endoderm. At E7.5 protein was revealed in all three germ layers. At E8.5 SRF expression was found to be very strong in the heart but almost not detectable in other tissues (Arsenian et al., 1998). In the chick, at stage HH8 *Srf* is coexpressed with *Nkx2.5* and *Gata4* in the cardiac crescent and combinatorial interaction among these proteins regulate the cardiac α -actin (α -CA) promoter (Sepulveda et al., 2002). *Srf* deficient mice are not able to form mesoderm and die at gastrulation (Weinhold et al., 2000). Cardiac-specific *Srf* null mutants die at mid-gestation due to abnormal sarcomeric structure and impaired muscle gene regulation (Miano et al., 2004; Niu et al., 2005). Around 160 genes have been predicted to be SRF target genes, approximately 60 of which are to date experimentally validated (Sun et al., 2006). Most of these genes contribute to cell growth, migration, cytoskeletal organization, and myogenesis (Norman et al., 1988). Regulation of downstream genes by SRF occurs via association of SRF with positive and negative cofactors (Treisman, 1994). Since SRF is ubiquitously expressed but is required for muscle gene expression, the existence of muscle specific SRF coactivators was predicted. Myocardin, a novel cardiac-restricted gene, is a very powerful SRF cofactor, which contributes to the tissue specificity of SRF-regulated target genes. Myocardin is a member of the SAP (SAF-A/B, Acinus, PIAS) domain

family of nuclear proteins, which act through chromatin remodelling and transcriptional regulation. Myocardin activates CArG-box cardiac promoters via binding to the MADS domain and ternary complex building with SRF. The SAP domain of myocardin provides specificity in this process (Wang et al., 2001).

2.2.4 The Mef2 family

The MEF2 subfamily of MADS box proteins is involved in cardiac differentiation. Four genes are expressed in vertebrates, *Mef2a-d* (Bretbart et al., 1993), whereas in *Drosophila* a single *mef2* gene product, D-MEF2 is present (Lilly et al., 1994). All MEF2 proteins have highly conserved MADS and MEF2 domains (Olson et al., 1995). MEF2 proteins can bind as homodimers as well as heterodimers to the consensus sequence C/T-T-A-(A/T)4-T-A-G/A which is similar to the SRF binding site and present in many heart specific genes. *D-mef2* ablation in *Drosophila* results in prevention of cardiac, visceral and skeletal muscle formation (Lilly et al., 1995). The *Mef2C* mutant mouse develops normal until about E9.0 and die at the beginning of cardiac looping. This is accompanied by severe right ventricular hypoplasia and downregulation of a subset of cardiac contractile protein genes (Lin et al., 1997). Since the MADS domain of MEF2 shares high homology with the SRF MADS domain, it was proposed that myocardin might be able to bind and activate MEF2. In fact, a 935bp myocardin isoform, which is produced by alternative splicing and contains a unique motive, can act as a MEF2 cofactor. This unique protein-protein interaction motif confers the ability to bind and activate MEF2 gene promoter of another SAP domain transcription factor called MASTR (MEF2 activating SAP transcriptional regulator) (Creemers et al., 2006).

2.2.5 The T-box transcription factor family

Another transcription factor family, which is essential for normal heart development, is characterized by the presence of a T-box, a highly conserved DNA binding domain. There are at least 8 T-box genes identified in *Drosophila* and 18 T-box genes in mammals (Showell et al., 2004). Several T-box genes are found to be very important for early embryonic patterning and organogenesis (Showell et al., 2004), but the most severe defects in case of altered T-box gene function are observed in the cardiovascular system (Plageman and Yutzey, 2005). Thus, a dominant mutation in *TBX5* is responsible for Holt-Oram syndrome associated with skeletal and cardiac malformations (Basson et al., 1997; Li et al., 1997), and a mutation in *TBX1* is

responsible for DiGeorge syndrome implicated in malformations of the cardiac outflow tract and pharyngeal arches (Baldini, 2004). Additional T-box genes that are expressed in the developing heart are *Tbx2*, *Tbx3*, *Tbx18*, and *Tbx20*. *Tbx2*, *Tbx3*, *Tbx5*, and *Tbx20* are found in early cardiac progenitors (Plageman and Yutzey, 2005). *Tbx2* and *Tbx3* are expressed in the primitive heart tube and subsequently contribute to chamber formation. *Tbx2* and *Tbx3* are both found in the cardiac primordial, posterior primitive heart tube, and atrioventricular canal (AVC) of chicken and mouse embryos (Yamada et al., 2000; Hoogaars et al., 2004). In contrast to *Tbx5*, *Tbx2* and *Tbx3* are transcriptional repressors and implicated in development of the atrioventricular canal (AVC) and the cardiac conduction system (CCS; Habets et al., 2002). In the mouse heart the temporal and spatial pattern of *Tbx2* mRNA and protein expression was found to be mutually exclusive to that of *Nppa*, *Cx40*, *Cx43*, and *Chisel*, which are genes that demarcate the forming atrial and ventricular chamber myocardium (Christoffels et al., 2004). *Tbx2* is thought to compete for binding with *Tbx5* and thereby repress chamber gene expression in AVC and IC (Inner Curvature; Harrelson et al., 2004). Hearts of mouse embryo with transgenic expression of *Tbx2* in the primitive heart tube do not form chamber myocardium (Christoffels et al., 2004). *Tbx3* is expressed in the sinoatrial node (SAN), atrioventricular node (AVN), His bundle and bundle branches and serves in mouse as specific marker for the central CCS. Despite this feature, no conduction system disorders were found in *Tbx3* mutant mouse, however this is probably due to functional redundancy and overlapping expression of *Tbx2* (Hoogaars et al., 2004; Davenport et al., 2003). In man *TBX3* haploinsufficiency causes ulnar mammary syndrome, but no data is present about anomalies in CCS (Bamshad et al., 1997). Another Tbx factor essential for heart chamber development is *Tbx20*. *Tbx20* is expressed in the cardiac crescent and later in primitive heart tube, with subsequent enrichment in AVC, outflow tract (OFT), and developing valves (Stennard et al., 2003). *Tbx20* null mice die prenatal due to severe cardiovascular defects (Singh et al., 2005). Like *Tbx2* and *Tbx3* but not *Tbx5*, *Tbx20* is induced by *Bmp2* in chick cardiac mesoderm, implying that all three genes are at least partially regulated by *Bmp2* (Plageman and Yutzey, 2004). *Tbx20* is thought to regulate the progression from the tubular heart stage to the chambered heart by repressing *Tbx2* in the myocardium (Singh et al., 2005).

Similar to *Nkx2.5* and *Gata4-6* genes, *Tbx5* is expressed in the bilateral precardiac mesoderm in zebrafish, *Xenopus*, chick, and mouse embryos (Chapman et al., 1996). Later expression is found in regions, which originates from the primary heart forming fields: the left ventricles, atria and inflow of the heart (Bruneau et al., 1999). *Tbx5* deficient mice die before E10.5, due to severe cardiac malformations. Mice with *Tbx5* haploinsufficiency similarly to patients with HOS demonstrate septal defects and CCS disease. In addition, a mouse with *Tbx5* haploinsufficiency has reduced expression of genes encoding connexin 40 (Cx40), and atrial natriuretic peptide (ANF) (Bruneau et al., 2001). Mouse embryos with *Tbx1* null mutation exhibit cardiovascular defects like aortic arch malformations, outflow tract and ventricular septal defects (Plageman and Yutzey, 2005). Mice heterozygous for *Tbx1* gene exhibit only some of the anomalies found in the DiGeorge syndrome (Jerome and Papaioannou, 2001).

2.2.6 The HAND genes

Basic helix-loop-helix (bHLH) transcription factors are implicated in cardiac morphogenesis and gene regulation in various species. Mouse *Hand1* and *Hand2* encode bHLH transcription factors, which are expressed in an overlapping manner in the developing heart. *Hand1* is expressed in the linear heart in segments, which contribute to the conotruncus and left ventricle. *Hand1* null mouse embryos die at E8-8.5 from severe placental and extra-embryonic abnormalities. *Hand2* is expressed throughout the linear heart. At later stages expression is localized to the developing right ventricle and to a lesser extent in the atrial and left ventricular chambers (Thomas et al., 1998). *Hand2* null mouse embryos develop until stage E10.5 and then die from right ventricular hypoplasia and vascular disorders (Srivastava et al., 1997). Mutation in the single zebrafish hand gene results in early severe defects in myocardial development. There are a reduced number of myocardial precursors and the resulting myocardial tissue does not form properly (Yelon et al., 2000). Functional redundancy is also suggested by the severe phenotype that is seen in a Hand double null mutant (Mac Fadden, 2005).

2.2.7 The Hey genes

Hey genes form a small subfamily of bHLH transcription factors that are related to the *Drosophila hairy* and Enhancer-of-split genes. These genes are characterized by the

presence of three conserved motifs: basic domain for DNA binding, helix-loop-helix domain for protein dimerization, Orange and four amino acid WRPW domains which mediate specificity and transcriptional repression (Steidl et al., 2000). There are three Hey genes (*Hey1*, *Hey2*, *HeyL*) found in human and mouse, one highly related homologue *dHey* in *Drosophila* and a mouse *Hey2* ortholog is encoded by the *gridlock* locus in zebrafish. In mouse, *Hey1* gene expression is first detected in the lateral part of the cardiac crescent, which subsequently contributes to the formation of the sinus venosus and the atria. The *Hey2* gene is expressed first in the anterior part of the heart tube and later expression is restricted to the ventricles (Chin et al., 2000). All three genes *Hey1*, *Hey2* and *HeyL* are expressed in blood vessels from the earliest time point onward. Hey genes can act as repressors of GATA4 and GATA6 activity and their target genes ANF and CARP. *Hey1* and *Hey2* are essential transducers of Delta-Notch signalling pathway during cardiovascular development (Fischer et al., 2005). Recently published data demonstrate that both *Hey1* and *Hey2* in the chick model participate in a process which allows strictly the demarcation of two gene-specific programs; one associated with myocardium and another one required for the developing AVC and IC (Inner Curvature) during heart looping. *Hey1* and *Hey2* repress *Bmp2* in myocardium, while *Tbx2*, which is induced by *Bmp2*, inhibits both, *Hey1* and *Hey2* in a negative feedback loop (Rutenberg et al., 2006). Loss of the *Hey1* gene in mouse leads to no visible defects. Loss of *Hey2* gene results in a high postnatal lethality due to cardiac malformations (Fischer et al., 2004; Gessler et al., 2002). Mice lacking both *Hey1* and *Hey2*, die early in development due to severe vascular defects and impaired arterial-venous differentiation. Interestingly, a similar phenotype was exhibited by the *Notch1/Notch2* double-knockout and in the zebrafish *gridlock* mutant (Fischer et al., 2004; Zhong et al., 2001).

2.2.8 The transcriptional repressor CDP

The CCAAT- displacement protein, CDP (*Cutl1*) belongs to a family of evolutionary conserved homeodomain transcription factors that are involved in the regulation of cell cycle progression and differentiation. CDP was originally isolated as a transcriptional repressor, but subsequently its ability also to act as a transcriptional activator was demonstrated (Santaguida and Nepveu, 2005). CDP is also known as *cut* in *Drosophila melanogaster*, *Clox* in dogs, *Cux1* and *Cux2* in mice and Cut-like (*CUTL1*, *CUTL2*) in human (Nepveu, 2001). CDP proteins contain four DNA-binding

domains, three Cut repeats (CR1, CR2, and CR3) and a Cut homeodomain (Neufeld et al., 1992). Single Cut repeats are not capable of binding to DNA, which is the result of interaction between two repeats or between one repeats and the Cut homeodomain. For acting as a repressor, CDP utilizes two distinct mechanisms. It can compete for a binding site with transcriptional activators. This CCAAT displacement activity depends on interaction between 1 and 2 Cut repeats (Moon et al., 2000). Another way to repress gene transcription is exerted through the binding of CDP protein carboxy-terminal sequence to target gene promoters and recruitment of histone deacetylases (HDAC; Li et al., 1999; Mailly et al., 1996). The CDP/Cux p110 isoform is found to be capable of activating the DNA polymerase α promoter (Truscott et al., 2003). Mutations within the *cut* coding sequence in *Drosophila* lead to embryonic lethality during larval development (Johnson and Judd, 1979). Multiple viable mutations resulted in different developmental malformations in wings, legs, tracheal system, Malpighian tubules and others (Nepveu, 2001). Mice lacking *Cux1* display different phenotypes, including perinatal lethality, curly whiskers, growth retardation, delayed differentiation of lung epithelia, impaired hair follicle morphogenesis, male infertility and a deficit in T and B cells (Ellis et al., 2001; Luong et al., 2002; Sinclair et al., 2001). Mice transgenic for *Cux1*, in contrast, displayed multiorgan hyperplasia and organomegaly (Ledford et al., 2002).

2.3 The cardiac conduction system

The heart is the first organ to form and function in the developing embryo. While growing and getting mature, the heart starts to function, i.e. contract rhythmically to pump blood, providing the basis for growth and development of the whole embryo. The key component that enables the vertebrate heart to contract is a cardiac conduction system (CCS), the specialized tissue network that initiates and transmits electrical impulses. The CCS consists of the sinoatrial (SA) node, atrioventricular (AV) node, His-bundle branches and Purkinje fibers (Pennisi et al., 2002) (Fig. 3). In higher vertebrates, the SA node is located at the boundary of the superior caval vein and is responsible for generating a pacemaker cardiac action potential (AP). Once generated in the SA node, this AP propagates through the electrically coupled atrial myocytes and arrives at the AV node. The AV node is situated at the junction of the atria and ventricles and is required for generating a delay in the propagation of the AP. This delay allows the separate activation of the atrial chambers and the

ventricles, ensuring directional blood flow. From the AV node the depolarization wave propagates along the His bundles and reaches the ramified network of Purkinje fibers, activating both ventricles from apex to base (Gourdie et al., 2003).

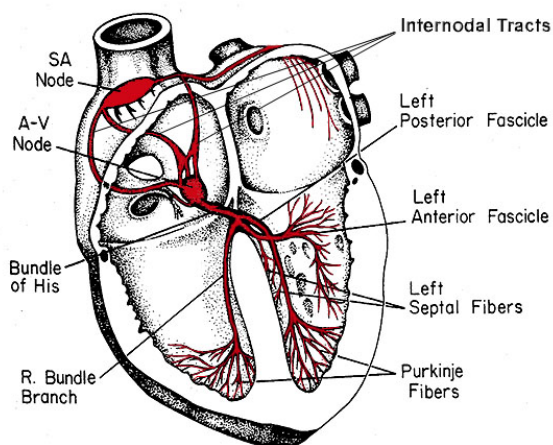


Figure 3. Position of the major elements of the cardiac conduction system in the feline heart (After Tilley, 1977). Elements of the CCS are labelled in red and consists of the SA node, specialized internodal tracts in the atrium (questioned by some authors), the AV node, the His bundle and the right and left bundle branches, the CCS terminates with the Purkinje fibers which make contact to the ordinary working myocardium.

The first impulse propagation, seen as slow irregular peristaltic waves, is observed in the heart at the end of E8. By stage E9, the developing heart already consists of the sinus venosus, a single atrial chamber, the atrio-ventricular canal (AVC), the common left ventricle, the bulbus cordis, the future right ventricle and the outflow tract. At this stage regular sequential contractions of the primitive chambers occur, where the AVC similar to the function of the AV node in older mice, delays AP propagation. First signs of trabeculation appear around E9 and by E10 chamber septation becomes apparent. Staining is found in the SA node region of the *mink-lacZ* knockin mouse, which specifically express LacZ in CCS. By E13.5 four distinct chambers are formed and separation of the ventricles is accomplished. Except for Purkinje fibers, all the definitive components of the mouse CCS in this period of development are definable by microscopy, periodic acid Schiff's (PAS) staining and *mink-lacZ* (Kaufman 1999; Kondo et al., 2003; Viragh and Challice 1982).

Heterogeneity of CCS structure and diverse functions of its components accounts for a complex pattern of gene expression. *Msx2*, a homeobox gene related to the *Drosophila msh* (Dr) transcription factor that was found to be expressed in the CCS (Chan-Thomas et al., 1993). *Nkx2.5* and *Tbx5* are essential genes for CCS specification. *Nkx2.5* is expressed in the embryonic and adult CCS (Takebayashi-Suzuki et al., 2001). Mutation in *Nkx2.5* results in CCS defects in both human and mice (Biben et al., 2000; Schott et al., 1998). Transgenic mice overexpressing one of the mutant forms of *NKX2.5* identified in humans exhibit significant AV conduction defects and heart failure (Kasahara et al., 2001). The *Tbx5* gene is reported to play an essential role in development and maturation of the CCS. *Tbx5* is expressed in AV node, His bundle and bundle branches. In addition to defects mentioned above, *Tbx5* haploinsufficient mice show abnormalities in the proximal ventricular conduction system (Moskowitz et al., 2004). *Tbx3* as mentioned above is expressed in the developing CCS. *Tbx3* is absent in the cardiac cells as soon as they turn on the atrial gene specific program. *Tbx3* is important in positive regulation of the SAN expression program and in repression of the atrial phenotype in SAN. Thus ectopic expression of the *Tbx3* in mice heart leads to the formation of functional ectopic pacemakers and arrhythmias (Hoogaars et al., 2007).

Shox2 encodes a homeodomain transcription factor which is known to be implicated in craniofacial, limb and brain development (Blaschke et al., 1998; Rovescalli et al., 1996). In human the related transcription factor SHOX causes various short-stature syndromes (Rao et al., 1997). Expression of the *Shox2* was also detected in the heart during development. At the beginning at E9.5 *Shox2* expression is found in the mesenchyme of the transitional zone between the sinus venosus and common atrium (Blaschke et al., 2007). Later at E11.5 and at least till E13.5 *Shox2* expression is strongly expressed in the SAN region and the venous valves. *Shox2*^{+/-} do not show any prominent disorders, while null mutants are not viable. *Shox2*^{-/-} embryos die between E11.5 and E13.5. At this time point aberrant expressions of connexin 40, connexin 43 and *Nkx2.5* were observed within sinoatrial nodal region. In zebrafish *Shox2* is expressed in central and peripheral nervous system, the pectoral fin buds and in the inflow tract of the heart. Injection of the morpholino-modified antisense oligonucleotides which target *Shox2* in early zebrafish embryos resulted in a severe heart dysfunction. Embryos after 72 hours of development display pronounced sinus bradycardia and intermittent sinus exit block.

Endothelin 1 (Edn1), a shear stress responsive cytokine expressed in the coronary arterial bed and neuregulin 1 (Nrg1), a factor secreted from mouse endothelial cells both are able in vitro to recruit murine myocardial cells to the Purkinje fiber lineage (Gourdie et al., 1998; Rentschler et al., 2002).

Connexins (Cxs) are required for electrical coupling of myocytes. They are a major component of gap junction channels. In the mammalian heart three most abundant connexins are Cx40 (*Gja5*), Cx43 (*Gja1*) and Cx45 (*Gja7*). At the stage of the first impuls propagation observed in the mouse heart (E8.5), Cx45 mRNA is identified in all cardiac structures including inflow tract, AV canal, and outflow tract. At this time of mouse development Cx45 is the only connexin gene, which is expressed in the heart. Beginning at E11.5 Cx45 expression declines and in the adult heart expression remains in the slow-conducting tissues and in atrial myocardium (Alcolea et al., 1999). Cx43 expression was found in the ventricle at E9.5 and in the atria at E12.5. In adult heart Cx43 is the main gap junction protein. It is expressed in all atrial and ventricular myocytes but is absent in the SA and AV nodes, His bundle, and bundle branches (Delorme et al., 1997). Cx40 is strongly expressed in the atrial myocytes as well as in the central portion of the AV node, His bundle, and distal part of the CCS. Cx40 expression has never been found in ventricular myocytes. The pattern of Cx40 expression makes this connexin the best marker of the fast-conducting pathway (Delorme et al., 1995). Mutation in Cx40 gene leads to aberrant AP propagation through all components of the CCS (Gros et al., 2004).

2.4 The Popeye domain-containing gene family

The *Popeye domain containing* (*Popdc*) gene family has been isolated in a screen for novel genes with preferential expression in the heart. The first cDNA (known as *Popdc1*, or *Bves*) was independently cloned from the chick by two groups by means of subtractive hybridization (Andrée et al., 2000; Reese et al., 1999). Orthologues were also found in mouse and man, *Xenopus laevis* and zebrafish (Hitz et al., 2002; Ripley, 2004), and in lower chordates *Branchiostoma*, *Ciona intestinalis*, and *Boltonia vilosa* (Davidson and Levine, 2003). In insects *Popdc* genes have been identified in *Drosophila*, bees and mosquito (Lin et al., 2002). In vertebrates, three genes, *Popdc1*, *Popdc2*, and *Popdc3* have been identified. *Popdc1* and *Popdc3* are localized adjacent to each other on the same chromosomal loci (6q21 in human,

chromosome 10 in mouse, and 3 in chick). The *Popdc2* gene is mapped on chromosome 3 in human, chromosome 16 in mouse, and chromosome 1 in the chick (Andrée et al., 2000). In lower chordates two *Popdc* genes are present, which are homologous to *Popdc1* and *Popdc3* in vertebrates. In *Drosophila*, bees and mosquito only single gene is present (Brand, 2005).

The *Popdc* gene family encodes proteins with 300 – 350 amino acids and are characterized by the presence of a unique *Popeye* domain, which is 150 amino acids long and present in all known *Popdc* proteins. Another feature of the *Popdc* protein family is a 70 amino acid long hydrophobic domain, located between the *Popeye* domain and the N-terminus. By computer prediction this part of the protein forms three transmembrane domains (Andrée et al., 2000). In all three proteins, *Popdc1*, *Popdc2*, and *Popdc3* N-glycosylation sites were predicted to be present at the N-terminus (Thomas Brand, personal communication). In *Popdc1* these two amino-terminal N-glycosylation sites were experimentally shown to be functional and extracellularly localized (Knight et al., 2003). Thus, the *Popeye* domain and the C-terminus are located in cytoplasm. In the presence or absence of a reducing agent, *Popdc1* protein has an apparent molecular weight of a 58 or 120 kDa, respectively (Knight et al., 2003; Vasavada et al., 2004). The dimerization motif sequence has been mapped and shown to be part of the *Popeye* domain (Ripley, 2004). Direct interaction between *Popdc1* and ZO-1 was shown by a GST pull-down assay. Other evidence came from results obtained by an antisense morpholino oligonucleotide (MO) knockdown approach. *Popdc1* morpholino treatment caused a decrease in transepithelial resistance, disruption of the epithelial sheet and loss of membrane localized ZO-1 that indicates an essential role of *Popdc1* for epithelial integrity (Osler et al., 2005). However these data are contrast to the mutant phenotype in mice, which suggested no essential role of *Popdc1* during development (Andree et al., 2002).

In every species examined, all three *Popdc* genes are expressed preferentially in the heart and skeletal muscle. In mouse, *Popdc2* is predominantly expressed in the heart at all stages of development, whereas *Popdc1* and *Popdc3* have a broader pattern of expression and expression is especially prominent in skeletal muscle. In the chick embryo *Popdc1* mRNA was detected in different organs such as stomach, gut, brain,

kidney, lung, and spleen (Andrée et al., 2000). In addition, information received from the expressed sequence tag (EST) and serial analysis of gene expression (SAGE) databases suggests expression of *Popdc* genes in non-muscle cells such as the embryonic pancreas and melanocytes (Brand, 2005). In the chick, strong expression of all three *Popdc* genes was demonstrated in the myocardium, while in the proepicardium no transcripts were found (Breher et al., 2004). In contrast, a monoclonal antibody (D033) that reacts with a conserved peptide of *Popdc1* detects expression in the proepicardium and in smooth muscle cells of the coronary arteries in the developing chick embryo (Reese et al., 1999). This finding was supported by demonstration of *Popdc1* expression in a rat epicardial cell line (Wada et al., 2003). Another monoclonal antibody raised against a glutathione-S-transferase fusion protein with the carboxy terminus of *Popdc1* provided no evidence for expression of *Popdc1* in the epicardium or coronary arteries in the chick (Vasavada et al., 2004; DiAngelo et al., 2001). The controversy on the expression pattern of *Popdc1* could be explained by the presence of multiple splice isoforms that are produced by each of the *Popdc* genes. In addition, such processes as dimerization and posttranslational modifications may also affect the detection of *Popdc* proteins (Brand, 2005).

Popdc1 mouse null mutant, that was generated by replacing the first coding exon of *Popdc1* with a *LacZ* reporter gene is viable and has no apparent embryonic and postnatal phenotype. The *Popdc1-LacZ* expression pattern in most cases resembles the expression pattern previously obtained by whole mount in situ hybridization. In heterozygous mice the first *LacZ* expression was seen at E7.5 in the cardiac crescent. From this stage onward *Popdc1-LacZ* expression maintained in cardiac myocytes. During embryonic development no *LacZ* expression was found in the epicardium or any others non-muscle cells of the heart. At E11.5 *Popdc1-LacZ* expression became downregulated in the trabecular layer but remained present in the myocardial compact layer. Expression of *Popdc1-LacZ* was downregulated in the postnatal heart (Andrée et al., 2002). In addition to the previously reported expression pattern of *Popdc1* by whole mount in situ hybridization, *Popdc1-LacZ* staining was detected in the brain and CCS (Fig. 4 A, B). Detailed phenotype analysis of the *Popdc1* null mutant revealed a retarded ability to regenerate damaged skeletal muscle (Andrée et al., 2002). In addition, hearts of *Popdc1* null mutants subjected to ischemia in a Langendorff perfusion model showed impaired ability to recover and

developed larger infarcts than wild type hearts (Kessler-Icekson, personal communication).

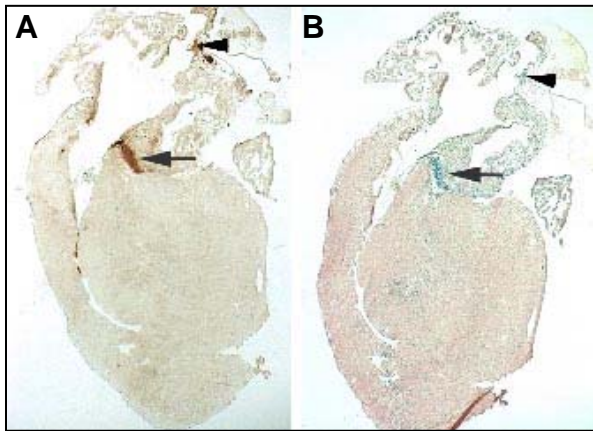


Figure 4. *Popdc1-LacZ* expression in the CCS (After A. Fleige, Diplomarbeit). (A, B) Consecutive cryosections of *Popdc1⁺LacZ* mouse heart stained with the acetyl-cholin esterase (AChE) (A) and LacZ (B). Arrowheads point on the SA node and arrows on the His bundle.

Based on whole mount in situ hybridization results, *Popdc2* is first detectable at E7.5 in the cardiac crescent (Fig. 5). Sections through the cardiogenic region of E8.0 embryo demonstrate strong expression of *Popdc2* in myocardial but not endocardial cells. From this stage onward *Popdc2* was expressed in the whole heart with the exception of the outflow tract. At E8.5 expression is in the whole heart tube. At E9.5 and E10.5 *Popdc2* expression is seen in the trabeculated layer. Beginning around stage E14.5 *Popdc2* expression in the ventricle becomes more restricted to the compact layer myocardium (Andrée et al., 2000).

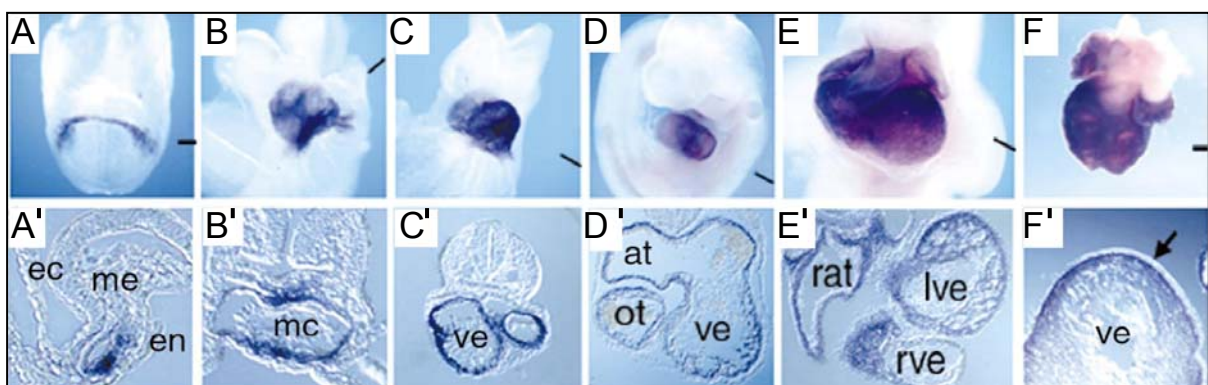


Figure 5. *Popdc2* expression during embryonic development (After Andrée et al., 2000). Whole mount in situ hybridization. (A-F) Mouse embryos hybridized with *Popdc2* probe. (A) At E7.5, two somite stage, *Popdc2* is expressed in cardiac crescent. (B) At E8.0, six-somite stage expression is observed in whole heart but not in the outflow tract. (C, D) At E8.5 and 9.5, respectively, expression is seen in the myocardium of the tubular heart (C, C') and both, atrium and ventricle (D, D'). (E, F) At E10.5, and 14.5, respectively, expression is seen in the myocardium of both atrium and ventricle, but absent in

outflow tract. (A'-F') Transverse sections through the heart of the embryos shown in (A-F). (A') Expression is restricted to the cardiogenic splanchnic mesoderm. (B') Expression is observed in myocardium, but not in endocardium. (C') Strong expression of *Popdc2* is seen in the whole heart tube. (D'-E') *Popdc2* expression is present in the atria (at) and both in the trabeculated area and in the compact layer, and absent in the outflow tract (ot). (F') At E14.5 expression is mainly confined to the subepicardial compact layer of the ventricle. ec, ectoderm; en endoderm. Bars indicate approximate plane of section.

Recently, some progress was made with regard to the subcellular localization analysis of Popdc proteins and its function. Osler et al. demonstrated colocalization of Popdc1 with the tight junction proteins ZO-1 (*Tjp1*) and occludin (*Ocln*) (Osler et al., 2005).

PAX3 is transcription factor essential for development in vertebrates. In a search for novel PAX3-regulated genes using a CASTing (Cyclic Amplification and Selection of Targets) strategy one of the identified candidates was *Popdc1*. Subsequently, transfection assays demonstrated upregulation of *Popdc1* by PAX3. Moreover, mice homozygous for PAX3 have a significant decrease in the expression level of *Popdc1* (Barber et al., 2002).

Despite the implication of Tbx5 in several developmental processes and its association with Holt-Oram syndrome, only few genes regulated by Tbx5 are known. Search for new genes potentially regulated by Tbx5, was carried out using microarray technique. One of the candidate genes, modulated by Tbx5 during heart development was *Popdc2* (Plageman and Yutzey, 2006).

2.5 Aim of the study

The aim of this work was to generate and characterize the *Popdc2* gene knockout mouse. For this purpose gene targeting by homologous recombination in ES cells was used. Different methods including histology, immunohistochemistry and physiological measurements etc. were applied for phenotype characterization and for expression analysis of the introduced reporter gene. Through this analysis a phenotype in the cardiac conduction tissue and more specifically in the sinus node tissue was observed in the aging null mutant. Therefore this mouse mutant might be a unique and novel model of sick sinus syndrome, a disease condition that affects about 400.000 patients per year in the western world. Sick sinus syndrome is a common indication for pacemaker implantation. Our mouse model might therefore be suitable for studying the cause of the disease and for the development of biological pacemaker tissue. An additional aim of this work was to study the regulation of the *Popdc2* expression by promoter analysis. For this purpose, the *Popdc2* promoter region was subjected to deletion analysis in primary chick embryo cardiomyocytes. Using this approach several transcription factor binding sites were identified. Transcriptional activity of the *Popdc2* promoter was also analyzed in transgenic embryos. An enhancer, a silencer and a basal promoter were identified in this way.

3. Materials and Methods

3.1 Chemicals

If not otherwise stated chemicals and kits used in this thesis were supplied by the companies Amersham, Aplichem, Bayer, Biolabs, Biorad, BRL Difco, Gibco, Merck, Miles, Prenner, Roche, Pharmacia, Qiagen, Seromed, Serva and Sigma. Enzymes were purchased from New England Biolabs, BRL, Merck, Perkin-Elmer, Promega, Roche, Serva and USB. Oligonucleotides were purchased from the companies Carl Roth GmbH and Thermo Fisher Scientific, Inc.

Chemicals and suppliers considered of specific interest to this thesis are listed below.

Amplification solution	Amersham Bioscience
BCIP (5-Bromo-4-chloro-3-indolyl-Phosphat)	Boehringer
Big Dye	PE Applied Biosystems
Chicken Embryo Extrakt	ICN
Complete™ Mini Protease Inhibitor Cocktail	
Tablets	Roche
DAPI (4', 6-Diamidino-2-phenylindol)	Applichem
Digoxigenin-11-UTP	Boehringer
DMEM (Dulbecco`s Modified Eagle Medium)	Gibco
DMSO (Dimethylsulfoxid)	Roth
Formamid	Merck
FCS (Fetal Calf Serum)	PAA
Gancyclovir	Sigma
G418, geneticin	Invitrogen, Sigma
HBSS (Hank`s Balanced Salt Solution)	Gibco
Hefe-tRNA	Roche
Heparin	Sigma
HEPES	Roth
Magnesiumsulfat	Roth
Metafectene	Biontex
Dual-Glo-Luciferase-Reagent	
Reagent	Promega

Dual-Glo-Stop+Glo-Reagent	Promega
NBT (Nitro blue tetrazolium chlorid)	Boehringer
Nuclear Fast Red	Sigma
OCT, Polyfreeze Tissue Freezing Medium	Polysciences, Warrington, USA
PEG-6000 (Polyethylenglykol)	Merck
Percoll	Amrsham Bioscience
Redivue Pro-Mix, ³⁵ [S]- Methion/ Cystein, 14,3 µCi/ µl	Amersham Bioscience

3.2 Enzymes

Collagenase Typ II	Gibco
DNase	Promega
Proteinase K	Boehringer/ Mannheim
Restriktionsendonucleasen	New England BioLabs
RNasin	Promega
RNase	Roth
T4-Ligase	Promega
Taq-Polymerase	TaKaRa
T3-RNA-Polymerase	Promega
Trypsin	PAA

For amplification the homologous arms of the *Popdc2* targeting construct as well as for generation *Popdc2* promoter region deletions and in all other amplifications where high fidelity proofreading amplification was required, Pwo (Roche Diagnostics GmbH, Mannheim, Germany) enzyme was used.

3.3 Eggs

SPAFAS (virusfree)	Charles River
--------------------	---------------

3.4 Clones and vectors

XL-1 Blue	Stratagene (Heidelberg) RecA1 endA1 gyrA96 thi-1 hsdR17 supE44 relA1 lac [F'proAB lacI ^q ZΔM15 Tn10 (Tet ^r)]
-----------	--

pBluescript II SK phagemid vector	Stratagene
pPD 46.21	Fire et al., 1990 (kindly provided by Dr. R. Zweigerdt)
pGL3 vectors	Promega

3.5 Primers

Primers used for amplifying the 5' arm of targeting construct:

LA Not Asc up	5'-NNNGCGGCCGCGGCGCG- -CCTGAAGCACAAACAGCTGC-3'
Pop2 FLAG dn	5'-NNGGATCCTTGTCGTCGTCGTCCTT- -GTAGTCACTCATCTTTGGGGCCCTCGA-3'

Primers used for the probe amplification for Southern blot analysis of ES cell lines:

LES probe up	5'-CCCTCTAGATTAAAACTTCCC-3'
Probe ES dn	5'-GAGTCCCTGCCAGCTGTCAAT-3'

Amplicon generated using these two primers is approx. 700 basepairs.

Primers used in analysis of ES cell lines:

ES PCR up	5'-CTGTCTTGCTGACGAAATTCT-3'
LacZ-S	5'-CGATTAAGTTGGGTAACGCC-3'

Primers used in analysis of removal neo cassette:

Pop2 rev	5'-TGCCTCATGATCTAGCTT-3'
LacZ 3060	5'-CCAGTTCAACATCAGCCGCTAC-3'

Primers used in genotyping of tail biopsies:

Pme1	5'-GTTTTGGAGCCTGCAAAGGC-3'
START-Pop2	5'-TTCTACATCCGGTTTCCAGC-3'
LacZ-S	5'-CGATTAAGTTGGGTAACGCC-3'

Primers used for amplification of hypertrophy specific markers and *Popdc2* genes:

Popdc2	5'-GGGCTTTATGGCAGGCAGTGGAGT-3' 5'-GAAGGCGGATGTCTGAAGCGTAACC-3'
--------	---

GATA4 5'-GCACAGCCTGCCTGGACG-3'
 5'-GCTGCTGCTGCTGCTAGTGG-3'

Atrial Natriuretic Factor (ANF)
 5'-GAGAGACGGCAGTGCTTCTAGGC-3'
 5'-CGTGACACACCACAAGGGCTTAGG-3'

β Myosin Heavy Chain (β -MHC)
 5'-GCCAACACCAACCTGTCCAAGTTC-3'
 5'-TGCAAAGGCTCCAGGTCTGAGGGC-3'

β -actin was used as a reference gene:

β -actin 5'-TGGAATCCTGTGGCATCCATGAAAC-3'
 5'-TAAACGCAGCTCAGTAACAGTCCG-3'

Primers used in promoter study:

Primers used for generation different size *Popdc2* 5' sequences plus 550bp of the 5' UTR fragment:

Nhe-pop2-dn 5'-NNGCTAGCTGCCATTGGCACTCATCTTTG-3'
 -77 5'-NNNNNGAGCTCACCTTTCTTCCGGCGCC-3'
 -282 5'-NNNNNGAGCTCCTGTTTCTGTTAGTAGTCCC-3'
 -418 5'-NNNNNGAGCTCACAGTGATGTTTGCTGAGTG-3'
 -517 5'-NNNNNGAGCTCTGGGCAGATATTTGCAGA-3'
 -581 5'-NNNNNGAGCTCTTAGGCAGTCATTCTAACTT-3'
 -691 5'-NNNNNGAGCTCCGTGTTGGAACACGTTAC-3'
 -1051 5'-NNNNNGAGCTCCTTAGTGTTATTCAGGTC-3'
 -1750 5'-NNNNNGCGGCCGCGTCACACCTGTAACCCCAGC-3'

Primer used for generation 1.7 kb fragment for subcloning into AUG-LacZ:

Nhe-transgene 5'-NNNNNGCTAGCAACTTCAGCAACACGGGACG-3'

Oligonucleotides used in SRF gelretardation assays:

Oligonucleotides with wild type binding site for SRF:

WT-SRF1 5'-TGGATTCCAATTCAAACATGGTATCCCTCTGGGGT-3'
 WT-SRF2 5'-GGGTGACCCCAGAGGGATACCATGTTTGGAATTGG-3'

Oligonucleotides with mutated binding site for SRF:

MUT-SRF1 5'-TGGATTCCAATTCCAAACATCTTATCCCTCTGGGGT-3'

MUT-SRF2 5'-GGGTGACCCCAGAGGGATAAGATGTTTGAATTGG-3'

Oligonucleotides used in CDP gelretardation assays:

Oligonucleotides with wild type binding site for CDP:

WT-CDP1

5'-CAGCTGCTTTTGTGATCGAAAGTCAACTTTTGTGATCGAAAGTCAA-3'

WT-CDP2

5'-CAGTGTTGACTTTTCGATCAACAAAAGTTGACTTTTCGATCAACAAAAG-3'

Oligonucleotides with mutated binding site for SRF:

MUT-CDP1

5'-CAGCTGCTTTTGTGGAAGTACAGTCAACTTTTGTGGAAGTACAGTCAA-3'

MUT-CDP

5'-CAGTGTTGACTGTACTTCAACAAAAGTTGACTGTACTTCAACAAAAG-3'

3.6 Mice

Specific pathogen-free outbred CD1 (ICR) mice were purchased from Charles River laboratories and used for blastocyst aggregations.

Identified *Popdc2* chimeric mice were backcrossed with C57BL/6J mice for at least six generations (>98% C57BL/6J background) for strain maintenance.

Animal colonies were kept in pathogen free conditions at the Animal Facility of the Universities of Braunschweig and Würzburg.

3.7 General molecular biology techniques

The range of the molecular biology techniques used during the course of this thesis such as PCR, isolation and purification of the plasmid/cosmid DNA and RNA, agarose gel electrophoresis, restriction enzyme digestion, subclonings of DNA, DNA fragments ligation, colony hybridization, DNA isolation from the agarose gel, polyacrylamid gel electrophoresis, bacterial transformations etc, were performed by standart protocols described in "Molecular Cloning" (Sambrook et al., 1989). Methods considered of specific impotency to this thesis are outlined under the headings below.

3.8 Database analyzes of the mouse genome

For database analyzes of the mouse genome the EBI database of the Sanger Institution (<http://www.ensembl.org>) and the NCBI (<http://www.ncbi.nlm.nih.gov>) database were used.

3.9 Cosmid library screening

A filter-spotted cosmid library of the mouse strain 129/ola (library no. 121, Burgtorf, Poch and Wiles, RZPD, Resource Centre and Primary Database, Berlin). was hybridized with a ³²P-labeled *Popdc2* full cDNA. Nine cosmid clones have been identified and obtained from the RZPD. Cosmid DNA was prepared using DNA Midiprep kit (Qiagen, Hilden), ends sequenced and analysed.

3.10 Site-directed mutagenesis

To create mutation at a defined site in a DNA sequence Quickchange™ site-directed mutagenesis kit from Stratagene was utilized. The principle of site-directed mutagenesis approach is that a mismatched oligonucleotide is extended, incorporating the "mutation" into a strand of DNA that can be cloned.

3.11 Cell culture

3.11.1 ES cell line

TBV2 ES cells (Gene trap consortium, GSF, München) were cultured on Mitomycin growth-inactivated feeder cells in the presence of leukemia inhibitory factor (LIF).

500ml ES cell culture medium:

In 425 ml DMEM:

75 ml FCS (hit inactivated by 56°C for 30min)

5 ml Glutamine (100x stock)

5 ml Non-essential amino acid (BRL product)

5 ml Penicillin-Streptomycin (100x stock)

4µl β-mecaptoethanol (Fluka)

250 µl LIF (10⁶ U/ml, GibcoBRL, Paisly, Schottland)

Freezing medium (2x)

60% Medium, 20% DMSO, 20% FCS

3.11.2 Mouse Embryo Fibroblast (MEF)

MEFs were prepared from β 2-Microglobulin embryos at embryonic day 13.5. Cells of β 2-Microglobulin embryos are expected to be G418 resistance since they contain Neomycin cassette. The head and internal organs were removed, and the torso was minced and incubated in 0.1% trypsin for 30min at 37°C. Cells were grown and then viably frozen in liquid nitrogen. Subsequently, when needed primary MEFs were thawed, expanded and treated with mitomycin to halt their proliferation.

3.11.3 Electroporation and selection of ES cells

The day before transfection the ES cells were plated on 100 mm gelatin coated dishes. For electroporation, the cells were trypsinized, washed with PBS and centrifuged. The cell pellets were resuspended in 500 μ l cold PBS (up to 10^8 cells) and pipetted into an electroporation cuvette together with 120 μ g DNA. Electroporation was carried out at 0.8kV V and 3 μ F. After that the cells were plated on mitotically inactivated MEFs in ES growth medium.

2 days after transfection selection with G418 and gancyclovir of stably transfected cells was started. Medium exchange was done every 2 to 3 days. The selection is finished in general after 7-12 days.

3.11.4 Isolation and cryopreservation of ES cell clones

Colonies which appeared after 7-10 days of selection were picked in HEPES buffer piped up and down to dissociate the cells and split into two 96 well plates. After growing 3-4 days, one 96 well plate was frozen down and the second plate was used for DNA isolation and PCR/Southern blot analysis.

3.11.5 In vitro differentiation of ES cell

In vitro differentiation of ES cells into cardiomyocytes was performed as previously described (Maltsev *et al.*, 1993).

3.11.6 Isolation of primary embryonic chick cardiomyocytes

Embryonic chick cardiomyocytes were isolated using a Percoll gradient density method. Briefly, hearts were removed from 10-11-day-old chick embryos and washed in Hanks' balanced salt solution (HBSS) lacking magnesium and calcium (Life Technologies). The ventricular tissue was minced and then dissociated using 1 cycle

(15min) of trypsin (0.025%, Life Technologies) digestion and 4-6 cycles (each 30min) of collagenase digestion at 37°C. The cardiomyocytes were then enriched by Percoll gradient density centrifugation, counted with a hemacytometer, assessed for viability using trypan blue (0.4%), and plated out. Next day after they reached approx. 70% cardiomyocytes were used in transfection assays. Tissue culture plates used in cardiomyocyte primary culture: Primaria™ 24 wells, 96wells (Becton Dickinson Labware).

3.12 Luciferase assay

Primary chick cardiomyocytes culture was transiently transfected in 96-well plates using Metafectene (Biontix) (0.3 µl pro well) with the indicated plasmids (200ng *Popdc2* deletion construct DNA and 100ng of Renilla Luciferase Reporter Vector DNA pro well); 36 to 48 h posttransfection cells were washed with phosphate-buffered saline and luciferase activity was measured in a luminometer (1420 Luminescence Counter, Victor Light, Perkin Elmer) using the Dual-Glo™ Luciferase Assay System (Promega). Each experiment was repeated at least two times with each reaction measured in triplicate.

3.13 Ex ovo electroporation

Chicken embryos at Hamburger Hamilton stage 8 were cultivated on agar plates (Chapman et al., 2001). The DNA constructs (EGFP-reporter and *Popdc2-lacZ*) were diluted in a ratio of 2:1 in adjunct solution and coinjected into the cardiac crescent. The cardiac progenitor cells were immediately transfected via dorsal-ventrally directed low-voltage pulses using platinum wire electrodes. The embryos were incubated until they reached the desired age and the EGFP signal was detected by fluorescence stereomicroscopy. Subsequently the embryos were harvested and prepared for lacZ-staining.

Electroporation parameters:

Voltage: 15V
Pulse length: 30ms
Pulse interval: 300ms
Pulses: 4

Adjunct solution:

1% carboxymethylcellulose in PBS
0,05 % Fast green

3.14 DNA and RNA analysis

3.14.1 Extraction of Genomic DNA

A 2-3mm of mouse tail snip or cell pellet was incubated with 300 μ l lysis buffer containing 1 mg/ml Proteinase K at 56°C overnight until tissue is completely digested. The lysats were spinned down at maximal speed for 30 minutes. The supernatant was transferred to a new tube. For DNA precipitation the equal volume of isopropanol was added and mixed by gentle inversion. The DNA pellet was obtained after centrifugation at 14000 rpm for 15 min. The DNA pellet was washed with 70% ethanol, dried and resuspended in TE buffer.

Lysis buffer: 50 mM Tris
 0.4 M NaCl
 100 mM EDTA
 0.5 % SDS

3.14.2 Southern Blot Analysis

For Southern, 10 μ g of genomic DNA was overnight digested with the appropriate enzyme and run on 0.7% agarose gels in TAE solution. DNA was transferred to positive charged Nylon membrane in 0,4M NaOH and cross-linked to the membrane by drying at 80°C for 2h. Southern blot hybridisation was performed using standard techniques. Hybridizations were done in buffer consisting of 0,5 M $\text{Na}_x\text{H}_y\text{PO}_4$, pH 7,2, 7% SDS and 2mM EDTA.

The membrane has to be pre-hybridized for at least 30 min and then the denatured radioactively labeled probe is added to the tube and hybridization takes place overnight at 68°C. After hybridisation the membrane is washed with the following set of washes:

2x 5 minutes with	Wash buffer I:	40mM $\text{Na}_x\text{H}_x\text{PO}_4$, pH 7.2 1% SDS 2 mM EDTA
1x20 minutes with	Wash buffer II:	40mM $\text{Na}_x\text{H}_x\text{PO}_4$, pH 7.2 0.1% SDS, 2mM EDTA
3x10 minutes with	Wash buffer III:	100 mM $\text{Na}_x\text{H}_x\text{PO}_4$, pH 7.2 2 mM EDTA

The washes are carried out at 68°C while shaking.

3.14.3 DNA sequencing

DNA sequencing was carried out using the dideoxy nucleotide chain-termination method (Sanger et al., 1977). For this purpose ABI PRISM Big Dye Terminator Cycle Sequencing system was used.

3.14.4 Isolation of total RNA

Total RNA was isolated using Trizol reagent. The tissues were washed with cold PBS and 1 ml Trizol reagent was added to each 100 mg of the specimen and homogenized using power homogenizer (Ultra-Turrax, Bachofer Laboratoriumsgeraete, Reutlingen). 0.2ml chloroform per 1ml of TRIZol reagent was added to each sample. After vigorously mix and centrifugation at 13000 rpm 15 min at 4°C two phases are separated: lower red phenol-chloroform layer, interphase and colourless upper RNA phase. For RNA precipitation aqueous, upper clear RNA containing phase was transferred to a new tube, 0.5 ml isopropanol was added, mixed and centrifuged at 13000 rpm, 4°C for 15 min. RNA pellet was washed with 75% ethanol, air dried and redissolved in RNase-free water.

The concentration of the RNA was determined by measuring the A260 of the final preparation. A solution whose A260 = 1 corresponds to approximately 40 µg of mRNA per ml. The ratio between the readings at 260 nm and 280 nm gives an estimate of RNA purity. An A260/A280 absorbance ratio in the range of 1.8 to 2.0 indicates a pure preparation of RNA.

3.14.5 RT-PCR

RNA was reverse transcribed using the SuperScript™ First-Strand Synthesis System for RT-PCR (Gibco). Total RNA (1-5 µg) was combined with oligo-dT primer mix, dNTP mix and H2O and preheated at 65°C for 2 min to denature secondary structures. To the mixture was then added 5x RT Buffer, 10 mM DTT and RNase inhibitor. After 2min incubation at 42°C, Reverse Transcriptase was added to the samples. The RT reaction was incubated at 42°C for 50 min following by heating at 95°C for 5 min. To remove RNA complementary to the cDNA the samples were treated with 1 µl (2 units) of E. coli RNase H at 37°C for 20 min.

A control experiment without reverse transcriptase was performed for each sample to verify that the amplification was not caused by any residual genomic DNA. The cDNA for β -actin was examined as the reference cellular transcript in each PCR reaction.

3.14.6 Northern blot analysis

Northern blotting is a method for RNA analysis. Especially significant is to study how cells express different levels and types of mRNA. In this method RNA is loaded on denaturing 0.8% agarose gels containing 1.2% formaldehyde and run overnight by 26 V. Next, the RNA is transferred onto a nylon membrane by capillary action in highly concentrated salt solution 10xSSC. Once transferred, the RNA should be covalently cross-linked onto the membrane, by heating at 80°C for 2h. Detection of a specific mRNA in the total RNA sample is done by hybridization of the Blot with a specific, complementary radiolabelled DNA probe overnight at 65°C. This hybridization step followed by autoradiography.

Agarose gel: 1.2 g agarose,
10 ml 10×MOPS buffer,
18 ml formaldehyde (12,3M)

10×MOPS buffer: 200 mM MOPS,
50 mM Sodium acetate,
10 mM EDTA, pH 7.0

Running buffer: 100 ml 10×MOPS buffer

Hybridization buffer: 10% Dextransulfat
1% SDS
1 M NaCl
0,5 mg/ml Yeast-RNA
0,5 mg/ml salmon sperm DNA

5×GLB: 16 μ l bromophenol blue (1mg/ml),
80 μ l 500mM EDTA, pH 8.0,
720 μ l formaldehyde,
2 ml 100% glycerol,
3084 μ l formamide
4 ml 10×MOPS buffer

Post-hybridization washes were done as follows:

2x, room temperature, 20 minutes, 2x SSC/1% SDS
1x, 65° C, 20 minutes, 2x SSC/0.5% SDS
1x, 65° C, 20 minutes, 0.1x SSC/0.1% SDS

3.14.7 Probes and probe synthesis

Random priming with the "Redi-Prime DNA labeling system"

Labelling mix: dATP, dCTP, dTTP, exonuclease free Klenow enzyme, oligonucleotide primer (9-mer).

For this labeling reaction a commercially available system of the company Amersham is used. The reaction mix is available as a freeze-dried pellet in an Eppendorf tube. First 2.5-100ng DNA probe in 45 µl sterile water is denatured at 95°C for 5 min and put on ice immediately. The DNA and 5 µl of α [³²P] dCTP are added to the labeling mix, vortexed thoroughly and incubated for 10 to 30 min at 37°C. To stop the reaction 2 µl of 0.5 M EDTA is pipetted to the mix. After labeling, the probe is separated from unincorporated nucleotides over a Sephadex G50 column. For this purpose the ready to use stacked Micro-Spin™ G50 columns from the firm Pharmacia Biotech are used. The perfect packing of the column is reached by spinning the columns for 1 min at 2800 rpm. The labeling mix is put on the column and centrifuged through the column for 2 min at 2800 rpm. The labeled probe is denatured in a boiling water bath for 5 min, put on ice immediately and added to the hybridizing solution.

3.15 Protein analysis

3.15.1 Western blot

10-30 µg of protein per lane was separated on gradient 4-12% Bis-Tris gel (Invitrogen) and transferred by electroblotting onto nitrocellulose membranes (Amersham). The membranes were blocked in 5% non-fat dry milk dissolved in T-TBS (Tween Tris buffered saline) (20 mM Tris/HCl, pH 7,5, 137 mM NaCl and 0,1% Tween-20). Immunoblotting was performed using monoclonal antibody directed against CDP (M-222). Filters were then incubated with the secondary horseradish peroxidase conjugated anti-rabbit antibody. Proteins were detected using an enhanced chemiluminescence protein detection method (Pierce).

3.15.2 Preparation of nuclear extract

Nuclear extracts for Electromobility Shift Assay (EMSA) were prepared essentially as described by S. Parmecsek/ K.Chien on S. Parmecsek laboratory website

(http://www.med.upenn.edu/mcrc/parmacek_lab/NuclearExtract-cardiac.shtml) with little modifications.

Reagents:

1. PBS-ice cold

2. Buffer A (10 mM Hepes pH 7.9, 1.5 mM MgCl₂, 10 mM KCl, 0.5 mM DTT, 0.5 mM

PMSF):

500 ul 1M Hepes pH 7.9

75 ul 1M MgCl₂

500 ul 1M KCl

25 ul 1M DTT (added just prior to use)

250 ul 100 mM PMSF (added just prior to use)

48.5 ml ddH₂O

50 ml

3. Extraction Buffer (20 mM Hepes pH 7.9, 25% glycerol, 0.55M NaCl, 1.5 mM MgCl₂, 0.2 mM EDTA, 0.5 mM PMSF, 0.5 mM DTT, protease inhibitor cocktail

(Roche Applied Science):

1 ml 1M Hepes pH 7.9

12.5 ml glycerol

27.5 ml 1M NaCl

75 ul 1M MgCl₂

20 ul 500 mM EDTA

25 ul 1M DTT (added just prior to use)

250 ul 100 mM PMSF (added just prior to use)

3.6 ml 7x protease inhibitor cocktail

5 ml ddH₂O

50 ml

4. Dialysis Buffer (40 mM KCL, 15 mM Hepes pH 7.9, 1 mM EDTA, 0.5 mM PMSF, 0.5 mM DTT, 20% glycerol):

40 ml 1M KCl

15 ml 1M Hepes pH 7.9

2 ml 500 mM EDTA

500 μ l 1M DTT (added just prior to use)
200 ml glycerol
2.5 ml 100 mM PMSF (added just prior to use)
740 ml ddH₂O

1000ml

Method:

1. 10 hearts of 1-4 d neonatal mice are dissected, rinsed 3-4 times in ice cold PBS to get rid of blood cells, and transferred into 1.5 ml Eppendorf tube.
2. 1 ml of Buffer A is added to the hearts, and gently homogenized with microhomogenizer until tissues are homogeneous.
3. The homogenized tissues are centrifuged at 6000 rpm at 4°C for 15 min, and the supernatant is discarded.
4. The pellet is resuspended in 500 μ l buffer A and re-homogenized with microhomogenizer for 5 strokes.
5. The homogenized pellet is centrifuged at 6000 rpm, 4°C, 15 min, and the supernatant is discarded.
6. The nuclear pellet is resuspended in 200 μ l of Extraction Buffer and homogenized with microhomogenizer for 10 strokes.
7. The homogenized nuclear pellet is centrifuged in the microcentrifuge at 4°C at 14000 rpm for 30 minutes.
8. The supernatant is dialyzed in 1L dialysis buffer for 45min at 4°C.
9. The dialyzed nuclear extract is in 20 μ l aliquots quick frozen in dry ice ethanol and stored at -70°C.

3.15.3 Electromobility Shift Assay (EMSA)

EMSA were performed with 8 μ g of nuclear extract. The samples were incubated at 37°C for 15 min in a final volume of 40 μ l of 50 mM NaCl, 10 mM Tris, pH 7.5, 0.5 mM MgCl₂, 1 mM EDTA, pH8, 5% of glycerol, 1 mM of dithiothreitol, with 4 μ g non-labeled oligonucleotides and 100 ng of poly(dI-dC) as nonspecific competitors. End-labeled double-stranded oligonucleotides 40 pg were added and further incubated for 15 min at 37°C. To supershift the retarded complex, 2 μ g of antibodies were incubated with lysate, after the addition of oligonucleotides, for 20 min at room temperature. The samples were loaded on a 5% polyacrylamide gel (29:1), 1x TBE

buffer and separated by electrophoresis at 8 V/cm in 1x TBE buffer. The gels were dried and visualized by autoradiography.

The oligonucleotides used in this study were end-labelled with $\alpha^{32}\text{P}$ -dCTP by Klenow Fragment in the following reaction:

- 2 μl ds oligonucleotides (200ng/ μl)
- 2 μl Klenow buffer
- 2.5 μl dNTP mix without dCTP (4mM)
- 5 μl $\alpha^{32}\text{P}$ -dCTP (50 μCi)
- 1 μl Klenow Fragment (5U/ μl)
- 7.5 μl ddH₂O

The labelling reaction was carried out for 20min at room temperature and unincorporated nucleotides were removed with Sephadex G50 columns.

3.16 Histology

3.16.1 Paraffin sectioning

Stained embryos and whole organs were dehydrated through a series of ethanol followed by xylene and processed into paraffin blocks for sectioning. Serial 10 μm sections were obtained with a microtome and stained with hematoxylin and eosin (HE) or Masson's Trichrom according to the manufacturer's instructions.

3.16.2 Cryostat sectioning

Embryos and organs selected for cryostat sectioning were passed through an ascending series of sucrose-PBS solutions up to 30% sucrose in PBS. They were finally embedded in OCT compound and sectioned (Jung Frigocut 2800 E, Leica, Bensheim) at 10 μm .

3.17 LacZ staining and Acetylcholine esterase (AChE) enzyme histochemistry

Timed pregnant females, as well as, postnatal and adult mice were euthanized by cervical dislocation and their embryos or organs, respectively, were dissected out, washed in cold PBS, weighed when required and processed further.

Embryos up to E10.5 to be sectioned after staining and older to be shown only as whole mount stained (as well as organs at different stages) were fixed for 15 minutes up to 1hour depending on size, at room temperature in fix solution (2%

formaldehyde, 0.2% glutaraldehyde, 0.02% Nonidet P-40 (NP-40), 0.01% sodium desoxycholate in PBS). After fixation, tissues were rinsed 3 times in PBS and then stained 5 min to overnight at 37°C in the dark with stain solution (5 mM K₃Fe(CN)₆, 5 mM K₄Fe(CN)₆, 1 mg/ml 5-bromo-4-chloro-3-indolyl-2-D-galactopyranoside (X-gal), 2 mM MgCl₂, 0.02% NP-40, 0.01% sodium desoxycholate in PBS). Following a staining, specimens were washed at least three times with PBS, post-fixed in 4% PFA and washed again in PBS. The specimens which had to be cleared before documenting were dehydrated through an ethanol series and treated with benzyl alcohol/benzyl benzoate (1:2).

Embryos and organs to be sectioned before staining were subjected to the cryostat unfix. After specimens are cut sections are fix 5min in solution like in whole mounts experiments, washed in PBS, and stained in LacZ solution as described in whole mounts experiments for 5min to few hours.

LacZ stained sections and sections obtained by cutting whole mount stained embryos and organs were counterstained with 0.1% Nuclear Fast Red in 5% aluminum sulfate.

For acetylcholinesterase (AChE) staining, unfix sections were washed in running tap water for 10min and incubated with substrate solution containing 65mM sodium acetate (pH 6), 0.5mg/ml acetylthiocholine iodide, 0.5mM potassium ferricyanide, 0.3 mM copper sulphate and 5mM tri-sodium citrate in a 37°C for 2 hours; then passed through an ascending series of ethanol, immersed in xylene, and coverslipped with Entelan (E. Merck, Switzerland).

3.18 Image acquisition

Digital images were taken with a Leica MZFL III binocular equipped with Leica DC 100 or Polaroid DMC (Polaroid, Cambridge, USA), or with a Zeiss Axiophot microscope (Zeiss, Jena, Germany) equipped with a Pixelfly digital system (PCO Computer Optics, Kelheim, Germany).

3.19 Non-radioactive in situ hybridization on sections

Nonradioactive section in situ hybridization was performed as previously described (Moorman et al., 2001) with some adaptations. RNA probes complementary to the

mRNAs for *Popdc2* (Andree et al., 2000) and cardiac troponin I (cTnI) were labeled with digoxigenin UTP and hybridized to 10µm thick sections.

RNA probe labelling

Digoxigenin-labeled antisense RNA was produced by in vitro transcription using DIG RNA labeling mix (Roche Diagnostics GmbH, Mannheim, Germany) according to the manufacturer's instructions. After the labeling reaction the template DNA was digested using RQ-DNAse, phenol extracted and the labeled RNA probe was precipitated. The probe was dissolved in TE (10mM Tris-HCl and 1mM EDTA, pH 7.6) and its concentration measured.

Hybridization and posthybridization treatment

Embryos were fixed in PFA for 4 hours to overnight in freshly prepared 4% PFA in PBS by rocking at 4°C. Then embryos were dehydrated in a graded alcohol series and embedded in paraffin. 10µm thick sections were cut and mounted onto aminoalkylsilane-coated slides. After deparaffinization and hydration, sections were incubated with 20µg/ml proteinase K dissolved in PBS for 8-12 min depending on the developmental stage, at 37°C. The proteinase K activity was blocked by rinsing the sections in 0.2% glycine in PBST (PBS + 0.1% Tween20) for 5 min. After two washes in PBS for 5min the sections were post-fixed for 20 min in 4% PFA and 0.2% glutaraldehyde in PBS, followed by two washes in PBS for 5 min. To make a hydrophobic barrier around of each individual section which allows treatment with a different RNA probe, an ImmEdge pen (Vector Laboratories, Burlingame, USA) was used. After prehybridization for one hour at 70°C in hybridization mix (50% formamide, 5x SSC (20x SSC; 3M NaCl, 0.3M tri-sodium citrate, pH 4.5), 1% blocking solution (Roche Diagnostics GmbH, Mannheim, Germany), 5mM EDTA, 0.1% CHAPS (Sigma, Steinheim, Germany), 0.1mg/ml heparin, and 1mg/ml yeast total RNA (Roche Diagnostics GmbH, Mannheim, Germany), a digoxigenin-labeled probe was added to the hybridization mix in a final concentration series of 0.1 to 10 ng/µl. After overnight hybridization, the sections were rinsed with 2x SSC, followed by three washes with 50% formamide, 2x SSC, pH 4.5, at 65°C for 15 min, and finally three washes in PBS at room temperature. Subsequently, the sections were incubated for 1 hour in 2% blocking solution in PBST, followed by overnight incubation in 2% blocking solution in PBST containing 100mU/ml anti-digoxigenin Fab-fragment covalently coupled to alkaline phosphatase (AP) (Roche Diagnostics

GmbH, Mannheim, Germany). Probe binding was visualized using NBT/BCIP as the chromogenic substrate for anti-DIG-AP, according to the manufacturer's protocol (both NBT and BCIP are purchased from Roche Diagnostics GmbH, Mannheim, Germany). After staining times of 1 to 48 hours at room temperature, the color development was stopped by rinsing in double-distilled water. The sections were dehydrated in a graded ethanol series, kept for 2min in xylene, and embedded in Entellan.

3.20 Whole-Mount Immunostaining

The whole-mount atria preparations were fixed in methanol + DMSO 4:1 overnight at 4°C and then bleached with 30% H₂O₂ + DMSO + methanol 1:1:4 for 2-3 hours to block endogenous peroxidase. The preparations were blocked with PBS+2% BSA + 0.1% Triton for 2 h at room temperature, followed by overnight incubation with 1:500 diluted anti-HCN4 (Alomone Labs) at 4°C. The preparations were subsequently washed 5 times for 1hour in TBST and then incubated with 1:200 diluted (2mg/ml stock) goat anti-rabbit HRP-coupled (or 1:1000 diluted alexa 488 goat anti rabbit) secondary antibody at 4°C overnight. Staining was visualized by using 1mg/ml DAB (Sigma-Aldrich) and 0.03% H₂O₂ in Tris-HCl pH7.6.

3.21 Statistical analysis

The significance of the difference between the means of groups in the experiments was determined by Student's *t* test.

3.22 Three-Dimensional Reconstruction

Three-dimensional visualization and geometry reconstruction of HCN4 expression in SA node region was done on atria cryosections which were stained with rabbit polyclonal antibody against HCN4 (Alomone Labs), images were obtained by confocal laser scanning microscopy (CLSM) and reconstruction performed with Amira 3.0 (Mercury Computer Systems, Inc.) software.

4. Results

4.1 Generation of a *Popdc2* knockout mouse

4.1.1 Isolation of a genomic clone for the *Popdc2* locus

A genomic *Popdc2* clone was isolated from a cosmid library (mouse cosmid library no.121 *Mus musculus* 129/ola, Burgtorf, Poch and Wiles, RZPD (Resource Centre and Primary Database), Berlin). Library filters were screened using a full-length mouse *Popdc2* cDNA probe under high stringency conditions. A total of 9 clones were identified and further analyzed. One of these clones, MPMGc121110192Q2, was 43kb and found to contain the complete coding region and was used for vector construction (Fig. 6).

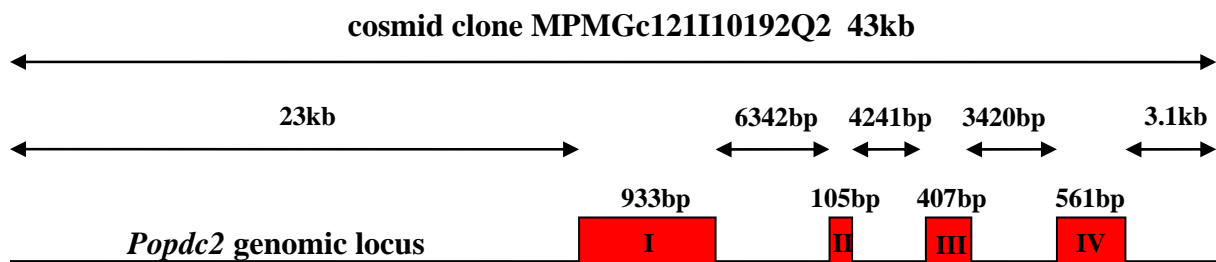


Figure 6. Schematic representation of the mouse cosmid clone MPMGc121110192Q2 and the *Popdc2* genomic locus including all four exons (red boxes).

4.1.2 Generation of a *Popdc2* null mutant in mice

A targeting vector was constructed in order to replace 490bp of protein coding sequence of exon 1 by a NLS-LacZ reporter gene (Fig. 7). For this purpose pPNT-2loxP was chosen as cloning vector. pPNT-2loxP contains a neomycine (*neo*) selection gene (pGKneo) for positive selection, which is flanked by two LoxP sequences and a HSV-thymidine kinase (TK) gene to allow for negative selection of random integration. A cassette containing a nuclear localized LacZ (NLS-LacZ) reporter gene was isolated from pPD46.21 and subcloned into the *Bam*HI and *Not*I sites of pPNT-2loxP upstream of the neomycine gene. Two fragments of homologous sequence flanking the protein-coding region of exon 1 of the *Popdc2* gene (Fig. 7) were isolated from the MPMGc121110192Q2 cosmid clone and subcloned into the targeting vector to ensure homologous recombination. The short arm was a PCR-

amplified 2.2kb fragment, which was subcloned into *SacI* and *BamHI* upstream of the LacZ gene. The 3' end this fragment contained an ATG start codon and a FLAG (Asp-Tyr-Lys-Asp-Asp-Asp-Lys) epitope in frame with the LacZ reporter gene. The long arm was isolated as a 2.8kb *EcoRI* fragment from MPMGc121110192Q2 cosmid clone and inserted into the targeting construct downstream of the *neo* gene. The targeting vector was *NotI* linearized and electroporated into 129 SvP-derived TBV2 embryonic stem cells (ES). Selection was performed with G-418 (positive selection) and gancyclovir (negative selection). 400 ES clones were picked and analysed. ES clones with homologous recombination at the *Popdc2* locus were identified by PCR and further analyzed by

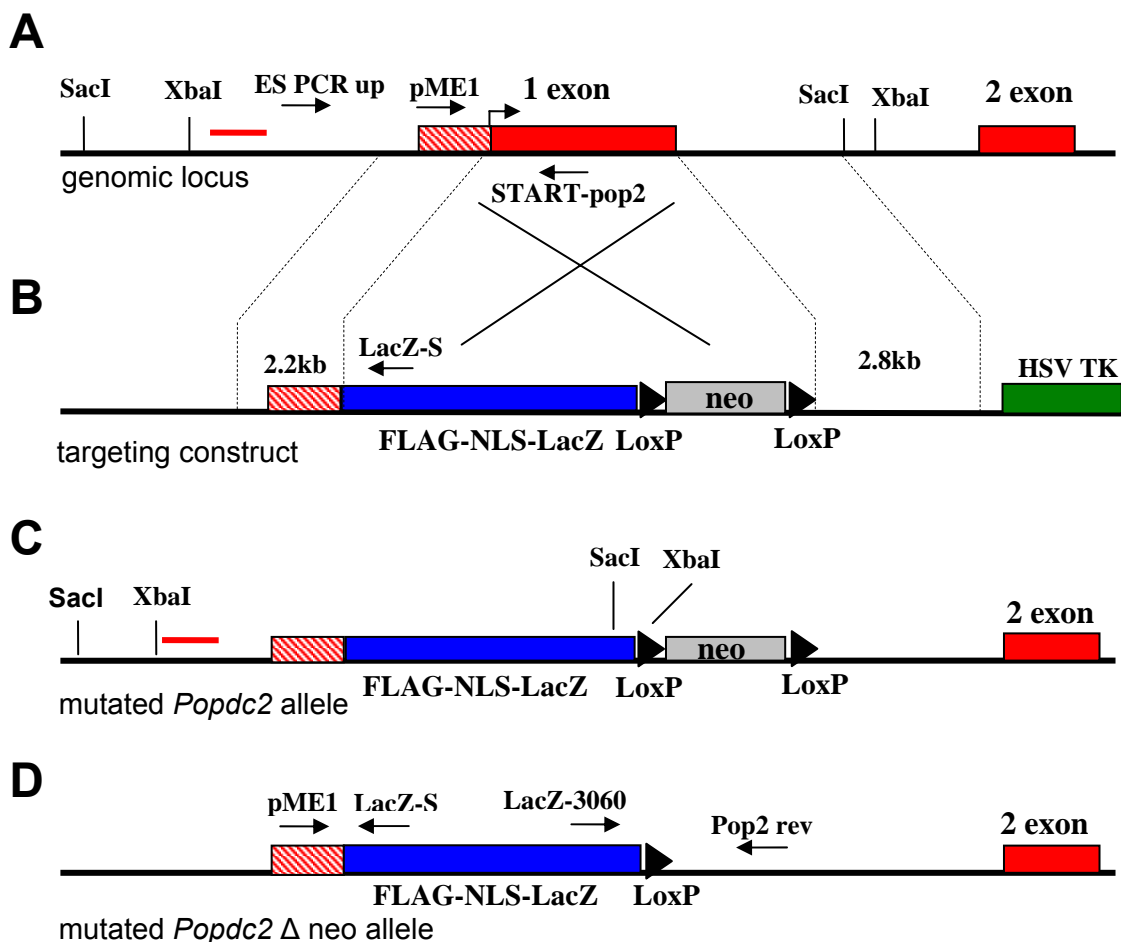


Figure 7. Schematic structure of the targeting vector and the genomic modifications in transgenic mice. (A) Schematic representation of the *Popdc2* locus. (B) Structure of the targeting construct. (C) *Popdc2* allele after homologous recombination. (D) Targeted *Popdc2* allele after Cre-mediated excision of the neomycine selection gene. A dashed box indicates the UTR of exon 1. Red line in (A) and (C) demarcate the position of the probe used for Southern blot analysis. Arrows demarcate the position of the various PCR primers that were used to genotype ES cells and mice.

Southern blot. Two ES cell clones were aggregated with CD1 morulae and the resulting chimeric male mice were bred to C57BL6 females to achieve germline transmission of the mutant allele.

Heterozygous F1 generation mice were bred with Zp3cre mice (Lewandowski et al. 1997) to delete the floxed *neo* cassette (Fig. 7). The further characterization of the *Popdc2* mutant was performed with animals having a deleted *neo* cassette and in the following will be referred to as *Popdc2* mice. These mice were backcrossed 5 times with C57-BI6J, maintained on this background by intercrosses and used for phenotype analysis throughout this work. For gene expression analysis also heterozygous and homozygous *Popdc2* mutant mice with a mixed genetic background (i.e. SV129/C57BI6J/CD1) have been used. No difference in the expression pattern was observed between embryos with a mixed or homogeneous genetic background (i.e. C57-BI6J).

4.1.3 Analysis of *Popdc2* gene inactivation in ES cells

ES clones, which survived selection with G-418 and gancyclovir were subjected to PCR analysis (Fig. 8). Primers were designed in such a way that the 5' primer sequence (ES PCR up) was located in a position upstream of the left arm used in the targeting vector, while the sequence of the 3' primer (LacZ-S) was derived from the LacZ gene (Fig. 7).

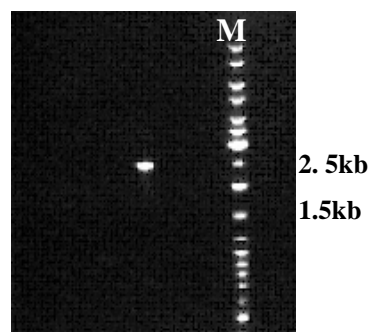


Figure 8. An example of a PCR positive ES cell clone. Genomic DNA was isolated from the targeted clones and tested by PCR using the primer pair ES PCR up and LacZ (position of primer Fig. 7A, B). The expected size of the amplicon was 2.4kb. M, marker.

To reconfirm results obtained by the PCR approach, putative positive clones were tested by Southern Blot analysis (Fig. 9). The position of the probe used in Southern Blotting is depicted in Fig. 7. Both, the probe for Southern blot analysis as well as the primer: *ES-PCR-up* was located external to the targeting sequences. The Southern Blot analysis provided further evidence that homologous recombination did occur. In addition Southern analysis allowed us to assess the relative amounts of the hybridizing bands representing the mutant and wild-type alleles, which was difficult to estimate by PCR. In case that wild-type and mutant bands were not of equal intensity, targeted clones were considered to be contaminated with wild-type ES cells and were discarded. The *Popdc2* targeted ES clones should give rise to a hybridizing DNA fragment of 5kb after *XbaI* restriction digestion and a 7kb restriction fragment after restricting DNA with *SacI*, whereas the wild-type allele is expected to give rise to a 6kb *XbaI* and a 8kb *SacI* fragment, respectively. Every clone that was analyzed displayed wild-type and mutant bands of equal intensity (Fig. 9). Based on PCR and Southern blot analysis a total 4 clones were isolated that harboured a mutant *Popdc2* allele.

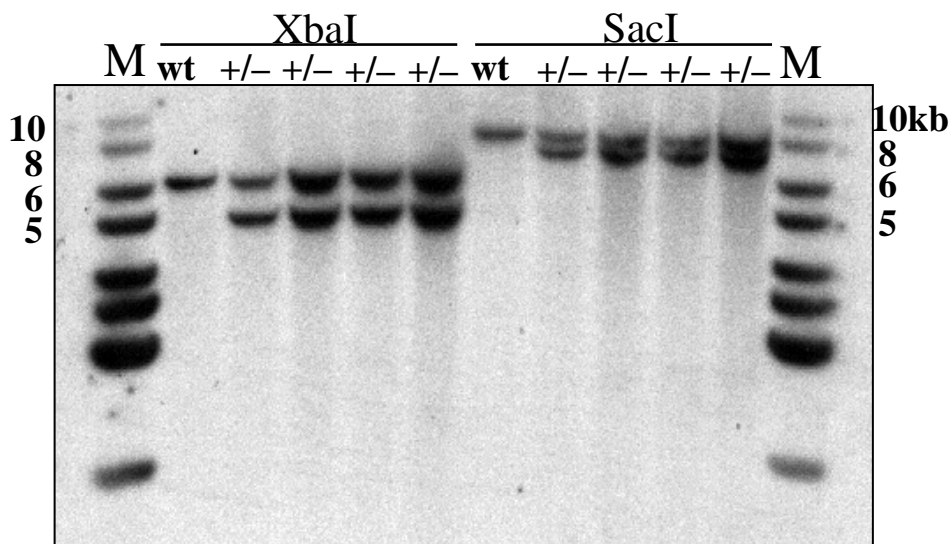


Figure 9. Southern blot analysis to confirm homologous recombination in the clones that were identified by PCR analysis. Genomic DNA of four targeted and one WT ES clone was digested with *XbaI* or *SacI* and hybridized with a PCR amplified probe. Position of the probe is shown in Fig.7. M, marker.

4.1.4 Analysis of *Popdc2* gene inactivation in mice and genotyping strategy

The *Popdc2* deficiency in knockout (KO) mice at the RNA level was demonstrated by Northern blot analysis. Total RNA used in this experiment was isolated from three organs (cardiac- and skeletal muscle, and bladder) representing different muscle types (striated and smooth muscle tissue) that express *Popdc2* in WT animals (Fig. 10). No truncated or otherwise aberrant bands hybridized with the probe in case of mutant tissue and thus it can be concluded that no *Popdc2* mRNA was made in the null mutant.

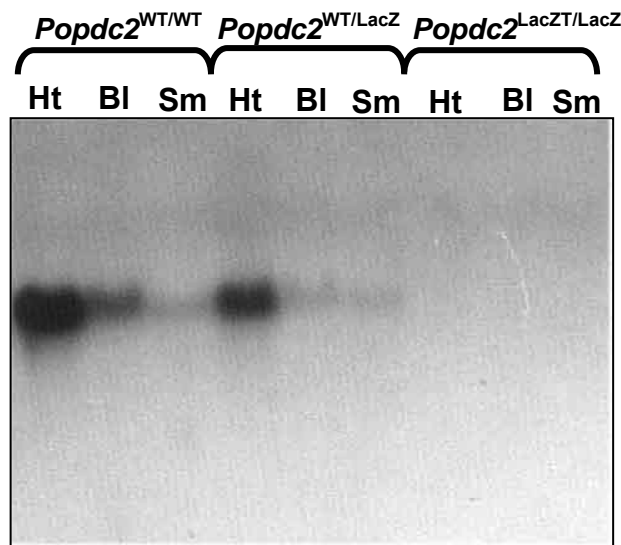


Figure 10. Northern blot analysis. Total RNA was isolated from different organs of *Popdc2*^{WT/WT}, *Popdc2*^{WT/LacZ}, *Popdc2*^{LacZ/LacZ} mice. As probe a full length *Popdc2* cDNA was used. Ht, heart; Bl, bladder; Sm, skeletal muscle.

To determine the genotype of every newborn mouse we designed a PCR based genotyping strategy (Fig. 11). This approach has the advantage that the genotype is known immediately after amplification, and no further work is required, which significantly reduces cost and time. In this approach different primer pairs were used for the amplification of the wild type and targeted alleles, resulting in the production of different amplicon sizes.

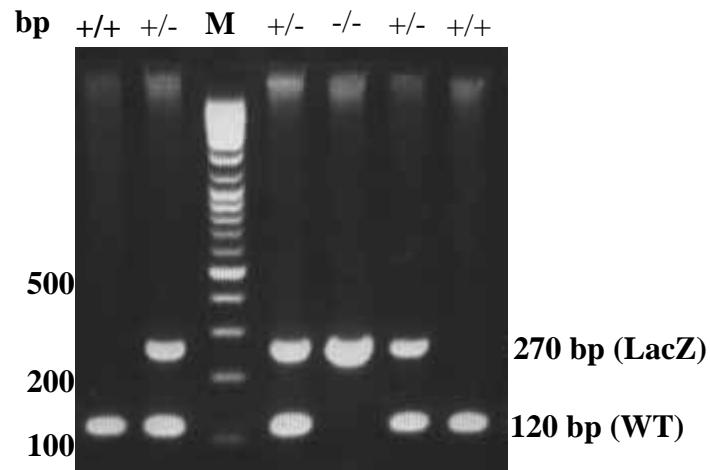


Figure 11. Genotyping of mice by PCR using tail biopsies. The upper band corresponds to the pME1–LacZ-S (position of the primers in Fig. 7 A) amplicon and the lower band to the pME1-START-pop2 (position of the primers in Fig. 7 D) amplicon. M, marker.

4.1.5 Deletion of the neomycin selection cassette from the *Popdc2-LacZ* allele in mice

The presence of the PGK-neo selection cassette in targeted loci can have effects on the expression of neighbouring genes and on the targeted gene itself (Olson et al., 1996). In the pPNT-2loxP vector, the PGK-neo selection cassette is flanked by two Lox-P sites. Thus it can be removed by site-specific Cre recombinase leaving behind a single Lox-P site in the targeted locus. From the few possible methods available we have decided to use the ZP3-Cre deleter mouse (Lewandoski et al. 1997). Cre expression in this mouse line is under the control of the zona pellucida 3 (*Zp3*) gene, which is expressed exclusively in growing oocytes (Fig.12A).

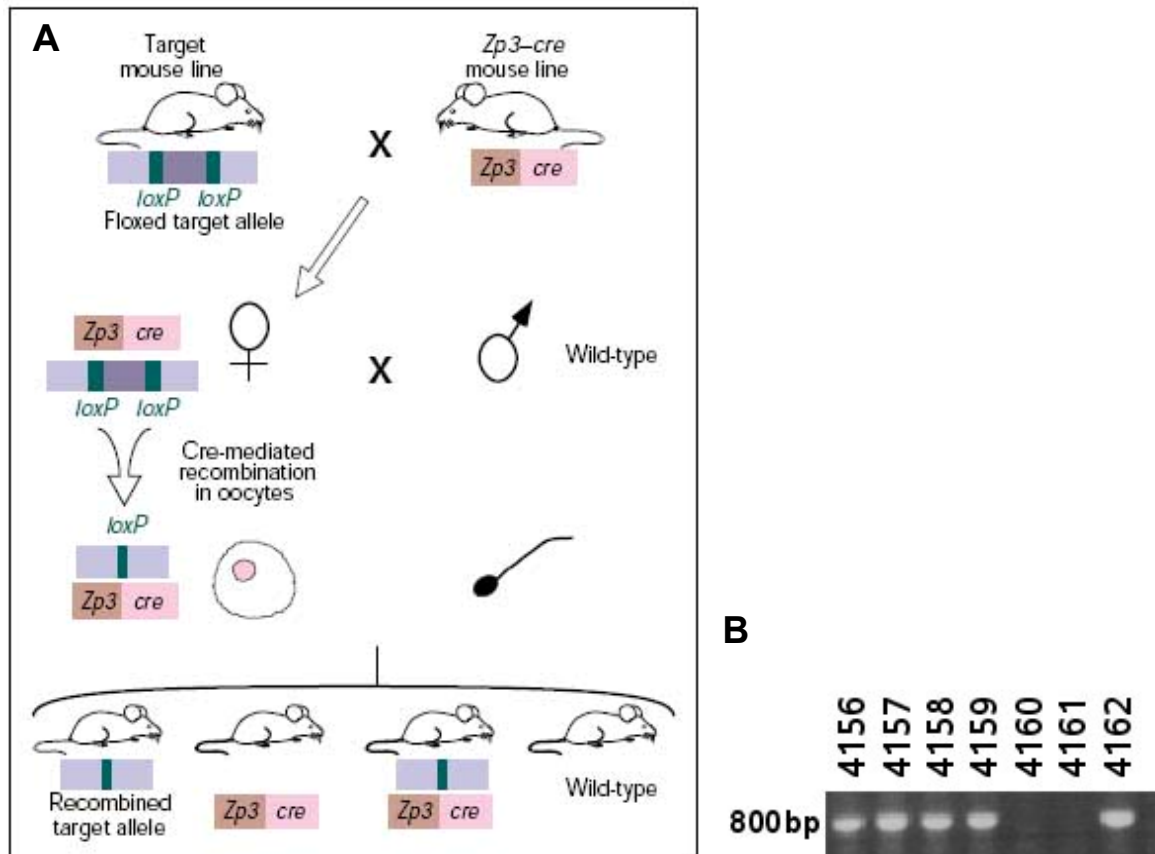


Figure 12. (A) Schematic demonstration of the strategy for removal of sequences that are flanked by LoxP sites by mating with *Zp3cre* transgenic line (after Lewandoski et al. 1997). Mice carrying the floxed target gene are first crossed to the *Zp3-cre* mouse. In female $cre^+/target^+$ progeny Cre mediates the recombination of two directly repeated target (*LoxP*) sites to a single *LoxP* site which results in the excision of the DNA sequence that is flanked by the LoxP sequences. In the next mating of such females with wild type males progeny four different genotypes can be produced. The target gene is inherited in recombined form independently of the inheritance pattern of *Zp3-cre* gene. (B) Example of the PCR strategy identifying the *Popdc2* Δ neo allele. Positions of primers (LacZ-3060 and Pop2 rev) are shown in Fig. 7 (D). Size of expected amplicon in case recombination occurred is approx. 800bp. 4156-4159, and 4162 are mice with recombined target allele i.e. *Popdc2* Δ neo. 4160 and 4161 are wild type or *Zp3-cre* mice.

In this way LoxP-flanked sequences were removed in the germ line of mice. *Popdc2* mice derived from the oocytes, which underwent Cre-mediated recombination, were identified by a PCR approach employing primers LacZ-3060 and Pop2 rev that amplified only the recombined allele (Fig. 12B).

4.2 Generation of a *Popdc2* null mutant ES cell line

4.2.1 Targeting strategy

Since the generation of a KO mouse is time-consuming, we have designed another experimental approach to learn about *Popdc2* function at the cellular level. For this

purpose we have produced a *Popdc2* null mutant ES cell line, which subsequently was used to study in in vitro differentiation experiments aiming at studying cardiac myocyte differentiation (Maltsev *et al.*, 1993). The null mutant *Popdc2* ES clone used in this experiment was generated by targeting the wild-type allele of a heterozygous *Popdc2*^{WT/-} ES clone using a construct described in Fig 7. The *Popdc2*^{WT/-} ES clone was previously isolated as described in 4.1.5. Before introducing the second targeting vector the *Popdc2*^{WT/-} ES clone was transfected with a Cre plasmid to remove the neo cassette (Fig. 13A). The targeting vector used for producing *Popdc2*^{WT/-} was similar to the targeting vector described in 4.1.5, but contained no LacZ cassette. Screening of multiple targeted ES cell clones was performed by PCR (Fig. 13B) with primers identical to those shown in Fig. 8. Two different types of ES cell clones were detected. In one of three ES cell clones recombination of the second targeting construct into the already targeted allele (Fig. 13A') occurred and thus resulted in the production of another heterozygous cell line. In the other two clones recombination occurred into the wild type allele and resulted in the generation of null mutant ES cell clones (Fig. 13 A''). A PCR approach with Start-pop2 and Pop2rev primers was utilized in order to distinguish between these two recombination events (Fig. 13C).

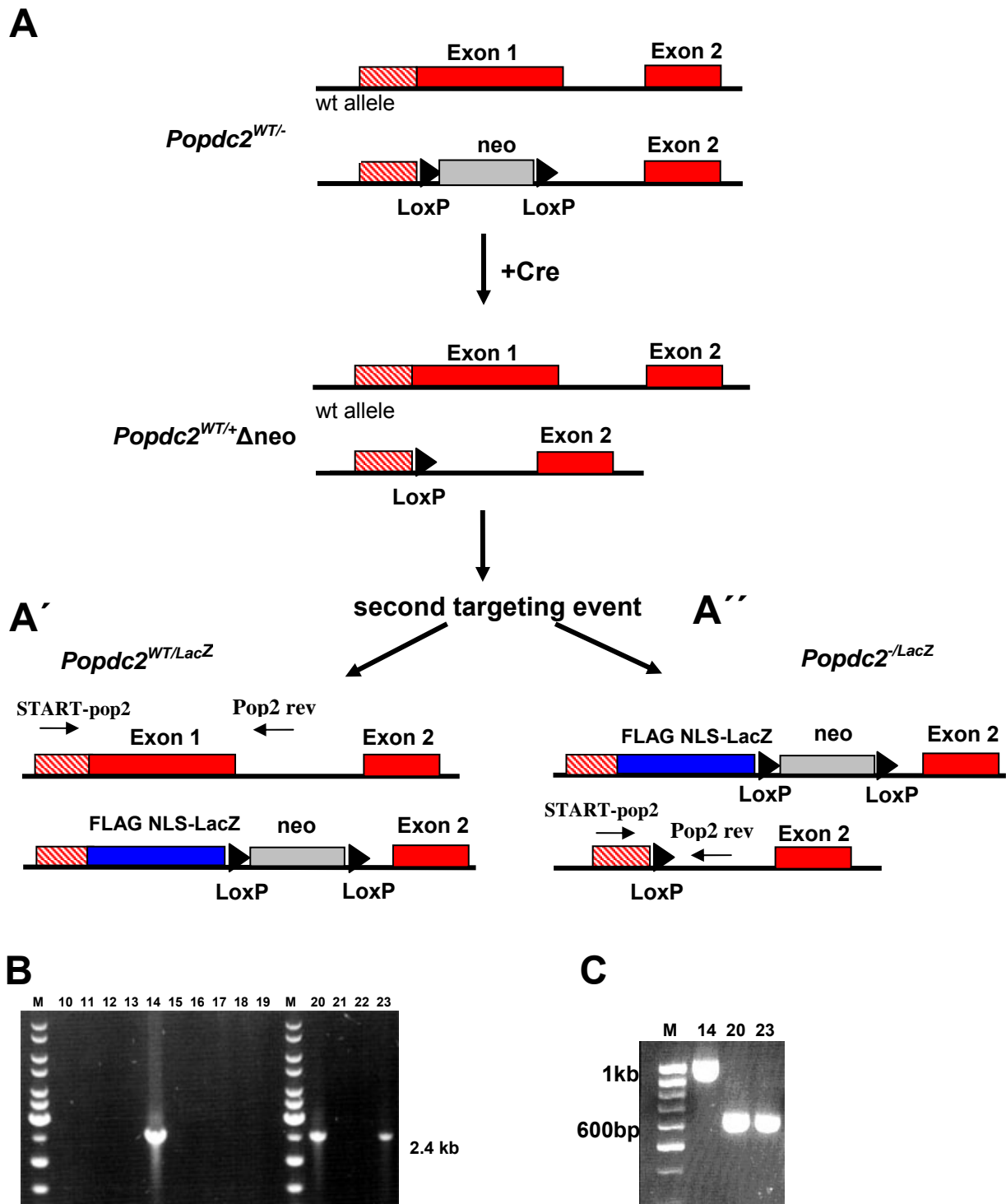


Figure 13. Schematic representation of the strategy for producing *Popdc2* KO ES cells clones. (A) Removal of the *neo* gene in *Popdc2*^{WT/-} ES clone. (A', A'') Two different clones can be produced as result of the second targeting of the *Popdc2*^{WT/+} Δneo ES cell clone with construct shown in Fig. 7 B. A dashed box indicates *Popdc2* exon 1 UTR. (B) Three ES clones positive for the first homologous recombination event were identified by PCR using primer pairs as outlined in Fig. 8. (C) PCR analysis (primers: START-pop2 and pop2 rev) of ES clones with the aim to identify clones in which homologous recombination occurred only in the WT allele (clone A') and not in the previously targeted allele (clone A''). M, marker.

4.3 Characterization of a *Popdc2* knockout mouse

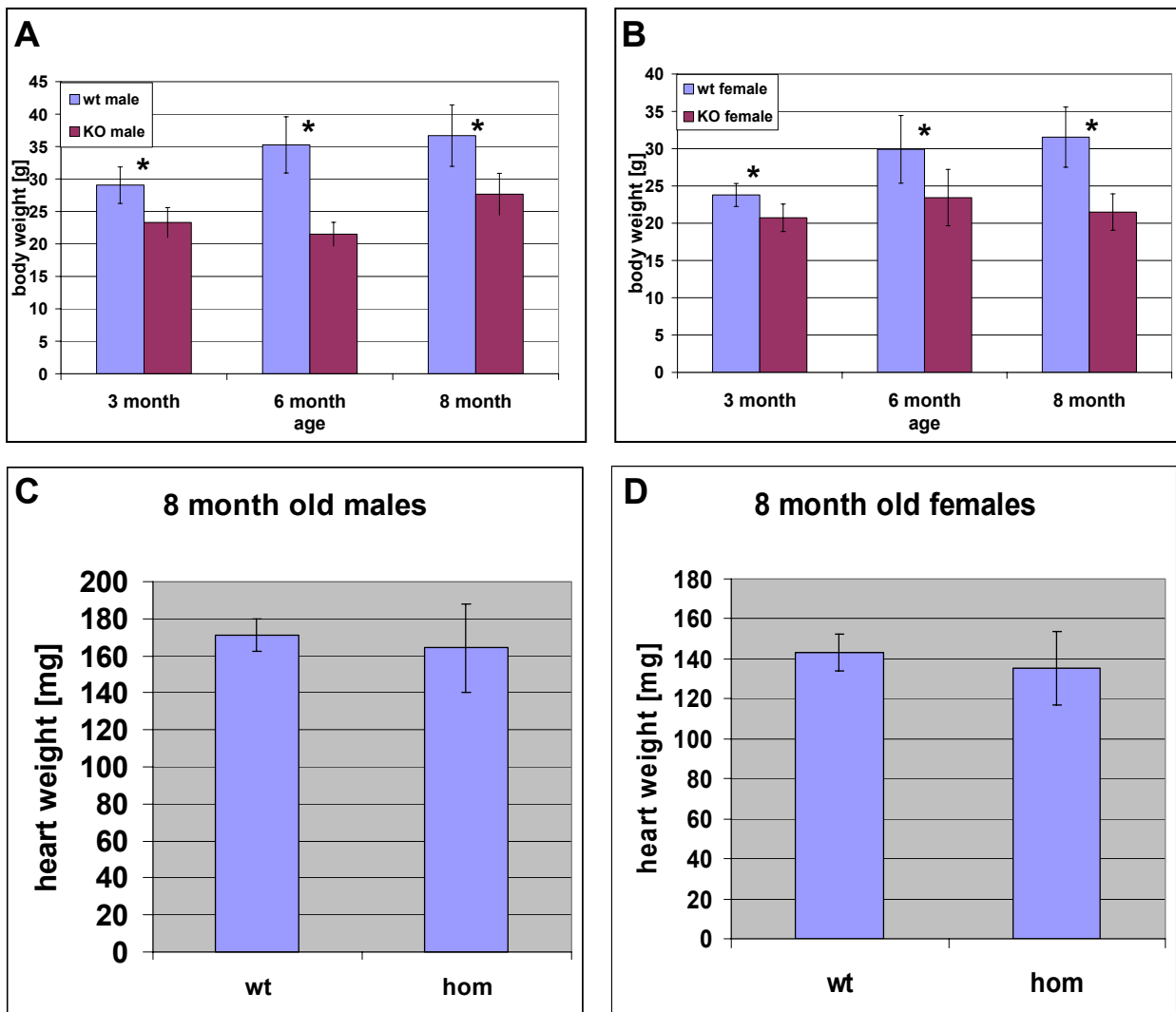
4.3.1 Effect of *Popdc2*^{LacZ/LacZ} deletion on the heart and body weight

Intercrosses of heterozygous *Popdc2*^{WT/LacZ} mice yielded *Popdc2*^{WT/WT}, *Popdc2*^{WT/LacZ}, and *Popdc2*^{LacZ/LacZ} offspring at the expected Mendelian ratio (Tab. 1).

Table1. Genotype of the offspring of heterozygous crossings

ear tag number male x femal(s)	genotype	offsprings date of birth	genotypes of the offsprings		
			wt	het	hom
9809 x 9801, 9806	het x het	6+9.10.04	1	6	3
4197 x 9805, 4200	het x het	7+6.10.04	2	1	10
9803 x 9815, 4198	het x het	7+11.10.04	5	3	3
9812 x 9825, 9829	het x het	7+11.10.04	3	11	2
138 x 159, 125	het x het	5+8.10.04	1	2	2
166 x 143, 127	het x het	6+7.10.04	10	7	4
165 x 149, 124	het x het	7.10.04	6	13	5
4157 x 4166, 4170	het x het	5+28.11.04	1	7	2
4156 x 4151	het x het	21.11.04	4	5	0
4158 x 4159	het x het	5.12.04	2	1	3
1221 x 1201, 196	het x het	6+8.10.04	1	6	0
o.m. x 153, 1203, 200	het x het	4+6.10.04	3	4	3
139 x 160	het x het	6+7.10.04	2	2	1
116 x o.m.	het x het	6.10.04	1	2	2
o.m. x 152, 168, 176	het x het	6+7.10.04	2	8	4
140 x 163,197	het x het	7+8.10.04	3	6	3
9812 x 111, 112	het x het	8+9.10.04	1	7	2
total offsprings of each genotype			48	91	49
expected ratio			47	94	47
total of all offsprings			188		

Popdc2 deficient mice were fertile and had a normal life-span. When getting disturbed the homozygous mutants displayed signs of hyperexcitation, which resulted in heavy breathing with a typical whistling sound. This phenotype was also observed in case of *Popdc1* null mutant mice, however at present we do not know the reason for this behavioural phenotype. *Popdc2*^{LacZ/LacZ} mice also had severe problems to recover after both ether and ketamin/xylazin anaesthesia. Comparison of body weight of males (Fig.14, A) and females (Fig.14, B) at three different time points (3 months, 6 months and 8 months) revealed body weight differences between wild type and KO mice. In the mean the mutants were approximately 20-25% lighter than their wild-type litter-mates.



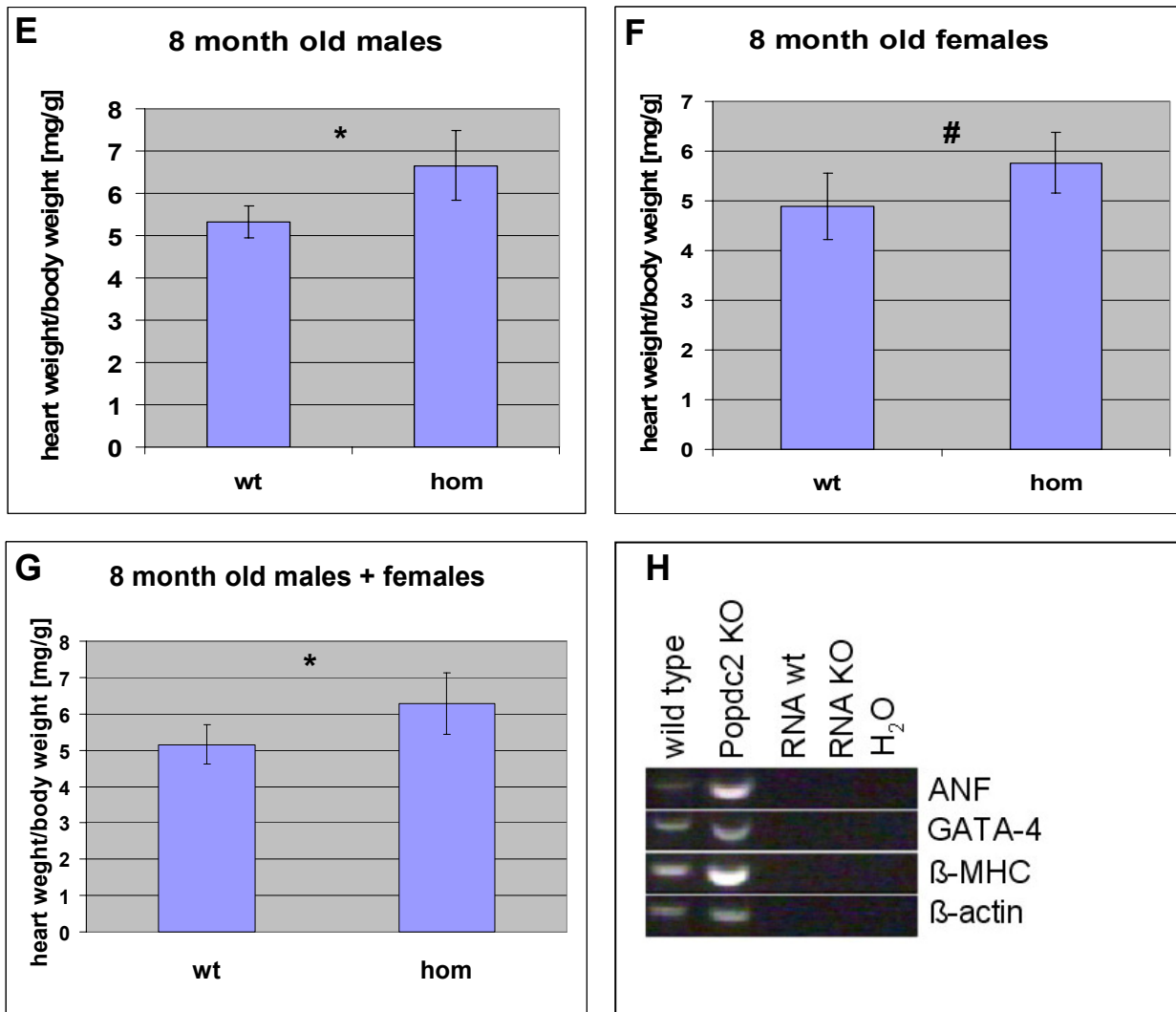


Figure 14. Body weight, heart weight and heart weight/body weight ratio for *Popdc2* mutant and wild type mice. (A, B) Statistically significant difference of body weight of wild type and *Popdc2* KO mice at different time points (* $p < 0.001$; $n \geq 10$). (C, D) Hearts of *Popdc2* KO males and females mice have similar weights as those of WT mice. (E, F) Heart weight/body weight ratios of 8 months old males (* $p < 0.001$; $n \geq 10$) and females (# $p < 0.03$; $n \geq 10$) as indicated. (G) Combined heart weight/body weight ratios of both males and females demonstrated a statistically significant difference between mutant and wild-type mice (* $p < 0.001$; $n \geq 10$). (H) RT-PCR analysis using RNA isolated from the ventricles demonstrates upregulation of markers of pathological cardiac hypertrophy (i.e. ANF, GATA-4 and β -MHC) in *Popdc2* KO in comparison to WT mice. β -actin served as a control.

Although 8 months old WT male and female mice were heavier than their *Popdc2* KO litter mates (Fig. 14 A, B), the hearts of WT females had comparable weights to those isolated from *Popdc2* mutants (Fig. 14 D). Significantly, hearts isolated from *Popdc2* mutants were heavier than those isolated from WT males (Fig. 14 C). As result, the mean ratios of heart/body weight of *Popdc2* mutants, irrespective of the sex were higher in the case of KO than in WT mice (Fig. 14 E, F.). Combined heart weight/body weight ratios (Fig. 14 G) reached a statistical significance between KO and wild type mice. These data indicate the presence of a pathological hypertrophy in

the *Popdc2* KO hearts. To further characterize the mutant hearts, cardiac hypertrophy marker genes, i.e. atrial natriuretic factor (ANF), β -myosin heavy chain (β -MHC), and GATA4 were amplified by RT-PCR. As shown in Fig. 14. H, all three markers were expressed at higher levels in the null mutant, which suggests a pathological hypertrophy in *Popdc2* mutant hearts. Real time PCR measurements of ANF and β -MHC also showed a 3-fold and 2.5 fold elevation of expression (data not shown).

In order to study this further we decided to analyze the histology of mutant and wild-type hearts. Despite evidence for the presence of a pathological hypertrophy in *Popdc2* mutant mice, no gross alterations were observed at the histological level (Fig. 15 A-F). Sections of the ventricles stained with hematoxylin-eosin (Fig. 15 A-D) or Masson's Trichrom (Fig. 15 E, F) of both WT and *Popdc2* mutant mice revealed a normal histology. Sections (Fig. 15 A, B) demonstrated normal thickness of the interventricular septum (IVS) and of free walls of the right and left chamber. Also the size of the right and left ventricular lumen appeared normal. Detailed analysis of the myocardial histology (Fig. 15 C and D) revealed the presence of mononuclear cardiac myocytes of apparently normal size and shape with well visible intercalated discs in both WT and mutant tissue. To exclude pathological processes which resulted in fibrotic tissue, we examined Masson's Trichrome stained ventricular sections of both WT and homozygous mutant hearts (Fig.15 E, F). No evidence for the presence of cardiac fibrosis was obtained. Likewise functional analysis using echocardiography did not reveal a major functional deficiency in case of the *Popdc2* mutant heart (L. Fabritz et al., pers. communication).

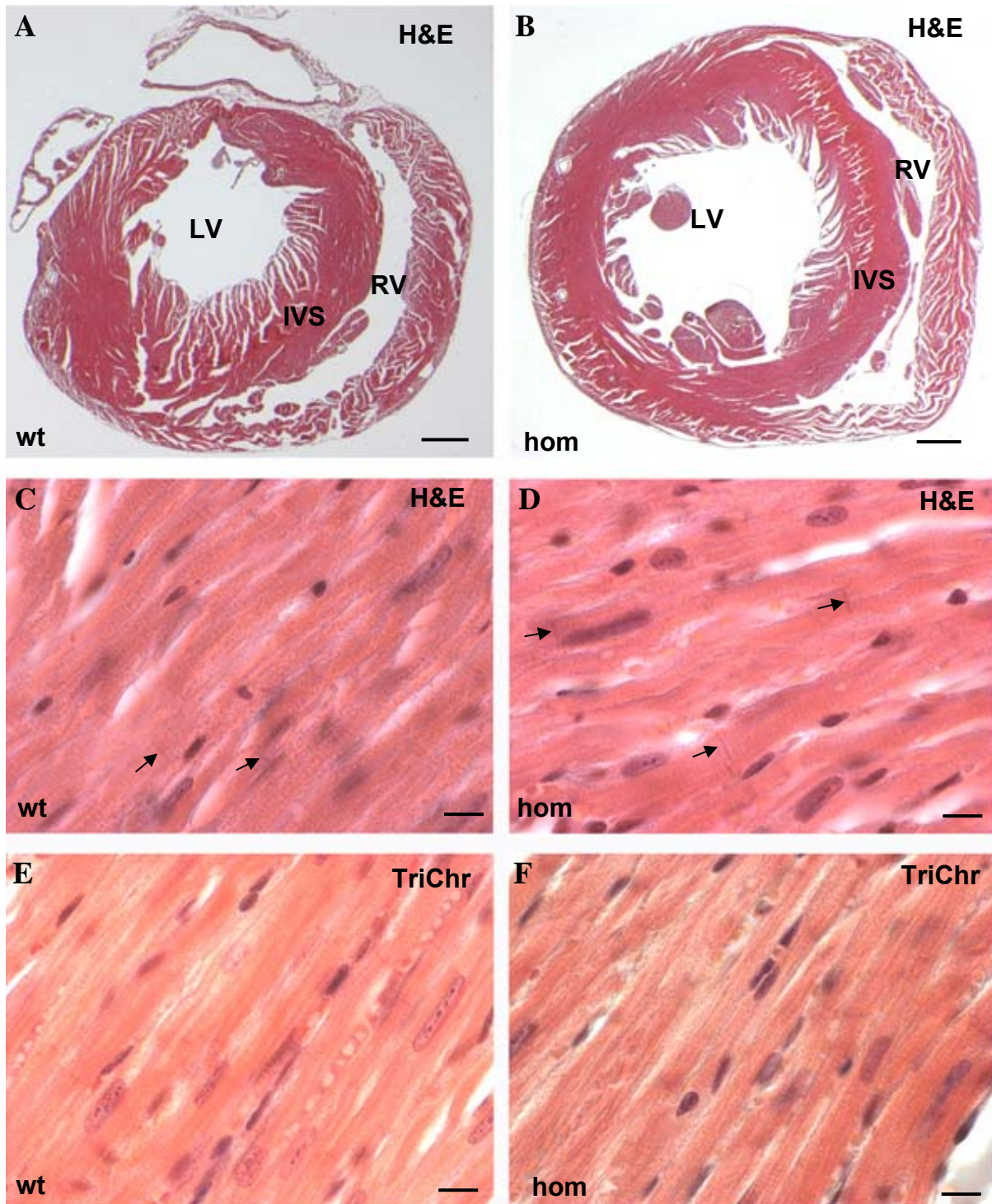


Figure 15. Histological analysis of 8 months old WT and *Popdc2* mutant (hom) mice. (A, B) Transversal sections through the ventricles of both WT and hom mice hearts stained with haematoxylin-eosin. (C, D) Enlarged view of longitudinally sectioned myocytes (arrows point to intercalated discs). (E, F) Enlarged view of the longitudinally sectioned ventricular tissue of WT and homozygous mice, which was stained with Masson's Trichrom. IVS, interventricular septum; LV, left ventricle; RV, right ventricle. Scale bars: A and B, 500 μ m; C, D, E and F, 10 μ m.

4.3.2 *Popdc2-LacZ* expression analysis in early embryo

To learn about developmental and postnatal expression of *Popdc2-LacZ* in the heart and different organs and tissues, embryos of different stages as well as postnatal and adult tissues and organs were whole mount or section stained utilizing various methods.

Popdc2-LacZ expression was first detected in heterozygous *Popdc2*^{WT/LacZ} embryos at E6.0 when differentiation of the egg cylinder commences (Fig. 16, A). The LacZ labelled cells belonging to the visceral layer of extra-embryonic mesoderm. At E7.0 (early to mid-primitive streak stage), LacZ staining was seen in the allantois, embryonic mesoderm and in the node (Fig. 16, A). At E7.5 (3-5 pairs of somites), *Popdc2-LacZ* activity was seen in the cardiac crescent (Fig. 16, B), which is consistent with the endogenous *Popdc2* expression at this stage as previously reported (Andree et al., 2000). In a more advanced embryo at E7.5 staining was also observed in amnion cells which spread out into the direction of the ectoplacental cone (Fig. 16, B-C). At E8.5 (8-10 pairs of somites) LacZ activity was seen in the tubular heart, the pericardial sac and in the amnion (Fig. 16, D). At E9.5 (21-29 pairs of somites), β -gal activity was detected in some cells within the branchial arches, heart, lateral plate mesoderm and somites (Fig. 16, E). At E10.5 (35-40 pairs of somites), LacZ staining in the *Popdc2*^{WT/LacZ} embryos becomes more prominent in the branchial arches (Fig. 16, F). At E10.5 the expression pattern of the *Popdc2*^{WT/LacZ} embryos was very similar to that of the *Popdc1-LacZ* embryos (Andree et al., 2002). The only difference was that *Popdc1-LacZ* embryos had no staining in the lateral plate mesoderm, but was present in a posterior domain within the limb. At E12.5, 48-52 pairs of somites, LacZ staining was found in the heart, somites and gut (Fig. 16, G and H).

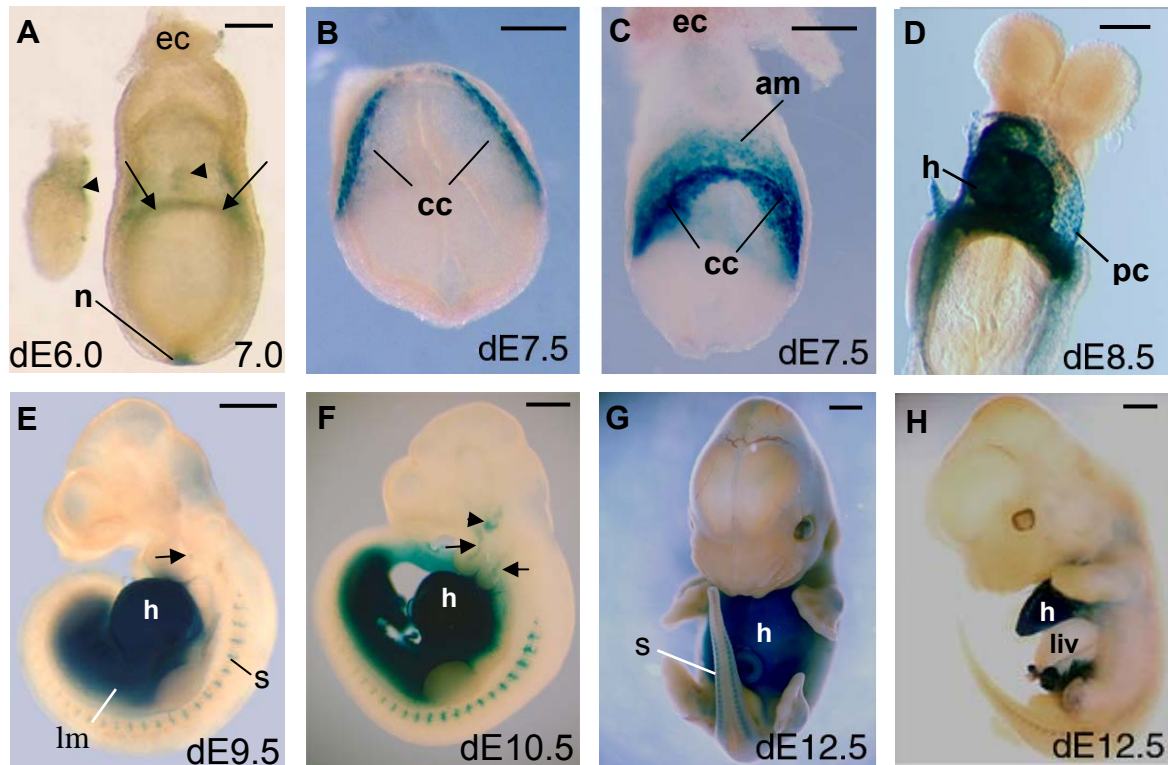


Figure 16. Expression of LacZ in *Popdc2*^{WT/LacZ} embryos at different developmental stages as indicated on the lower right of each panel. (A-H) Whole-mount LacZ staining. Embryos are viewed from the ventral side (A-D, G) or the left side (E, F, H). (A) At E6.0 LacZ staining was observed in the visceral layer of extra-embryonic mesoderm (arrowhead). At E7.0 LacZ activity was detectable in the node, allantois (arrowhead) and embryonic mesoderm (arrows). (B) At E7.5 LacZ expression was seen in the cardiac crescent (cc). (C) In a more developmental advanced embryo (E7.5) LacZ expression in the cardiac crescent becomes wider and stronger, and amniotic LacZ-stained cells appear to migrate in the direction of the ectoplacental cone (ec). (D) At E8.5 LacZ is strongly expressed in the tubular heart, pericardial sac and in the amnion. (E, F) At E9.5 and 10.5 LacZ staining is seen in the heart, lateral plate mesoderm (lm), and in somites. LacZ expression is also observed in some cells within the branchial arches at E9.5, which become more prominent at E10.5 (E, F arrows) and in facial skeletal muscle precursors at E10.5 (arrowhead). At E12.5 strong LacZ expression is present in the heart and somites and in the limb, (G, front view and H, lateral view of the embryo with the abdominal area skinned). ec, ectoplacental cone; h, heart; liv, liver; lm, lateral plate mesoderm; n, node; nf, neural fold; pc, pericardium; s, somites; sv, sinus venosus. Scale bars: A, B, C and D, 200 μ m; E and F, 500 μ m, G and H, 1mm.

4.3.3 In the gastrulating mouse embryo LacZ is expressed in the heart fields and in the somato- and splanchnopleura

E7.5-8 *Popdc2*^{WT/LacZ} whole-mount LacZ stained embryos revealed strong LacZ expression in the two heart fields and in the allantois (Fig.17, A and B). Sections through the heart regions of these embryos demonstrated significant *Popdc2-LacZ* transgene activity in the cardiogenic plate. Two derivatives of lateral plate mesoderm, somatopleura (formed by somatic mesoderm together with the ectoderm) and

splanchnopleura (formed by splanchnic mesoderm together with endoderm) were also labeled (Fig. 17, C-E).

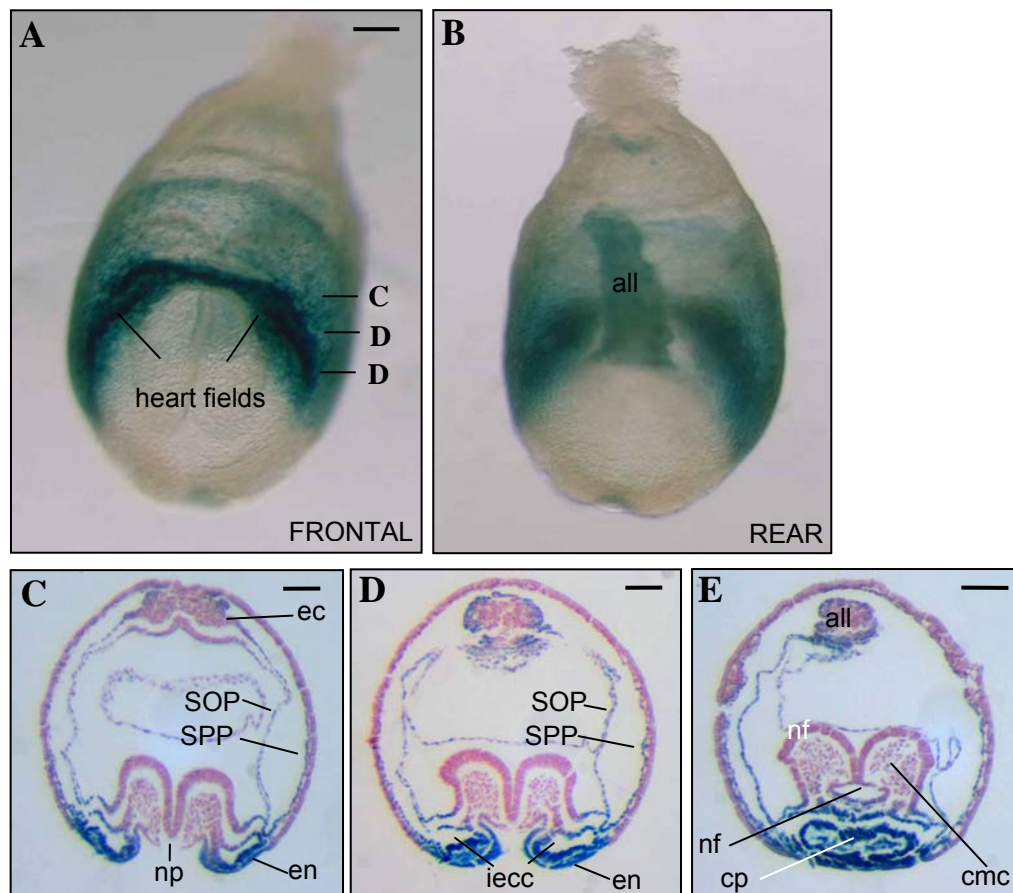


Figure 17. Expression of LacZ in *Popdc2*^{WT/LacZ} embryos at E7.5-8. (A, B) Whole-mount LacZ staining of embryos with intact chorion. (A) Expression is seen in the cardiac crescent and in the amnion. (B) Rear view demonstrates strong expression in the allantois (all). (C-E) Transverse sections of whole-mount LacZ stained embryo at the level of the heart fields as indicated in A. LacZ expression is observed in the cardiac plate (cp), and in both somatopleura (SOP) and splanchnopleura (SPP). (C-E) Sections are counterstained with Nuclear Fast Red. all, allantois; cmc, cephalic mesenchyme cells; ec, ectoderm cells; en, endoderm cells; fg, foregut; iecc, intra-embryonic coelomic channel; nf, neural fold; np, notochordal plate; SOP, somatopleura; SPP, splanchnopleura. Scale bars: A, C, D and E, 100 μ m.

4.3.4 Two distinct cell populations were labeled by LacZ during EB differentiation

Pluripotent embryonic stem (ES) cell lines have been established from the preimplantation mammalian embryo (Wobus et al., 1984). Under appropriate culture conditions ES cells have an unlimited ability to self-renew. When returned into developing blastocysts these cells have the potential to contribute to all three primary germ layers, including cardiac myocytes. Also in vitro, ES cells have been shown to

differentiate into a variety of cell types (Evans and Kaufman, 1981; Wobus et al., 1984). Protocols for the in vitro differentiation of ES cells into cardiac myocytes with atrial-, ventricular-, sinus node- and Purkinje-like cell identities have been established (Wobus et al., 1984). In most cases experimental protocols for differentiation of ES cells start with cell aggregation using hanging drops. This leads to the formation of structures termed embryoid bodies (EBs). For efficient cardiac myocyte differentiation in EBs the following parameters are important: (1) number of cells in hanging drops, (2) media, serum, additives, (3) ES cell line, and (4) the time of EB plating (Wobus et al., 2002). Cardiomyocytes are distinguishable within 1 to 4 days after plating since they spontaneously contract. Within the developing EB, cardiomyocytes are usually found between an epithelial layer and a basal layer of mesenchymal cells (Hescheler et al., 1997). The number of beating cells increases with time, which at the same time has a decreased beating rate (Boheler et al., 2002).

Two ES cell clones, a heterozygous *Popdc2*^{WT/LacZ} clone (Fig.7) and a homozygous *Popdc*^{-LacZ} (Fig. 13 A") were used in this experiment. Cells were cultivated and differentiated into beating cardiomyocytes as previously described (Maltsev et al., 1993). The principle of differentiation is schematically depicted in Fig. 18A. The first beating cell clusters in EBs were observed at day 7 (or 5+2d, 2 days in hanging drops and 2 days of suspension culture). With further differentiation at day 8 and 9 (or 2+5+1d and 2+5+2d, 5 days in hanging drops, 2 days in suspension and then 1 or 2 days after plating) these clusters increased in size and displayed strong LacZ staining. The second cell population which showed LacZ staining at day '8' and '9' consisted of small, round shaped cells, which we think represent mesothelial-like cells. These cells were never contractile and were weakly stained with LacZ, not organized into clusters and rapidly migrated out of the EB after plating (Fig.18 B).

No differences were observed between *Popdc2*^{LacZ/WT} and *Popdc2*^{LacZ/-} ES clones in their ability to attach to the substrate, their differentiation potential, or the time of acquiring contractility. Presumably the staining pattern that we observed in differentiating embryoid bodies reflects the expression pattern of embryos at E7.5. One population of cells with high LacZ activity are cardiac myocytes and the second population of the cells, which were weakly LacZ stained are mesothelial cells constituting the coelomic epithelium of both somato- and splachnopleura and these are probably the fast migrating cells in the periphery of plated EBs. To identify this cell

population as mesothelial cells will require the counterstaining with a specific marker protein. Staining with an mesothelin antibody however gave no clear result to unequivocally identify these cells as mesothelial cells.

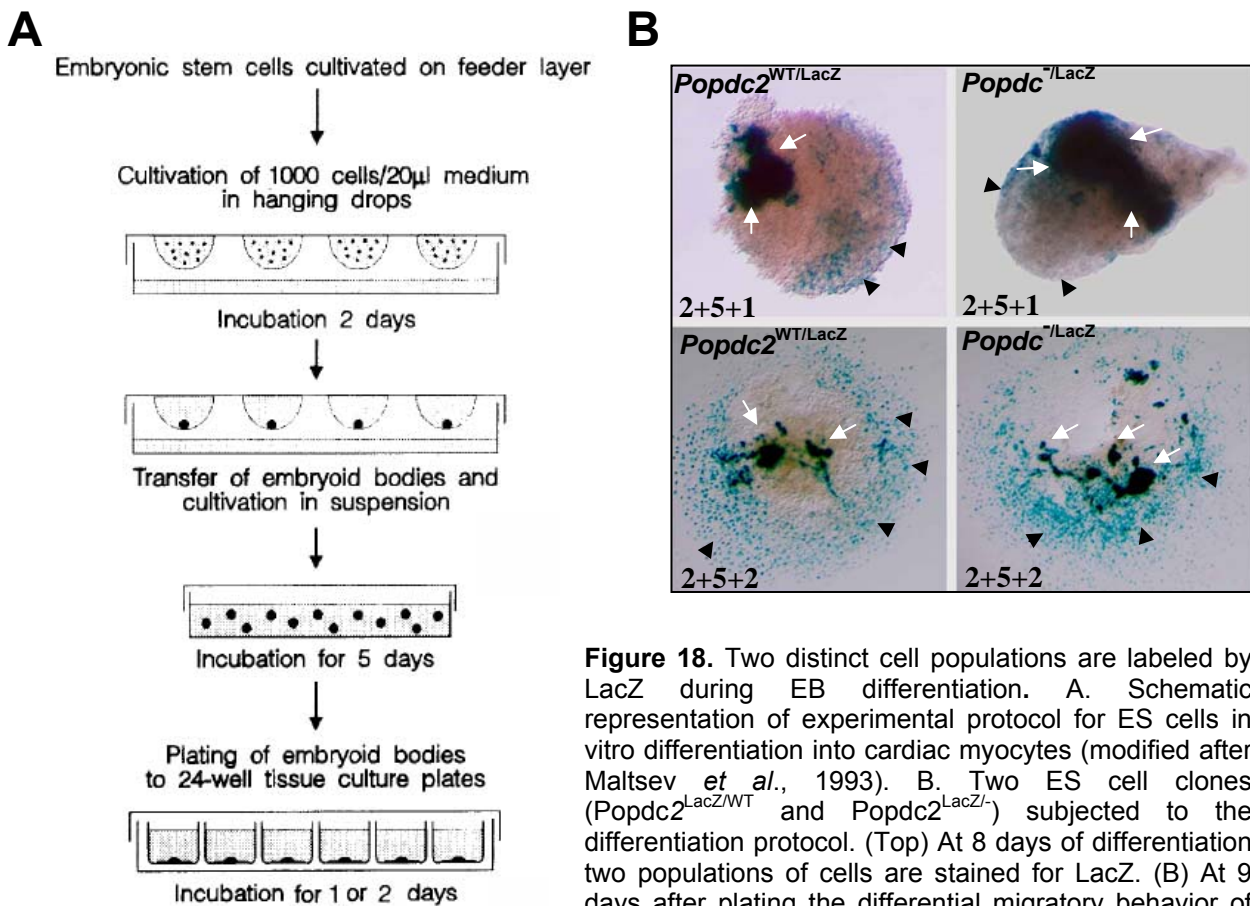


Figure 18. Two distinct cell populations are labeled by LacZ during EB differentiation. A. Schematic representation of experimental protocol for ES cells in vitro differentiation into cardiac myocytes (modified after Maltsev *et al.*, 1993). B. Two ES cell clones ($Popdc2^{LacZ/WT}$ and $Popdc2^{LacZ/-}$) subjected to the differentiation protocol. (Top) At 8 days of differentiation two populations of cells are stained for LacZ. (Bottom) At 9 days after plating the differential migratory behavior of the two different cell populations becomes apparent. arrow, strongly LacZ-stained cells; arrowheads, LacZ-stained round shaped methothelial-like cells. The number in the lower left of each panel indicates the incubation time in days under different conditions as shown in A.

4.3.5 Myocardial expression pattern of *Popdc2-LacZ* and *Popdc2* in selected developmental stages

In order to analyze developmental expression of the *Popdc2-LacZ* transgene in heterozygous embryonic hearts, embryos of different stages were either whole mount LacZ stained and then sectioned (E8.5) or first cryosectioned and then LacZ stained (E9.5 and older). At E8.5 expression of the *Popdc2-LacZ* was strongly evident in the myocardial tissue (Fig. 19 A) and to a lesser extent in the endocardium and amnion. The endocardium was also LacZ positive at E9.5 and E10.5 (Fig. 19 B, C), which is

in contrast to the expression pattern of *Popdc1-LacZ* staining at the same age (Andree et al., 2002). The expression in the endocardium was surprising since it is not reflected by the expression of the endogenous *Popdc2* gene and is most likely due to an early activation of the gene in the entire cardiogenic mesoderm. Since the endocardium is a derivative of the primary heart field it initially shares expression with the myocardium. Since LacZ most likely has a longer half-life than the *Popdc2* mRNA, its detection in the endocardium is probably due to the maintenance of LacZ activity and does not reflect endogenous gene expression in the endocardium. (Andree et al., 2000). This interpretation is also corroborated by the fact that endocardial expression is not maintained. At E9.5, E10.5, and E12.5 but not at E14.5 *Popdc2-LacZ* was expressed in pericardium (Fig. 19 B, C and D). The proepicardium also showed transient expression at E10.5, however at E12.5 *Popdc2-LacZ* activity was clearly absent from the epicardium. Since the *Popdc2* promoter also drives expression in the proepicardium, we believe that this transient expression is probably due to endogenous expression in the proepicardium. This is in contrast to data obtained in the chick embryo. Here proepicardial explants have been analyzed for *Popdc* gene expression. We could not detect *Popdc1*, *Popdc2*, or *Popdc3* expression in the proepicardium (Torlopp et al. 2006). However it has to be stated clearly that expression is not maintained in the epicardium or in epicardium derive cells. At E9.5, E10.5 and E14.5 (Fig. 19 B, C and D) *Popdc2-LacZ* expression was present in atrial myocardium and in the ventricles it was present in both, trabecular and compact layer. This is in contrast to the expression pattern that was recently reported for *Popdc1-LacZ*, which at E11.5 was found to be down regulated in the trabecular layer (Andree et al., 2002). Moreover the endogenous expression of *Popdc2* at E11.5 and older embryos was previously reported to show a distinction between compact and trabecular layer, being high in the compact layer and low in the trabecular layer (Andree et al., 2000). However, section in situ hybridization experiments performed in the E14.5 and E17.5 WT embryos (Fig. 19 D', E') corroborated the results of the LacZ staining, i.e. revealing strong staining in both compact and trabecular layer. This discrepancy between these two studies can be explained by the danger of producing staining artefacts if whole mount staining is performed with older embryos i.e. older than E10.5. The penetration of probes in dense tissues such as the heart will give structures in the inside of hollow structures a disadvantage in acquiring the same staining intensity, which results in differential staining, which however is

unrelated to the endogenous expression pattern. Therefore in older embryos section hybridization is the preferred method to prevent technical artefacts. Cardiac troponin I (cTnI) is a specific marker for cardiac myocytes. Section in situ hybridization using this marker in E14.5 and E17.5 old WT specimens (Fig. 19 D'', E'') demonstrated almost identical expression pattern of TnI and *Popdc2* (Fig. 19 D, E and D', E'). Cells lining the pulmonary veins (Fig. 19 E') are cardiac myocytes that were found to express strongly *Popdc2* and cTnI (Fig. 19 E'').

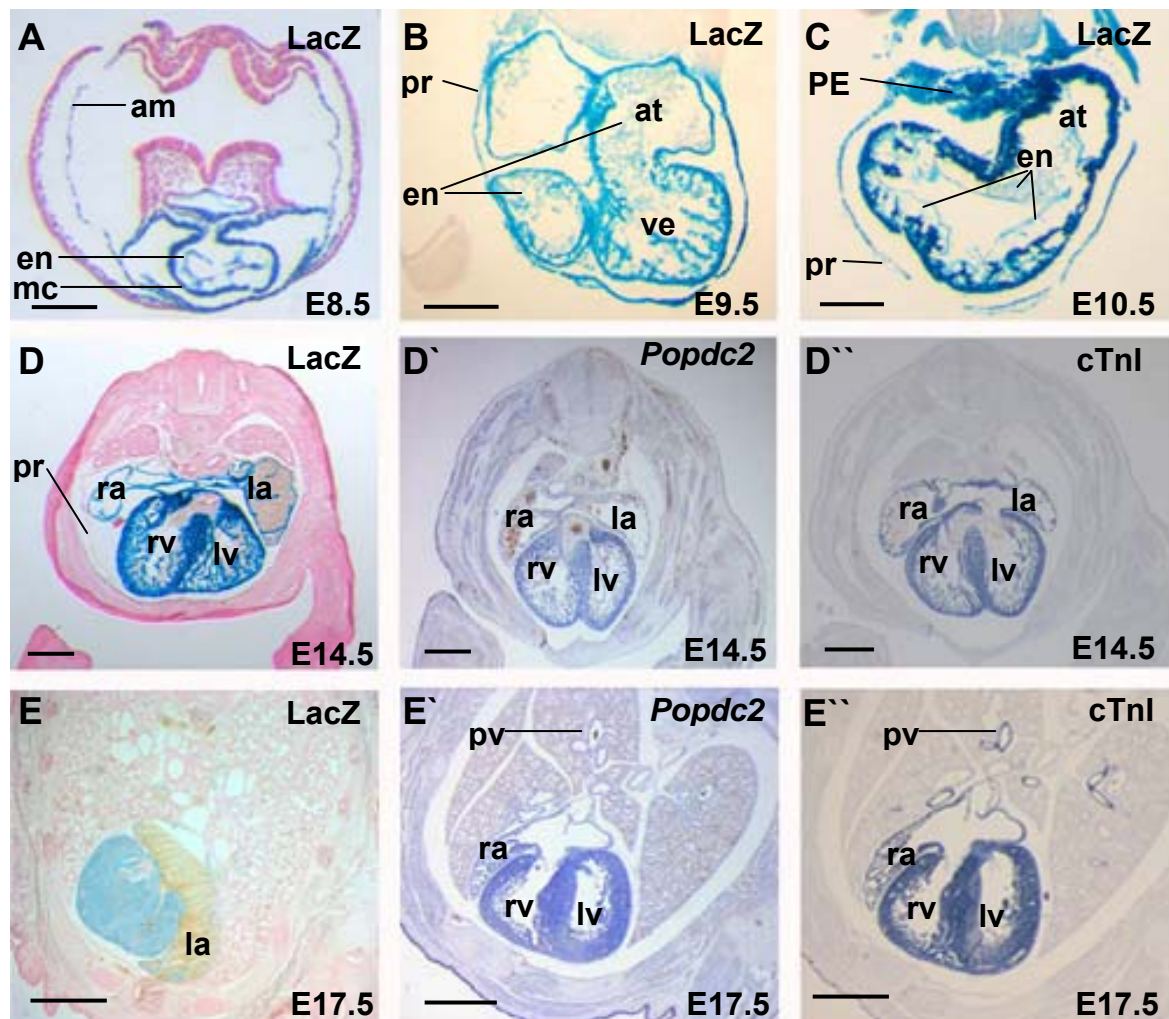


Figure 19. Myocardial expression of the *Popdc2-LacZ* and *Popdc2* at different stages as indicated in each panel on the lower right. (A) Section through the heart region of a whole mount LacZ stained E8.5 *Popdc2*^{WT/LacZ} embryo, which was counter-stained with Nuclear Fast Red. *Popdc2-LacZ* is strongly expressed in the myocardial cells forming the outer wall of primitive heart tube (mc). LacZ staining is also seen in the endocardial cells (endocardium, en) lining the inside of the heart tube and in the amnion (am). (B-D and E) LacZ and Nuclear Fast Red stained sections through the heart region of *Popdc2*^{WT/LacZ} embryos at E9.5 (B), E10.5 (C), E14.5 (D) and E17.5 (E), respectively. Expression of *Popdc2-LacZ* is present in the atria (at) and in the trabecular and compact layer of both ventricles. At E9.5 and E10.5 somewhat weaker staining is detected in the endocardium (en) and at E10.5 in the propepicardium (PE). At E9.5 and E10.5 but not at E14.5 LacZ staining is observed in the pericardium (pr). At E17.5 *Popdc2-LacZ* is detected in both, ventricles (rv, lv) and in the atria (ra, la), (E). (D', D'', E' and E'') Section in situ hybridizations of WT E14.5 and E17.5 embryos respectively. Expression pattern of the endogenous *Popdc2* gene (D') is very similar to that of the myocardial specific marker

cardiac troponin I (cTnI) (D'') and *Popdc2-LacZ* (D). In D', D'', E' and E'' stainings were performed together with Gert Van Den Berg, AMC, Amsterdam. pv, pulmonary vein extension. Scale bars: A, B and C, 200 μ m; D, D' and D'', 500 μ m; E, E' and E'', 1mm.

4.3.6 Myocardial expression of *Popdc2-LacZ* at E12.5

LacZ staining of sections through the heart of a E12.5 *Popdc2*^{WT/LacZ} embryo revealed homogeneous expression of *Popdc2-LacZ* in cardiac myocytes. Expression was present in both atria and ventricles. Strong expression was also observed in the pericardium whereas epicardial tissue was devoid of expression (Fig. 20, A, C and D). Two major cardiac cushions are present in the atrioventricular canal (AVC) and two minor in the outflow tract (OFT) of the mouse heart at E12.5. The cushions are filled with mesenchymal cells. Through a process called myocardialization that involves recruitment of mesenchymal cells to the myocardial cell lineage, the cushions are populated by cardiac myocytes (Kruithof et al., 2003). In *Popdc2*^{WT/LacZ} transgenic mouse presumptive cardiac myocytes within AVC and OFT displayed strong LacZ staining, whereas the mesenchymal tissue in the cushions was unlabeled (Fig. 20 A-C).

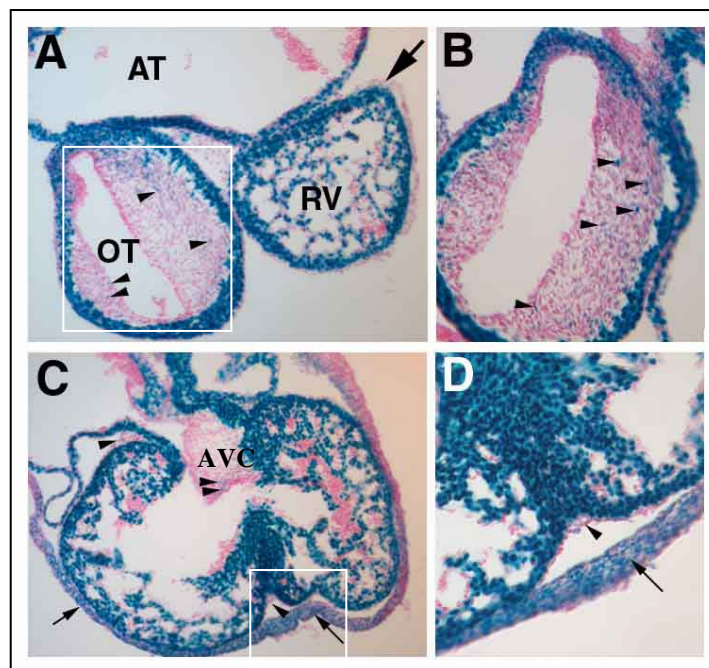
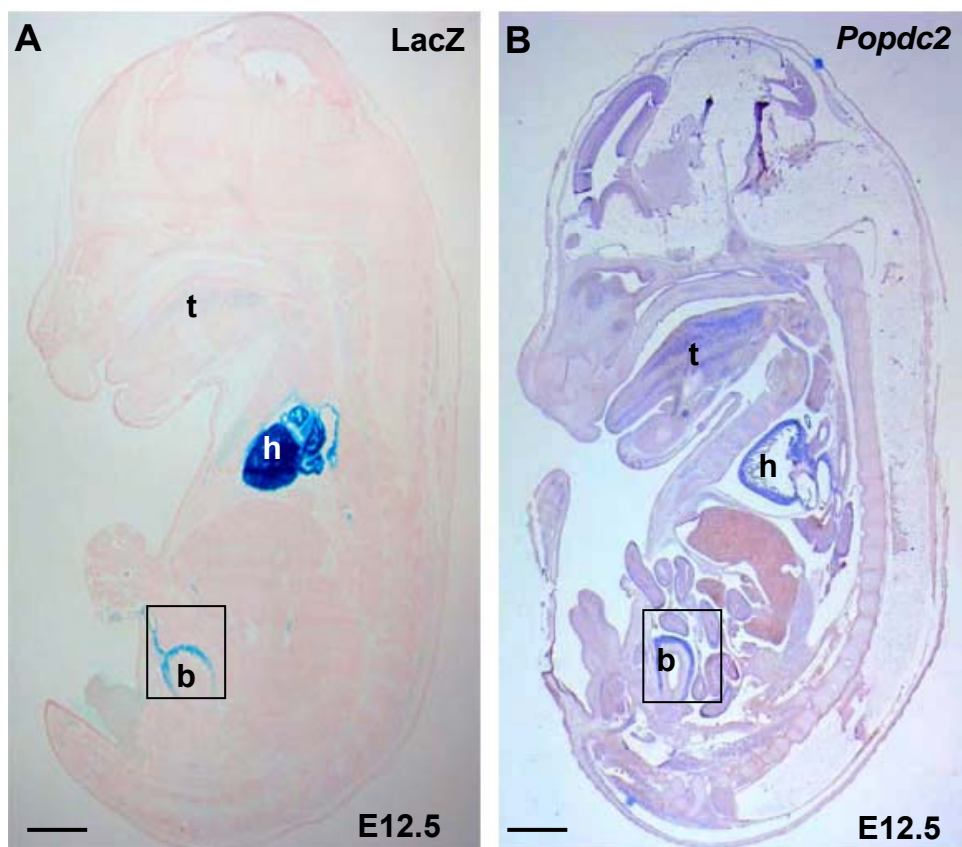


Figure 20. Expression of *Popdc2-LacZ* in the heart of a E12.5 embryo. (A-D) Transverse sections through the heart of a *Popdc2*^{WT/LacZ} embryo stained with LacZ and subsequently counter-stained by Nuclear Fast Red. (A) Section through the common atrium (AT) and outflow tract (OT). The arrow demarcates the epicardial cell layer, which is not labelled by *Popdc2-LacZ*. (B) Enlargement of the outflow tract area demarcated in (A) by a white box. Arrowheads in (A) and (B) point to cardiac myocytes within the outflow tract cushions. (C) Section through both right and left ventricle showing strong LacZ expression in cardiac myocytes but not in the endocardium (arrowheads) or epicardium (arrow), whereas the pericardium shows expression. (D) Enlargement of the area demarcated in (C) by a white box.

4.3.7 Expression of *popdc2* and *Popdc2-LacZ* in different organs at E12.5 and *popdc2-LacZ* at E17.5

In order to examine the developmental expression pattern of *Popdc2-LacZ* in further detail, I have stained sagittal frozen sections of *Popdc2*^{WT/LacZ} E12.5 mouse embryos for LacZ activity (Fig. 21 A). To determine whether *Popdc2-LacZ* expression is consistent with the endogenous expression pattern of *Popdc2* I have in parallel performed section in situ hybridization (Fig. 21 B). In both experiments similar expression domains were observed. Expression was seen in the tongue, heart, gut and bladder (Fig. 21 A-G). Within the tongue expression is seen in the skeletal muscle (Fig. 21 C and D). In intestine and bladder expression of both *Popdc2-LacZ* and *Popdc2* is restricted to the smooth muscle layer (Fig. 21 G and H).



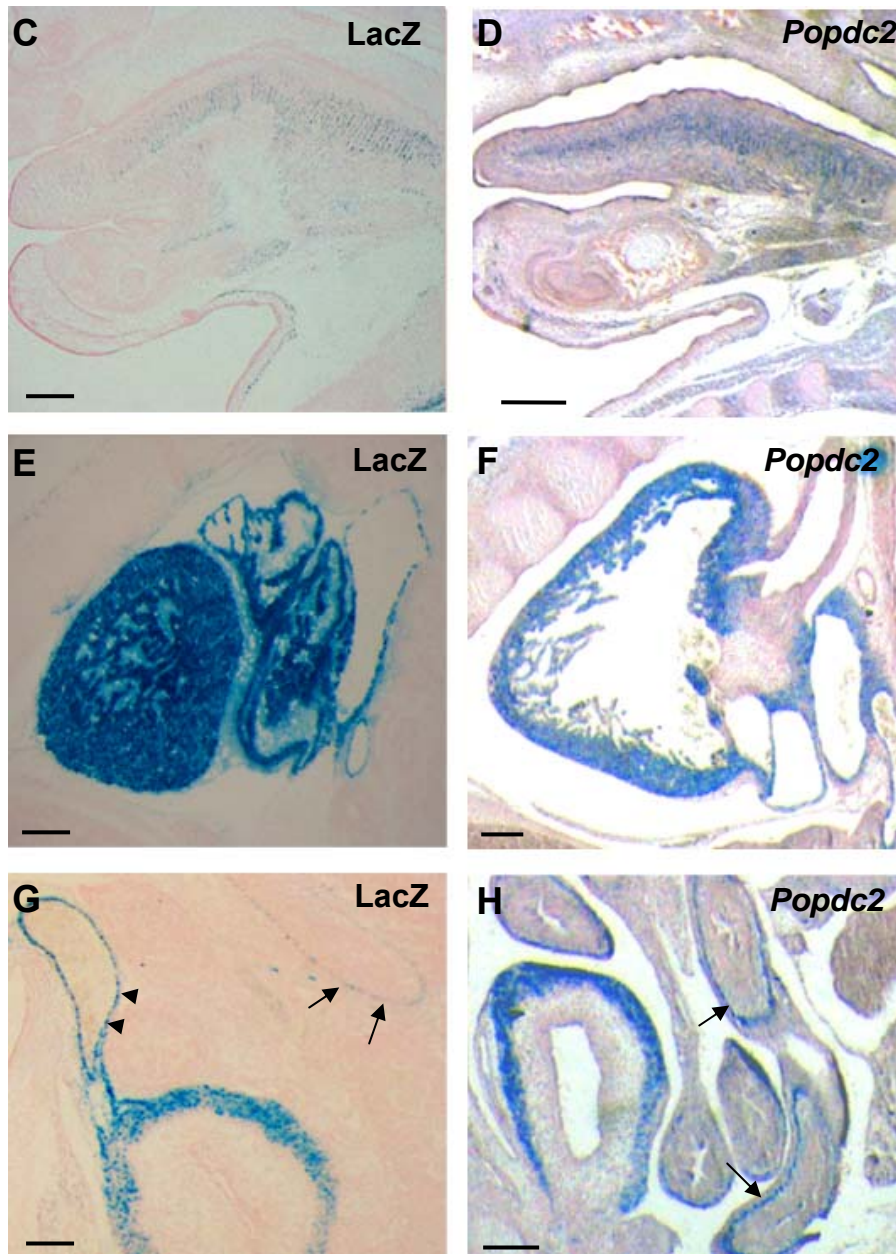


Figure 21. The endogenous *Popdc2* gene and the transgenic *Popdc2-LacZ* allele had a similar expression pattern at E12.5. (A) Sagittal section of a E12.5 *Popdc2*^{WT/LacZ} embryo stained for LacZ. (B) Section in situ hybridization of E12.5 WT embryo. Sections were counterstained with Nuclear Fast Red. In both cases expression was found in the heart, tongue (t), gut (g), and bladder (b). (C,E,G) and (D,F,H) are enlargements of the expression domains of tongue, heart and bladder areas shown in A and B, respectively. Arrows in G and H point on intestine smooth muscle layer and arrowheads in G point on the umbilicus vein. Scale bar: A and B, 1mm; C and D, 500µm; E, F, G and H, 200µm.

The LacZ expression in the *Popdc2*^{WT/LacZ} E17.5 mouse embryo (Fig. 22 A) has a very similar pattern to that of a E12.5 mouse embryo (Fig.21). Thus, LacZ staining was detected in the tongue, heart and bladder (Fig. 22 B, C and D). Within the tongue expression was confined to skeletal muscle (Fig. 22 B). In intestine and bladder expression of both, transgenic and endogenous *Popdc2* was restricted to the smooth muscle layer (Fig. 22 C and D). LacZ staining, which was detected in the intestinal epithelium (Fig. 22 D) represents non-specific activity since it was also seen

in non-transgenic wild type tissue (data not shown) reflecting the high level of endogenous β -gal activity in intestine.

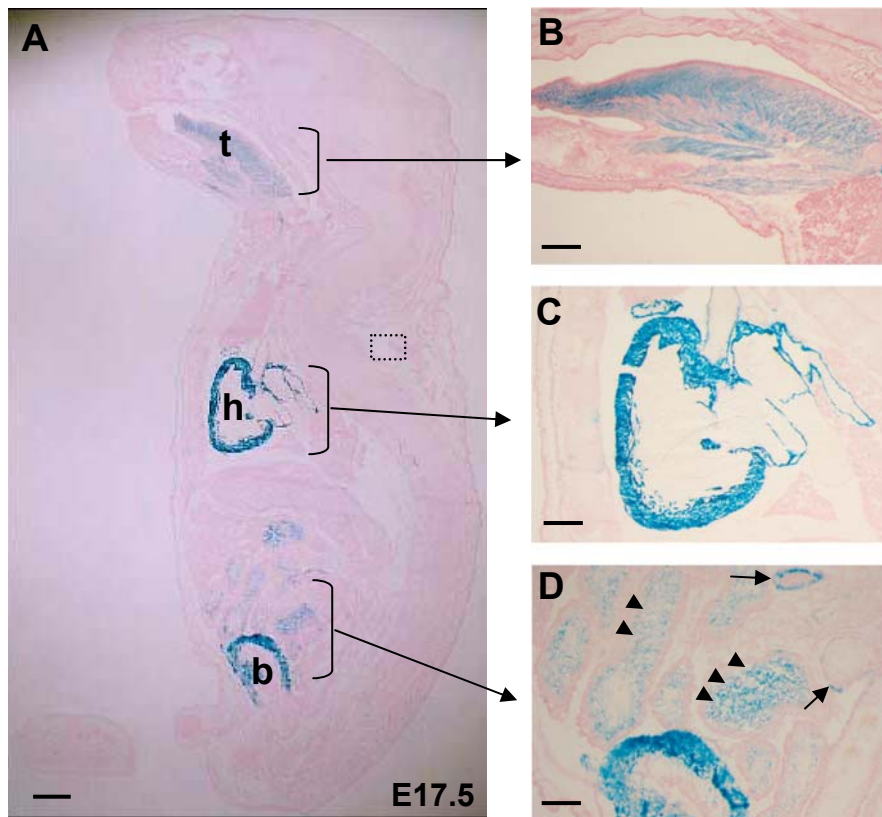


Figure 22. Expression of LacZ in *Popdc2*^{WT/LacZ} embryos at E17.5. (A) Sagittal cryosection stained for LacZ and counterstained with Nuclear Fast Red. View of whole section. (B, C and D) Enlarged views of selected regions in (A) as indicated. t, tongue; h, heart; b, bladder. (D) Arrowheads point to nonspecific LacZ staining in the intestine. Arrows point to LacZ stained intestinal smooth muscle. Scale bars: A, 1mm; B, C and D 500µm.

4.3.8 Expression of *Popdc2-LacZ* in skeletal muscle and absence of expression in the brain

It was previously reported, that *Popdc1-LacZ* mouse shows LacZ expression in the brain (Anne Fleige, Diplomarbeit). Since the phenotype of *Popdc2* KO mouse is similar in many respects to the phenotype of the *Popdc1* KO mice (see below), it was expected that *Popdc2-LacZ* activity would also be found in the brain as well. However, sections through the head of a E17.5 *Popdc2*^{WT/LacZ} mouse revealed absence of LacZ staining in neuronal tissue. Strong LacZ expression was found in skeletal muscle tissue of the head (Fig. 23 A, B) and in the tooth anlage (data not shown). β -gal activity was detected in all skeletal muscles examined including diaphragm (data not shown) and limbs (Fig. 23 C). LacZ staining in skeletal muscle

cells was localized to the nucleus like in other tissues (Fig. 23 D). Interesting, not all nuclei were LacZ positive. To give a general impression of the expression pattern within skeletal muscle tissue in the *Popdc2-LacZ* mouse a E15.5 embryo was whole mount LacZ stained and photographed after clearing (Fig. 23. E).

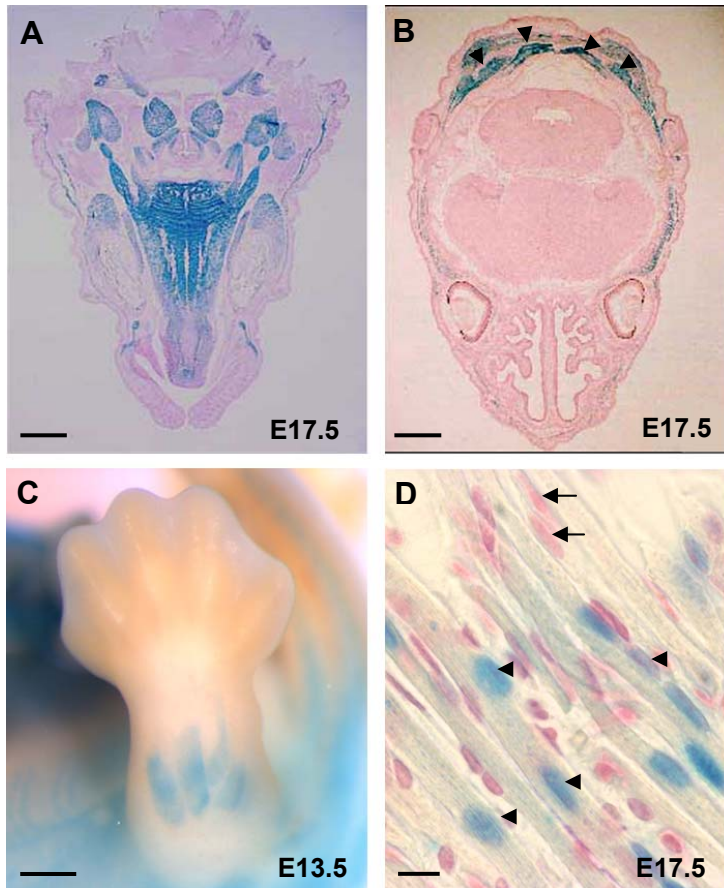




Figure 23. Expression of *Popdc2-LacZ* in the *Popdc2*^{WT/LacZ} brain and skeletal muscle at E17.5. Cryosections (A, B and D) stained with LacZ and counterstained with Nuclear Fast Red. Transversal sections at the level of the tongue (A) and eyes (B) showed strong LacZ staining in the head skeletal muscle tissue. No staining was observed in the brain. (C) Whole mount LacZ stained E13.5 hind limb. (D) Detail of a longitudinal section through skeletal muscle tissue of the region taken into the dotted line box in the Fig. 22 A. Skeletal muscles express *Popdc2-LacZ* (arrowheads point on LacZ stained and arrows on unstained nuclei). (E) Whole mount LacZ stained and benzylbenzoate/benzyl alcohol cleared E15.5 embryo demonstrates overall view of superficially located *Popdc2-LacZ* positive skeletal muscles and umbilicus vein (uv). Embryo at E15.5 was chosen for the whole mount LacZ staining since older embryos are not suitable for this purpose. Scale bars: A, B and E, 1mm; C, 500 μ m; D, 10 μ m.

4.3.9 Expression of *Popdc2-LacZ* in the newborn lungs

Whole mount LacZ staining of postnatal (7d) *Popdc2*^{WT/LacZ} heart and sections of the lungs revealed strong *Popdc2-LacZ* expression in the pulmonary veins (Fig. 24 A). This *Popdc2-LacZ* expression did not disappear even after pulmonary veins enter and ramify in the lungs (Fig. 24 B, B¹). Cells displaying LacZ staining were lining the pulmonary veins and their extensions into the lungs. These cells are believed to be cardiac myocytes. These cells were first described by Rauschel in 1836. In 1910 Favaro called them “pulmonary myocardium”. These cardiac cells are present in the

pulmonary veins in many species. In large mammals they are limited to extra pulmonary vein segments, while in rodents they are located in intrapulmonary vein extensions too (Jones et al., 1994). The myocardial origin of the cells shown in the Fig. 24 B and B' supports the data shown in the Fig. 19 E' and E'' which demonstrates identical expression of the *Popdc2* and cTnI in the cells lining lung vessels of the E17.5 embryo.

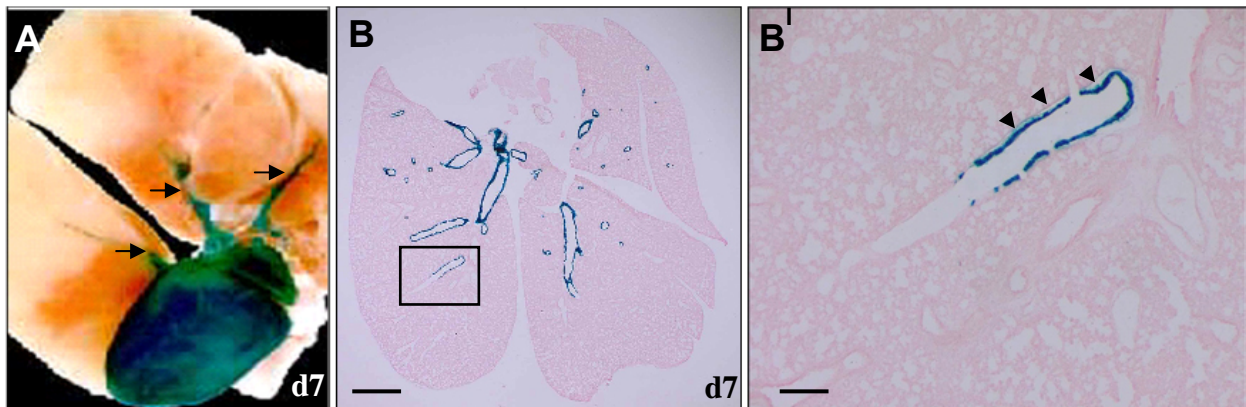


Figure 24. Expression of *Popdc2-LacZ* in 7 d *Popdc2*^{WT/LacZ} lungs, gut and bladder. (A, C and D) Whole mount LacZ staining of the heart, gut and bladder. (A) strong LacZ expression is observed in the whole heart and in the pulmonary veins (arrows). (B) LacZ stained section through the lungs shown in the (A). (B') Enlargement of black box in panel B. LacZ expression labels presumptively myocardial one cells layer lining pulmonary veins and its extensions into lung tissue (B', arrowheads). Scale bars: B, 1mm; B', 200µm.

4.3.10 Expression of *Popdc2* and *Popdc2-LacZ* in gastrointestinal tract, kidney, bladder and skeletal muscle of newborn mouse

In vertebrates the digestive tract as well as the parts of the respiratory tract is derived from the gut tube. The gut tube is the part of the gastrointestinal tract, which originates from splanchnic mesoderm and visceral endoderm. Morphologically, the stomach can be described as a thickened muscle derived from the mesoderm and specialized glands arising from the endoderm. The stomach consists of the two major parts: fundus and pylorus, which are functionally and structurally different (Fig. 25. A). The fundus, or anterior part of the stomach is characterized by unique gastric glands, which secrete pepsinogen and hydrochloric acid into the lumen. The pylorus or posterior portion of the stomach is characterized by glands, which secrete mucus (Smith et al., 2000). In *Popdc2*^{WT/LacZ} 7 days old mouse the fundus showed no *Popdc2-LacZ* expression, while the pyloric part did (Fig. 25 B). To localize the β -gal

activity at further detail in the pyloric part, LacZ staining of cryosections was performed (Fig. 25 C, D). LacZ expression was found to be restricted to the epithelium. In order to demonstrate specificity of LacZ expression in the pyloric epithelium, in situ hybridization on sections was performed (Fig. 25 E-G) showing an identical expression pattern and suggesting that the *Popdc2* gene is specifically expressed in the pyloric epithelium.

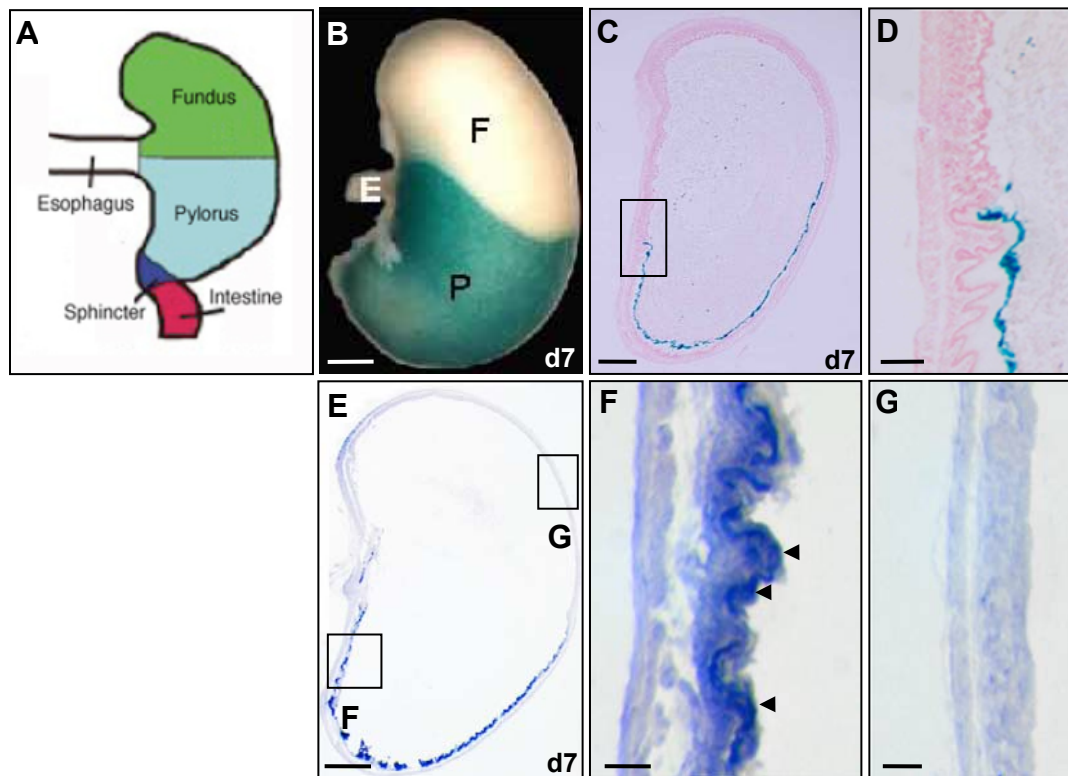


Figure 25. Expression of *Popdc2* and *Popdc2-LacZ* in the 7 days *Popdc2*^{WT/LacZ} neonatal stomach. (A) Schematic representation of the structural organization of a stomach (Modified after Smith et al., 2000). (B) Whole mount LacZ stained stomach demonstrating expression of *Popdc2-LacZ* in the pylorus region (P) and absence of staining in the fundus region (F). (C) Section through the specimen shown in (B) with strong expression of *Popdc2-LacZ* in the pyloric epithelium. (D) Enlargement of the area demarcated by a rectangle in panel C showing the transition from the fundus (unstained) into the pyloric epithelium (blue stained). (E) Expression analysis of *Popdc2* by section in situ hybridization shows expression of *Popdc2* mRNA is confined to the pyloric epithelium corroborating the LacZ expression pattern. (F, G) Enlarged views of the regions labelled by rectangles in panel E showing strongly stained pyloric epithelium (F, arrowheads), and unstained fundus epithelium (G). Scale bars: B, C and E, 1mm; D, F and G, 250µm.

In order to learn about *Popdc2-LacZ* expression in other parts of the digestive tract and in the bladder in neonatal animals (6-7 days old), these organs were removed from the abdominal cavity of WT and *Popdc2*^{WT/LacZ} mice, cryosectioned and stained

side by side with LacZ. Wild type mice in this experiment are especially required because of known endogenous β -gal activity in the some parts of the digestive tract. Bladder, kidney and the following parts of the gastrointestinal tract were used in this experiment: pancreas, liver, gall bladder, esophagus, duodenum, jejunum, ileum, cecum, ascending colon and rectum. *Popdc2-LacZ* activity was observed in the esophagus, ascending colon and bladder (Fig. 26 A-G) and was confined in all these organs to the smooth muscle layer.

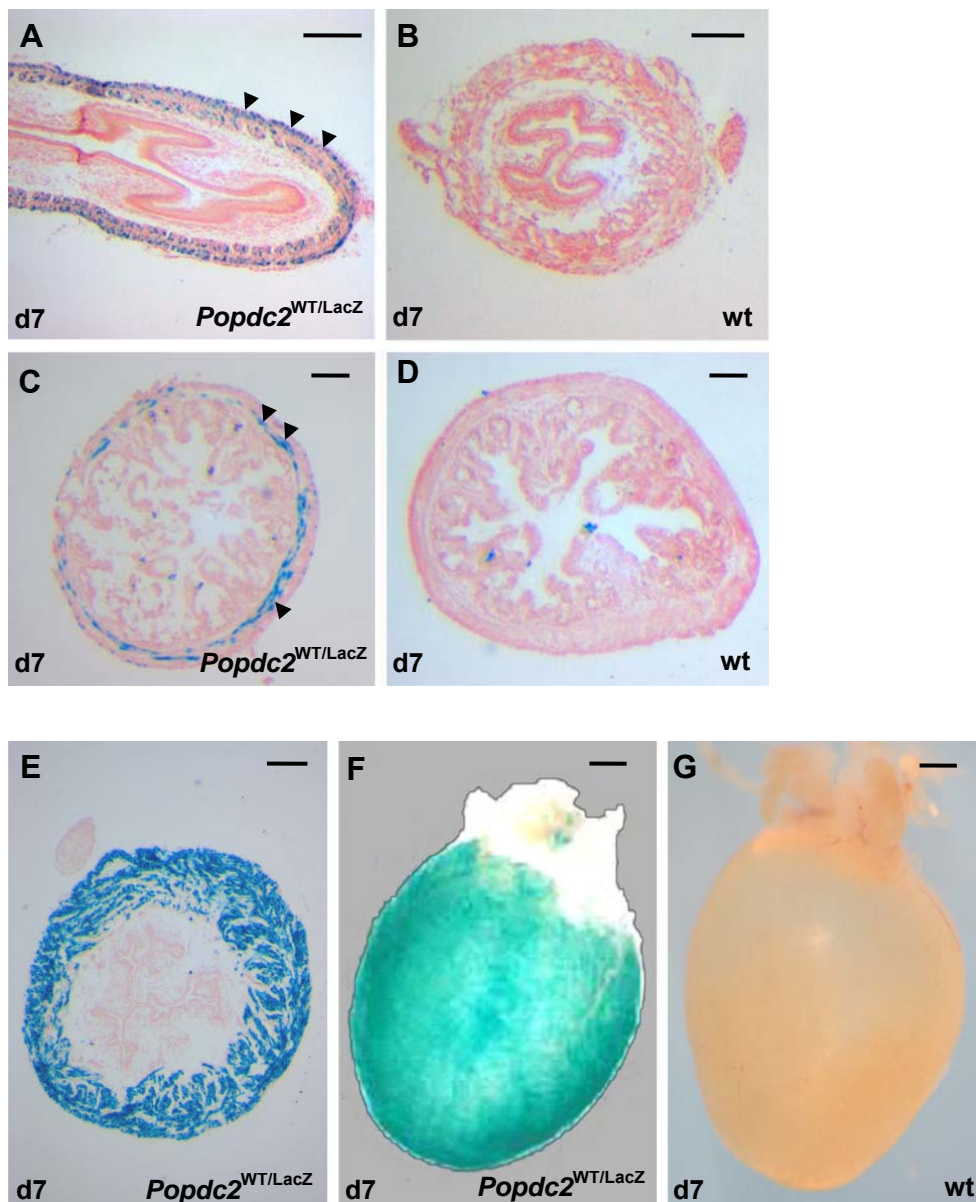


Figure 26. Expression of *Popdc2-LacZ* in the 7 days old *Popdc2*^{WT/LacZ} esophagus, intestine and bladder. (A-E) Cryosections of 7 days neonatal *Popdc2*^{WT/LacZ} and WT organs as indicated, were stained with LacZ and Nuclear Fast Red. (A, B) Esophagus (C, D) ascending colon. (E) bladder. (A, C and E) LacZ staining is seen in the smooth muscle layer (arrowheads in A and C). (F and G) Whole mount LacZ staining of *Popdc2*^{WT/LacZ} and WT bladders, respectively. (B, D and G) LacZ staining of WT tissues. Scale bars: A, E, 200 μ m; B, C, D 100 μ m; F and G, 500 μ m.

Cryosections of the newborn mouse stained with LacZ revealed activity of the β -gal in the bone marrow (Fig. 27 A) and in all skeletal muscles including diaphragm (Fig. 27 B-D).

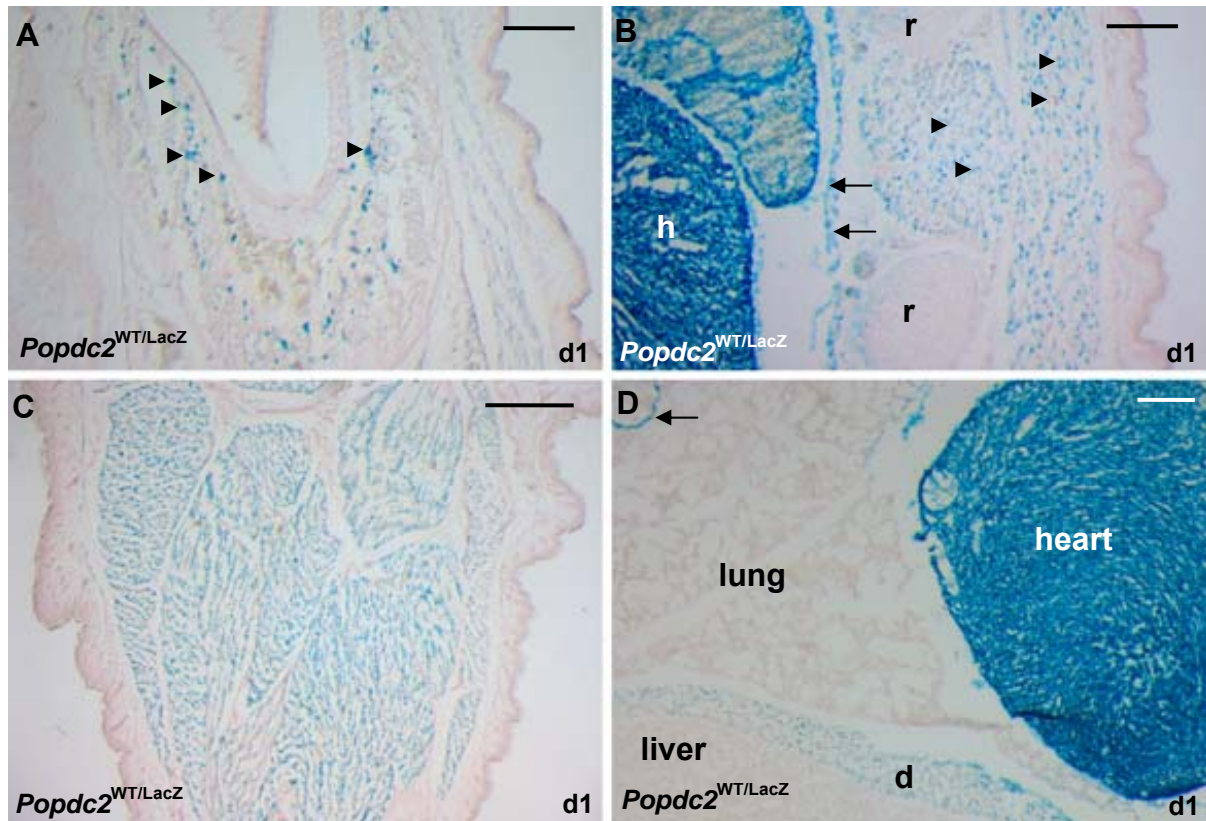


Figure 27. Expression of *Popdc2-LacZ* in the 1 day old *Popdc2*^{WT/LacZ} bone marrow and skeletal muscle. (A-D) Cryosections of 1 day neonatal *Popdc2*^{WT/LacZ} were stained with LacZ and Nuclear Fast Red. (A) Expression of the LacZ is observed in the cells of the bone marrow (arrowheads). (B) Skeletal muscle (arrowheads) and pericardium (arrows) displayed LacZ staining. (C) Entirely limb skeletal muscle express LacZ. (D) Diaphragm is LacZ positive. Arrow points on the LacZ positive cardiomyocyte layer of the pulmonary vein. h, heart; d, diaphragm; r, rib. Scale bars: A and B, 200 μ m; C, 500 μ m; D, 250 μ m.

4.3.11 Myocardial expression of *popdc2-LacZ* in 7d heart

Whole mount LacZ stained 7 days old *Popdc2*^{LacZ/LacZ} heart show strong *Popdc2-LacZ* expression in both atria and ventricles. 7 day old neonatal *Popdc2*^{WT/LacZ} heart cryosectioned and subsequently stained with LacZ and Nuclear Fast Red demonstrated β -gal activity in the myocardium of both atria and ventricles. No LacZ staining was observed in the coronary vessels and valves (Fig. 28 B). *Popdc2-LacZ* activity was homogenously expressed in the tissue of right and left ventricles and the IVS (Fig. 28 C). Within the cells LacZ was mainly localized to the nucleus (Fig. 28 C).

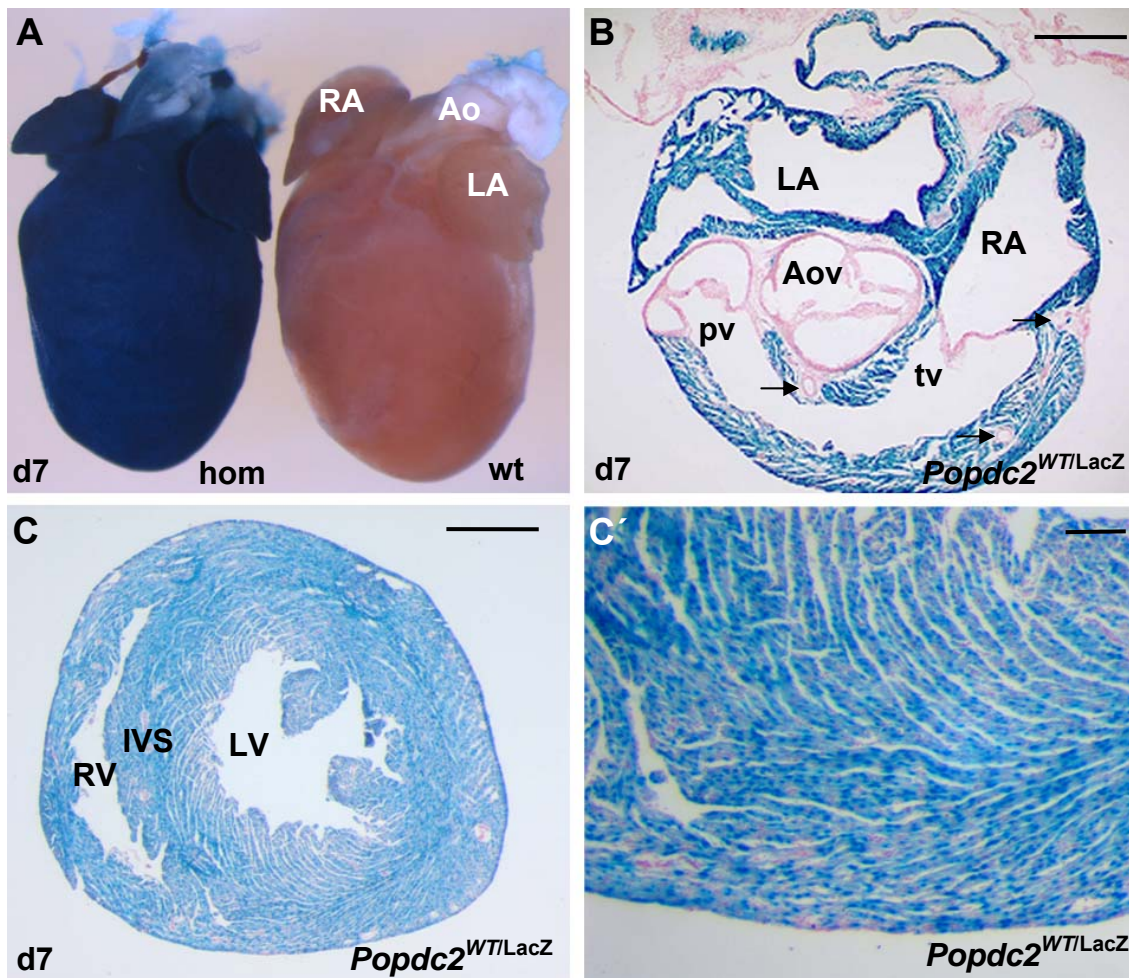


Figure 28. Expression of the *Popdc2-LacZ* in the 7 days old heart. (A) Whole mount LacZ staining of the *Popdc2^{LacZ/LacZ}* and WT control hearts reveal strong LacZ expression in the myocardium of the both, atria and ventricles (A). (B, C) Cryosections through the *Popdc2^{WT/LacZ}* heart stained with LacZ and Nuclear Fast Red. LacZ is strongly expressed in the myocardium and absent from coronary vessels (B, arrows) and valves. (C) LacZ staining of the cryosections through the ventricles demonstrates the homogenous *Popdc2-LacZ* expression. (C') Enlarged view of the myocardium LacZ staining in (C). Aov, aortic valve; IVS, interventricular septum; LA, left atrium; LV, left ventricle; RA, right atrium; RV, right ventricle; pv, pulmonic valve; tv, tricuspid valve. Scale bars: B and C, 500 μ m; C', 100 μ m.

Of note LacZ expression was observed in no other cell type than cardiac myocytes. Thus, coronary vessels, interstitial fibroblasts, epicardium and endocardium were devoid of any LacZ activity.

4.3.12 Expression of *Popdc2-LacZ* in gastrointestinal tract, bladder, kidney, spleen, skeletal muscle and heart of 3 months old mouse

In order to learn about *Popdc2-LacZ* expression in the adult digestive tract, bladder, kidney, spleen and heart, corresponding organs were removed from the abdominal

cavity of the WT and *Popdc2*^{LacZ/LacZ} mice, cryosectioned and stained side by side with LacZ in the similar way like in the experiment with newborn mice. 3 months old organs, i.e. bladder, kidney, spleen and the following parts of the gastrointestinal tract were used in this experiment: pancreas, liver, gall bladder, esophagus, duodenum, jejunum, ileum, cecum, ascending colon and rectum. Like in the case of neonatal animals *Popdc2-LacZ* activity was observed in the esophagus, ascending colon and bladder (Fig. 29 A-F) and was confined in all these organs to the smooth muscle layer.

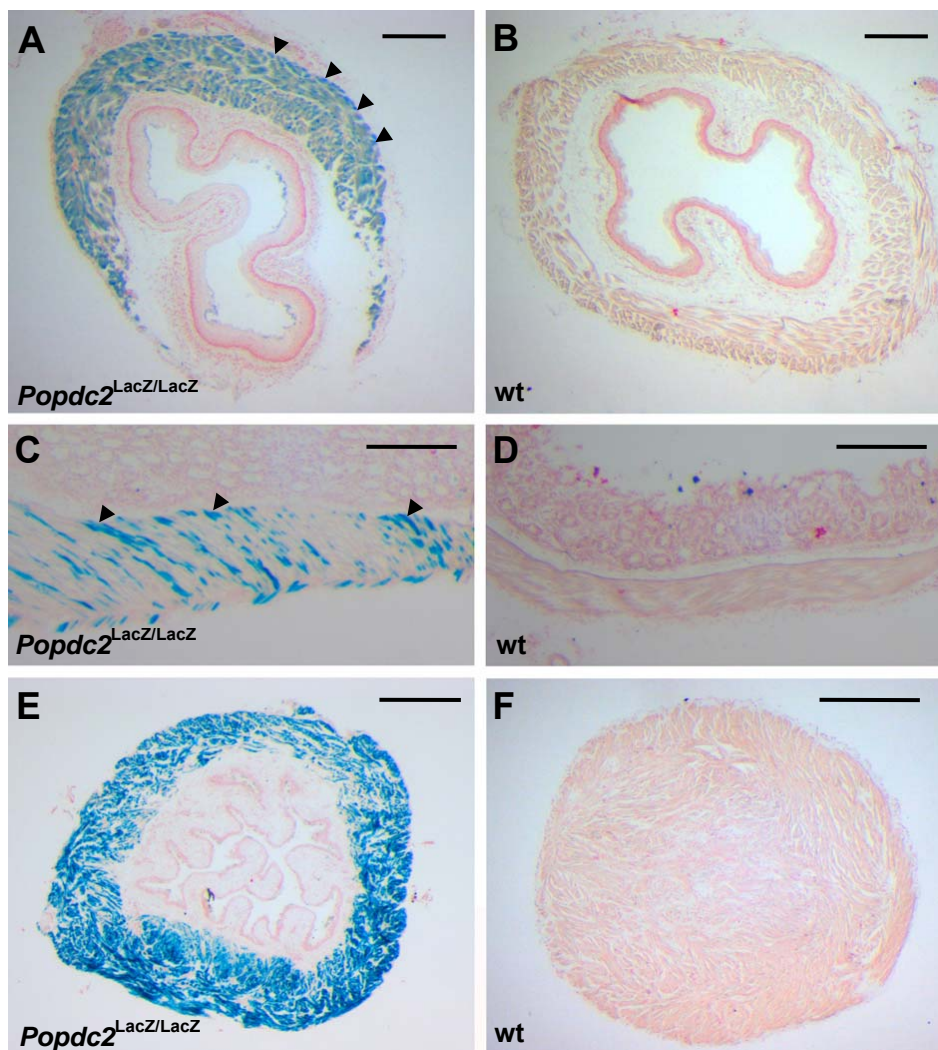


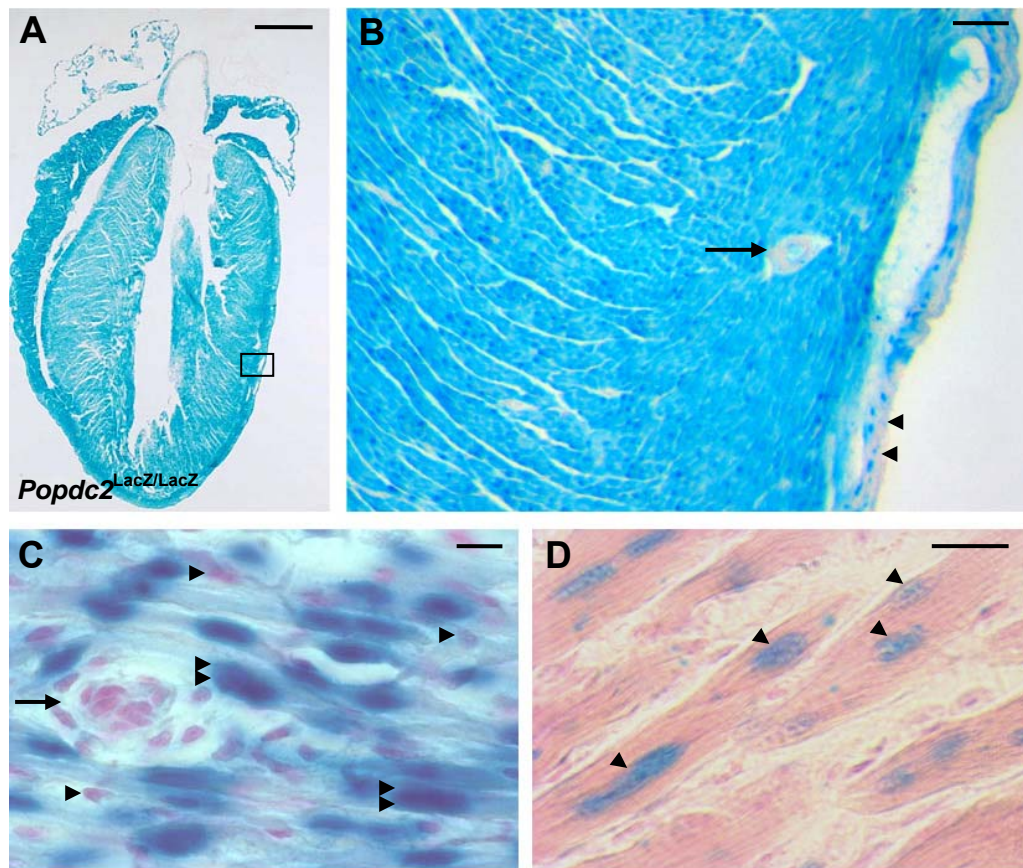
Figure 29. Expression of *Popdc2-LacZ* in the 3 months old *Popdc2*^{LacZ/LacZ} esophagus, intestine and bladder. (A-F) Cryosections of the 3 months old *Popdc2*^{LacZ/LacZ} and WT organs as indicated, stained with LacZ and Nuclear Fast Red. LacZ staining of sections through (A,B) Esophagus ; (C, D) ascending colon ; (E) bladder. Scale bars: A, B, C and D, 200µm; E and F, 500µm.

Also myocardial expression of the *Popdc2-LacZ* in the 3 months old *Popdc2*^{LacZ/LacZ} hearts was very similar to that of the 7 days old *Popdc2*^{WT/LacZ} hearts.

The heart of the *Popdc2*^{LacZ/LacZ} mice was cryosectioned and stained with LacZ and Nuclear Fast Red. Like in 7 days old neonatal hearts *Popdc2-LacZ* activity was homogenously expressed in the right and left ventricles and IVS (Fig. 30 A). Within the cells LacZ was localized to the nucleus (Fig. 30 B, C). No LacZ staining was observed in the coronary vessels, epicardium (Fig. 30 B, C) and fibroblasts (Fig. 30 C).

Also similar to the newborn, in the 3 month old animal expression in skeletal muscle was confined to the nuclei (Fig. 30 D).

In order to check whether *Popdc2-LacZ* expression obtained in this experiment coincides with the expression of the endogenous gene, RT-PCR analysis of different organs of a 3 months old mouse was carried out (Fig. 30 D). The results of the RT-PCR analysis correlated well with LacZ expression pattern. The only exception was the expression of *Popdc2* in the fundus part of the stomach, which was most likely due to a contamination of the mRNA preparation with pyloric tissue.



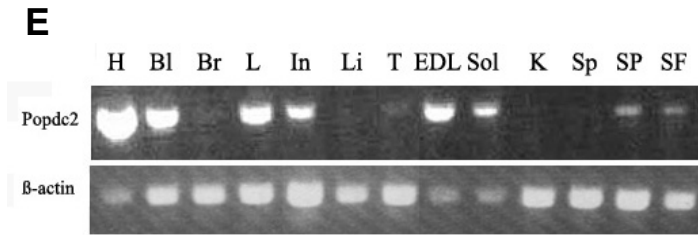


Figure 30. Expression of *Popdc2-LacZ* in the 3 months old *Popdc2^{LacZ/LacZ}* heart and skeletal muscle. (A) LacZ and Nuclear Fast Red staining of a sagittal *Popdc2^{LacZ/LacZ}* heart section. (B) Enlarged view of the ventricular wall of the section shown in (A), arrows and arrowheads demarcate a coronary vessel and epicardium respectively, which are unlabeled. (C) High magnification of the ventricle myocardium shown in A. Double arrowheads point on the LacZ positive cardiomyocytes nuclei; no LacZ is observed in the coronary capillary (arrow) and fibroblasts (arrowheads). (D) Cryosection LacZ stained skeletal muscle. Arrowheads point on LacZ positive nuclei. (E) *Popdc2* RT-PCR of different organs WT 3 months old mouse. H, heart; Bl, bladder; Br, brain; L, lung; In, intestine; Li, liver; T, testis; EDL, extensor digitorum longus; Sol, soleus; K, kidney; Sp, spleen; SP, pylorus part of the stomach; SF, fundus part of the stomach. Scale bars: A, 1mm; B, 100 μ m; C and D, 10 μ m.

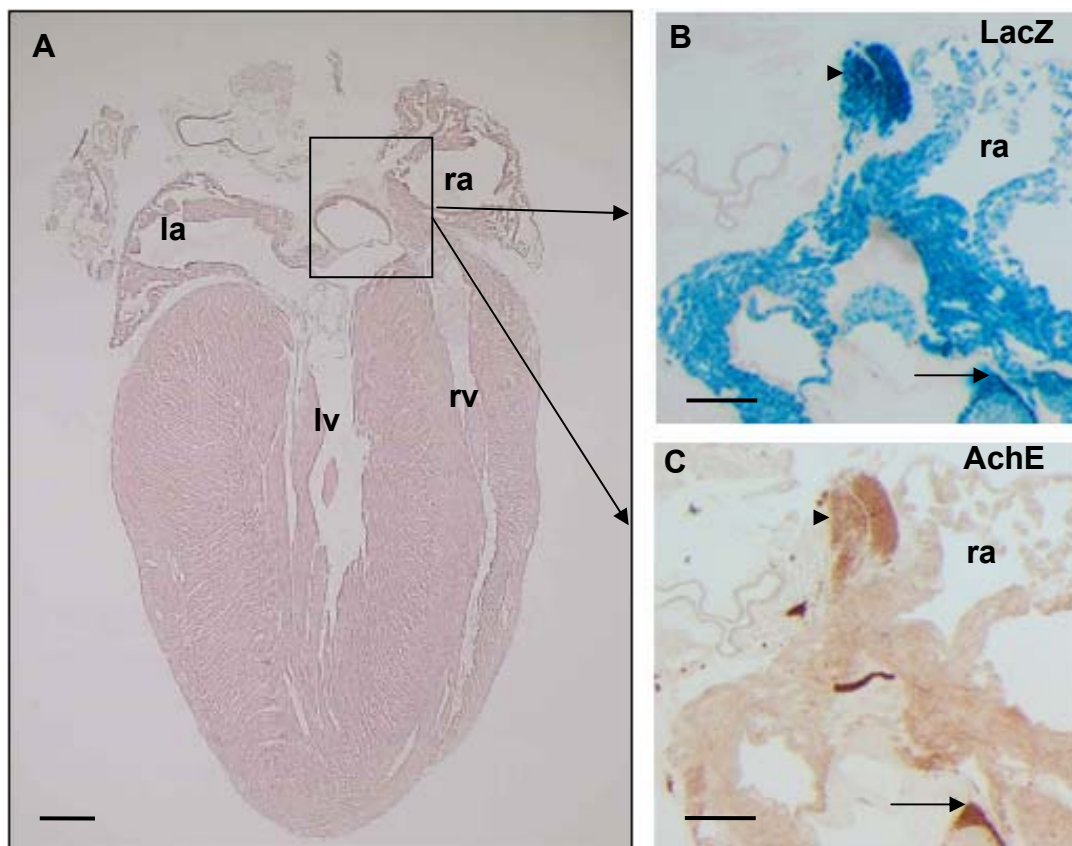
4.3.13 Expression of *Popdc2-LacZ* in conduction system

LacZ staining of sections through the adult *Popdc1* transgenic mouse heart revealed strong staining throughout the myocardium. However, when staining was performed for a short period of time, it revealed strong LacZ expression in the entire cardiac conduction system (CCS) (Fig. 4). In order to examine *Popdc2-LacZ* expression in the CCS of the *Popdc2* transgenic mice, consecutive sections of 3-4 months old *Popdc2^{WT/LacZ}* hearts (Fig. 31 A) were stained for LacZ (Fig. 31 B) and co-stained for acetylcholine esterase activity (AChE) (Fig. 31 C), which specifically demarcates the cardiac conduction system, which is due to the fact that the sinus and AV nodes are densely innervated by the parasympathetic nervous system (Ismat et al. 2005).

Staining for LacZ and AChE resulted in similar patterns, suggesting that indeed the sinus node shows higher levels of *Popdc2-LacZ* expression. Interestingly, higher levels of *Popdc1-LacZ* in CCS have previously been observed (A. Fleige, Diplomarbeit, S. Breher, unpublished observation), which would suggest that preferential expression in the CCS might be a common property of the Popeye gene family. To more specifically demonstrate *Popdc2-LacZ* expression in the sinoatrial node (SAN), section cut through the SAN of a 9 months old *Popdc2^{WT/LacZ}* heart was first stained for LacZ and subsequently for AChE activity, demonstrating co-localization in two stainings (Fig. 31 D, E).

Whole mount LacZ staining of a 3 months old *Popdc2^{WT/LacZ}* atrial preparation revealed LacZ expression in the SAN as well as in the atrioventricular node (AVN)

regions (Fig. 31 F). Whole mount *Popdc2* in situ hybridization confirmed specificity of *Popdc2-LacZ* activity in the SAN (Fig. 31 H). To learn about possible changes in SAN structure in homozygous versus wild type mice whole mount *Popdc2*^{WT/LacZ} and *Popdc2*^{LacZ/LacZ} atrial preparations were LacZ stained. *Popdc2*^{WT/LacZ} preparation LacZ staining resulted in SAN with multiple extensions (Fig. 31 G), while *Popdc2*^{LacZ/LacZ} SAN was seen somewhat smaller and appeared to be more compact (Fig. 31 I). Whole mount LacZ staining of a 3 months old *Popdc2*^{WT/LacZ} heart IVS preparation which was viewed an face from the right and left revealed β -gal activity in the bundle branches cells and Purkinje cells on both sides of the IVS (Fig. 31 J, K, L, M).



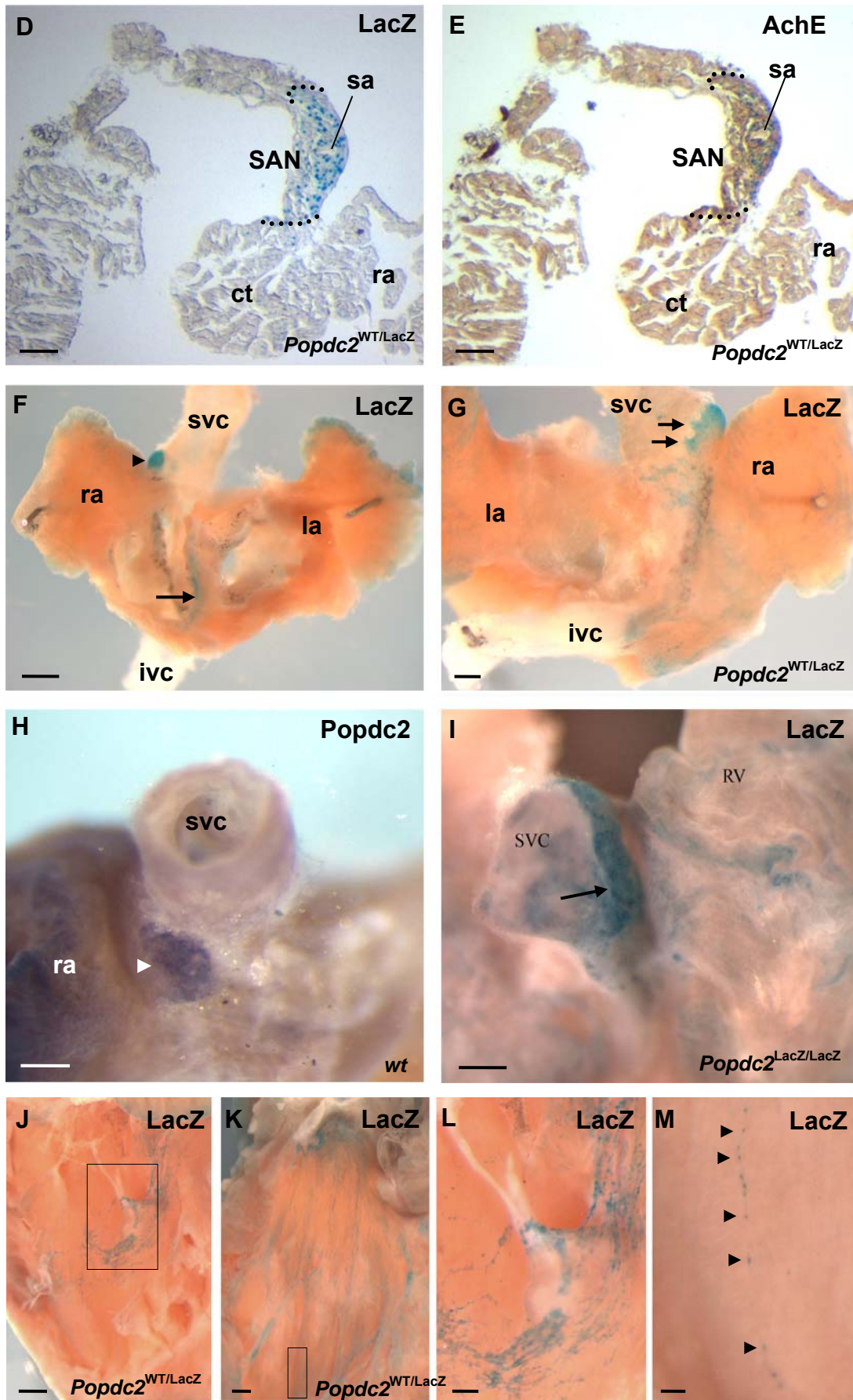


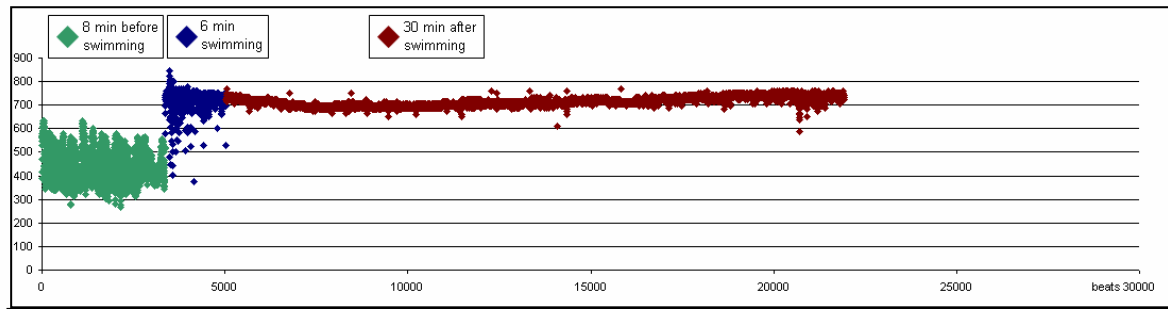
Figure 31. *Popdc2* and *Popdc2-LacZ* expression in the CCS. (A) Sagittal section through the adult heart stained with Nuclear Fast Red displays the location of the CCS components. Consecutive sections of adult myocardium isolated from *Popdc2-LacZ* mice are stained for (B) LacZ and (C) acetylcholine esterase activity (AChE). In both cases the SAN (arrowhead) and His bundles (arrow) were positively stained. (D, E) Section through the SAN, which was stained first for LacZ (D) and subsequently for AChE (E) activity. A dashed line demarcates the SAN. (F) Ventral view of an atrial preparation that was whole mount stained for beta galactosidase activity. Arrowhead points to the SAN and arrow to the AV node. (H) Whole mount in situ hybridization of an adult atrial specimen displaying strong *Popdc2* expression in the SAN (arrowhead) (Experiment performed together with J. Schlüter, Würzburg). (G) Ventral view of the vena cava of a *Popdc2*^{WT/LacZ} mutant (SVC, IVC) showing extensive beta galactosidase activity in presumptive sinus node cells (arrow). (I) Right-sided view of a beta LacZ stained *Popdc2*^{LacZ/LacZ} sinus node (arrow). (J, K) Left- and right-sided views of a whole mount LacZ stained IVS of a *Popdc2*^{WT/LacZ} mouse. (L, M) Enlargements of the region labelled by a rectangle in panel J and K, respectively. Arrowheads point to presumptive bundle branches. ct, crista terminalis; lv, left atrium; lv, left ventricle; ra, right atrium; rv, right ventricle; sa, sinus node artery; SVC, IVC, superior and inferior caval veins. Scale bars: A and F, 500µm; B, C, G, H, I, J and K, 300µm; D, E, L and M, 100µm.

4.3.14 *Popdc2* null mutants display a stress-induced bradycardia

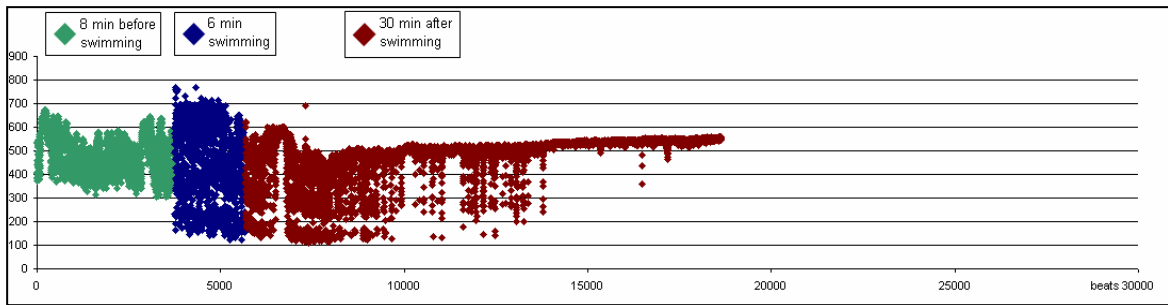
Since we observed strong LacZ expression in the *Popdc2*^{WT/LacZ} SAN we were interested to find out whether the mutant hearts showed any physiological alterations. In a collaboration with Dr. L. Fabritz, Münster we analyzed the electrocardiogram of 2.5, 5.5 and 8 months old mutant and WT littermates. The animals were implanted with telemetric ECG devices and subjected to three different stress regimens: isoproterenol infusion, mental stress and a swim exercise.

8 minutes (min) before the swim test, 6 min during and 30 min after the exercise Holter ECGs were recorded. No difference was observed during the experimental period between 2.5 month old WT and transgenic mice. In contrast, at 8 month of age mice during and after the exercise an abnormal heart rate compared to WT was detected (Fig. 32 A, B). ECGs recorded in these mice revealed significant sinus pauses compared to WT (Fig. 32 C). These results were consistent with the data obtained in another experiment where freely roaming 8 months old WT and *Popdc2* transgenic mice were subjected to mental stress produced by air-jet and ECGs were recorded (Fig. 32 D, E; Fig. 34).

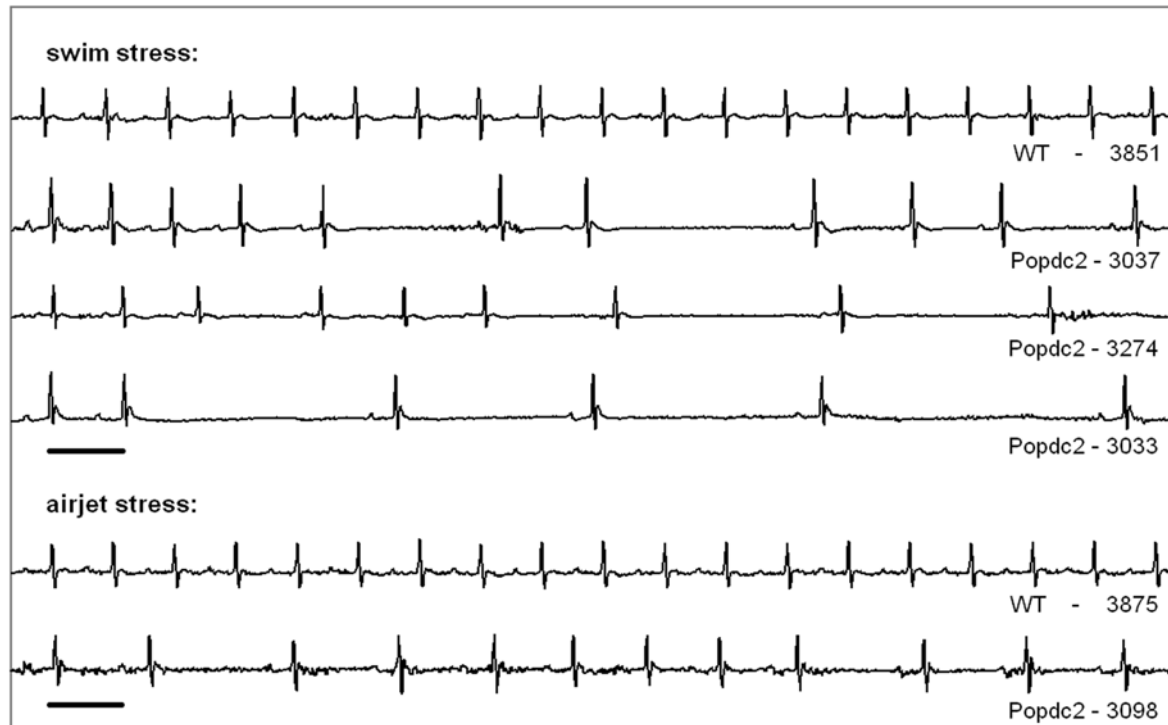
A



B



C



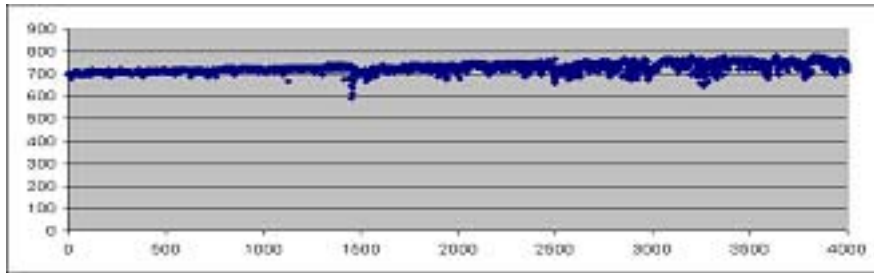
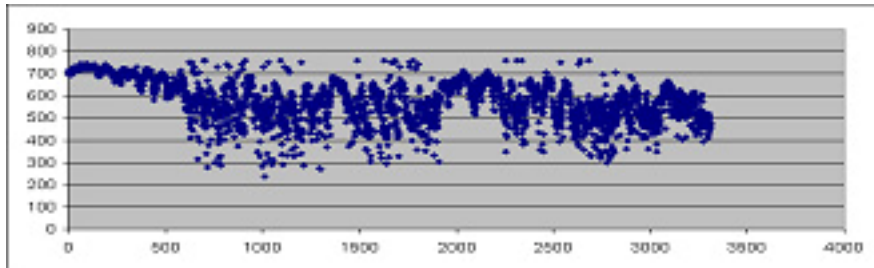
D**E**

Figure 32. Functional analysis of *Popdc2* null mutant hearts. Telemetric Holter ECG measurements from freely roaming mice with implanted transmitters. (A, B) Heart rate 8 min. before swimming (green traces), during 6 min. of swimming exercise (blue traces) and 30 min. after swimming (red traces) of (A) wild-type and (B) null mutants. (C) Examples of the ECG curves of wild-type (3851, upper trace in swimming and 3875, airjet stress) and mutant hearts (3037, 3274 and 3033, three lower traces in swimming and 3098, lower trace in airjet stress). Scale bar: 100ms. (D, E) Heart rate of wild-type (D) and *Popdc2*^{LacZ/LacZ} mice. (E) After applying air-jet stress.

Echocardiographic analysis performed in the 8 month old WT and *Popdc2* transgenic mice did not reveal any abnormalities in the heart rate and systolic function (L. Fabritz, data not shown, personal communication). However, after β -adrenergic stimulation with isoproterenol, which has chronotropic and inotropic effect on the heart, transgenic mice displayed a less pronounced increase in heart rate than WT litter mates (Fig. 33. A). Remarkably, the stimulation with isoproterenol did not lead to a significant difference in the PQ interval between WT and transgenic mice at heart rates of 600 beats per minute (bpm) (Fig. 33 B). Thus, despite prominent expression in the AV node and the ventricular conduction system there was only a defect observed in the SA node.

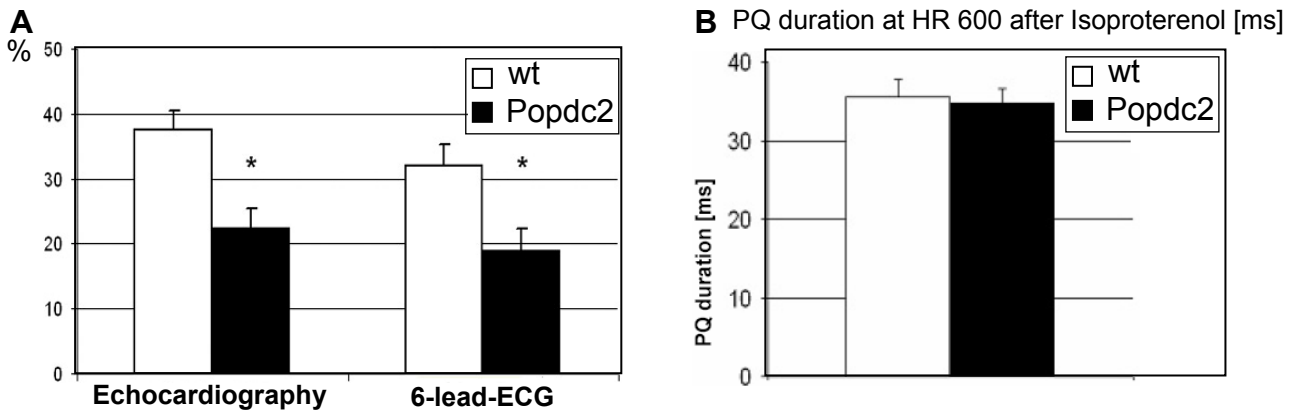


Figure 33. (A) Reduced response of heart rate on isoproterenol stimulation as recorded by echocardiography and by 6-lead-ECG (* $p < 0.05$). (B) PQ interval at the heart rate 600 bpm as measured by ECG after isoproterenol stimulation of 8 months old WT and *Popdc2* KO mice.

The phenotype found in 8 month old *Popdc2* KO mice in different experiments was absent in 3 month old mice and became only obvious around the age of 5.5 month. As shown in the Figure 34, A, B and C using three different stimulation protocols the experimentally-induced bradycardic phenotype reached its maximum by the age of 8 months. Although in all three experiments bradycardic events were already present by the age 5.5 months, but only in case of the swimming test the bradycardic events reached statistical significance. In *Popdc2* KO and WT mice after 6 min of swimming, sinus pauses were measured during next 30 min. The most significant difference between two groups of the animals was observed at the 8 months of age and a total of 542 syncopes were observed in *Popdc2* KO mice versus 2 in WT (Fig. 34 D).

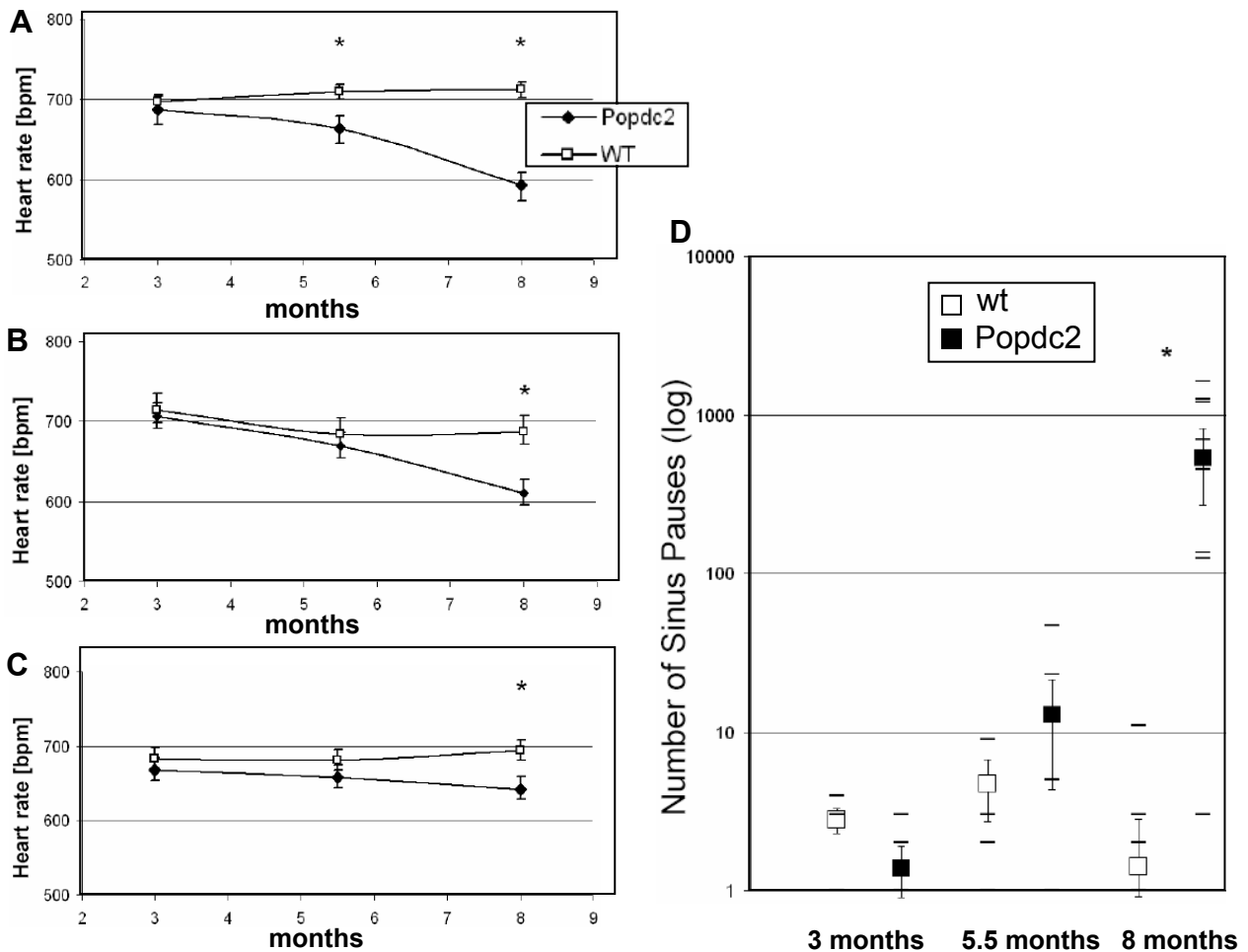


Figure 34. (A, B and C) Mean heart rates during 6 min of the stress load in WT and *Popdc2*^{LacZ/LacZ} mice at 3, 5.5 and 8 months old mice (**p*<0.05). (A) During swimming. (B) Airjet-stress. (C) Isoproterenol stimulation. (D) Mean of sinus pauses in WT and *Popdc2*^{LacZ/LacZ} mice at 3, 5.5 and 8 months old mice during 30 min after 6 min of the swim stress (**p*<0.05).

In contrast to β -adrenergic stimulation with isoproterenol, parasympathetic stimulation with the acetylcholine receptor agonist carbachol reduced the heart rate to a similar extent in 8 month old WT and *Popdc2* transgenic mice (Fig. 35).

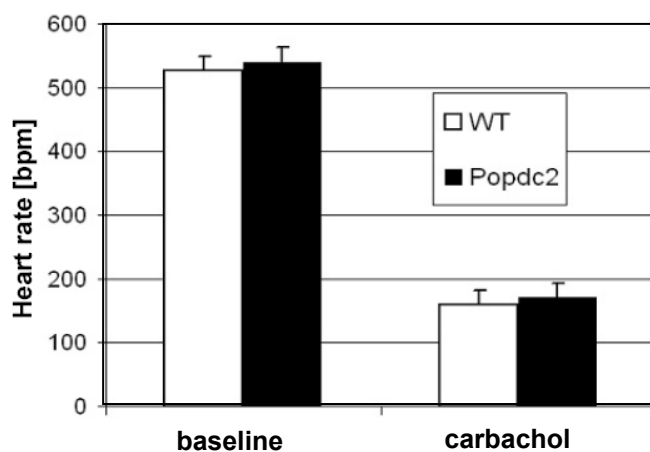


Figure 35. Similar response of heart rate on carbachol stimulation of the 8 months old WT and *Popdc2* KO mice. *n*=5 pairs of mice.

Taken together these results suggest that the absence of *Popdc2* resulted in the development of a stress-induced bradycardia. Moreover this phenotype develops in an age-dependent manner.

4.3.15 Structural alterations of sinus node cells in *Popdc2* null mutants as revealed by HCN4 whole-mount staining

Hyperpolarization-activated, cyclic nucleotide-gated cation currents, termed I_f or I_h , are generated by four members of the hyperpolarization-activated, cyclic nucleotide-gated cation (HCN) channel family (Yasui et al., 2001). Together with other ion channels HCN4 is believed to be critical for the generation and regulation of cardiac pacemaker activity. HCN4 is the prevalent HCN transcript in the adult mouse SAN as well as during embryogenesis (Yasui et al., 2001). Since HCN4 is a SAN-specific marker it was used here to determine possible structural alterations of the SAN in the *Popdc2* mutant. HRP staining revealed such alterations in the peripheral part of the SAN (staining has been done by A. Froese and J. Schlüter). In the SAN two different cell types are distinguished based on their morphology i.e. spindle cells and spider cells (Wu et al. 2001). Spindle cells in the WT possessed lengthy and more ramified extensions than in the mutant (Fig. 36 A, A', B, B'). Immunofluorescent detection of HCN4 by confocal microscopy revealed in addition to a reduction in the cellular extensions in the spindle cells also a severe reduction in the amount of spider cells in the pacemaker center (Fig. 36 C, D). Moreover there was a reduction of HCN4 immunoreactivity towards the inferior vena cava. Volume measurements using 3-D reconstructions of serial sections stained with HCN4 antibody revealed a volume reduction of about 30% in the mutant SAN (Fig. 37).

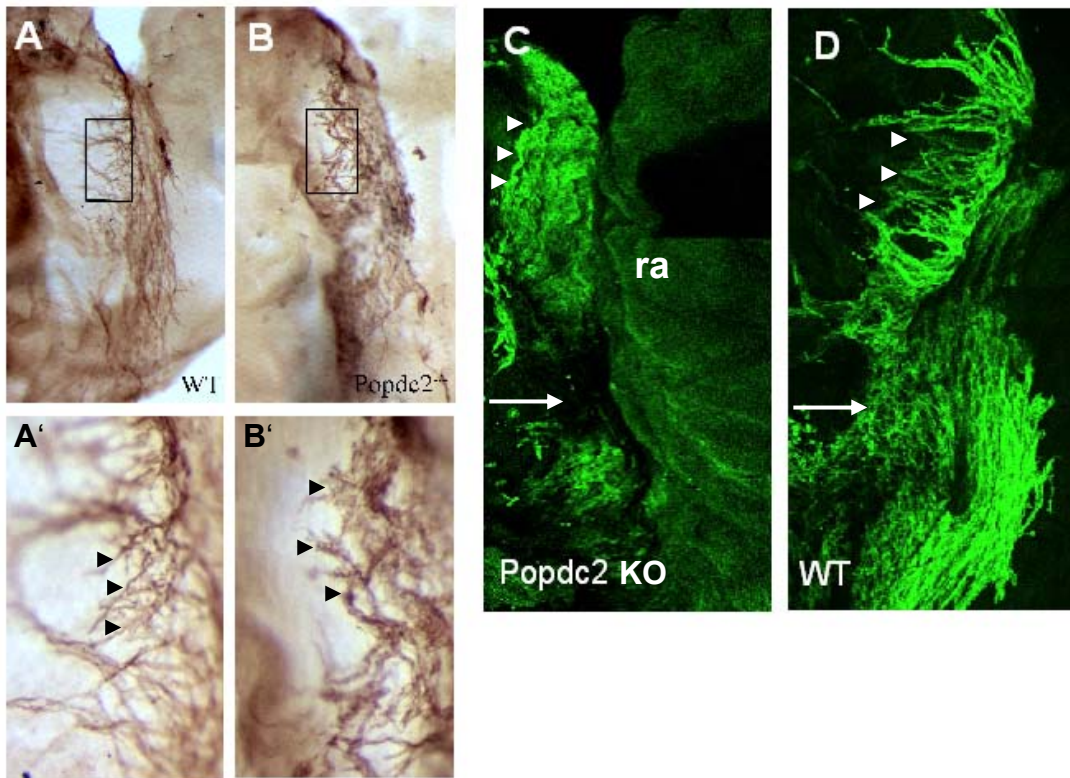


Figure 36. Whole mount immunostaining for HCN4 expression. (A,A',B,B') HRP immunostaining of sinus node cells in (A, A') wildtype and (B, B') *Popdc2* null mutant hearts. After staining the tissue was cleared in glycerol solution. (A', B') are enlarged views of spindle cells (arrowheads) in the sinus node. (C, D) Whole-mount immunofluorescent detection of HCN4 by confocal microscopy of (C) null mutant hearts and (D) wildtype. Arrowheads point on the spindle cells. Arrow in D points on the HCN4 positive area which is missing in C. ra, right atrium. (These immunohistochemical stainings were performed together with J. Schlüter, Würzburg).

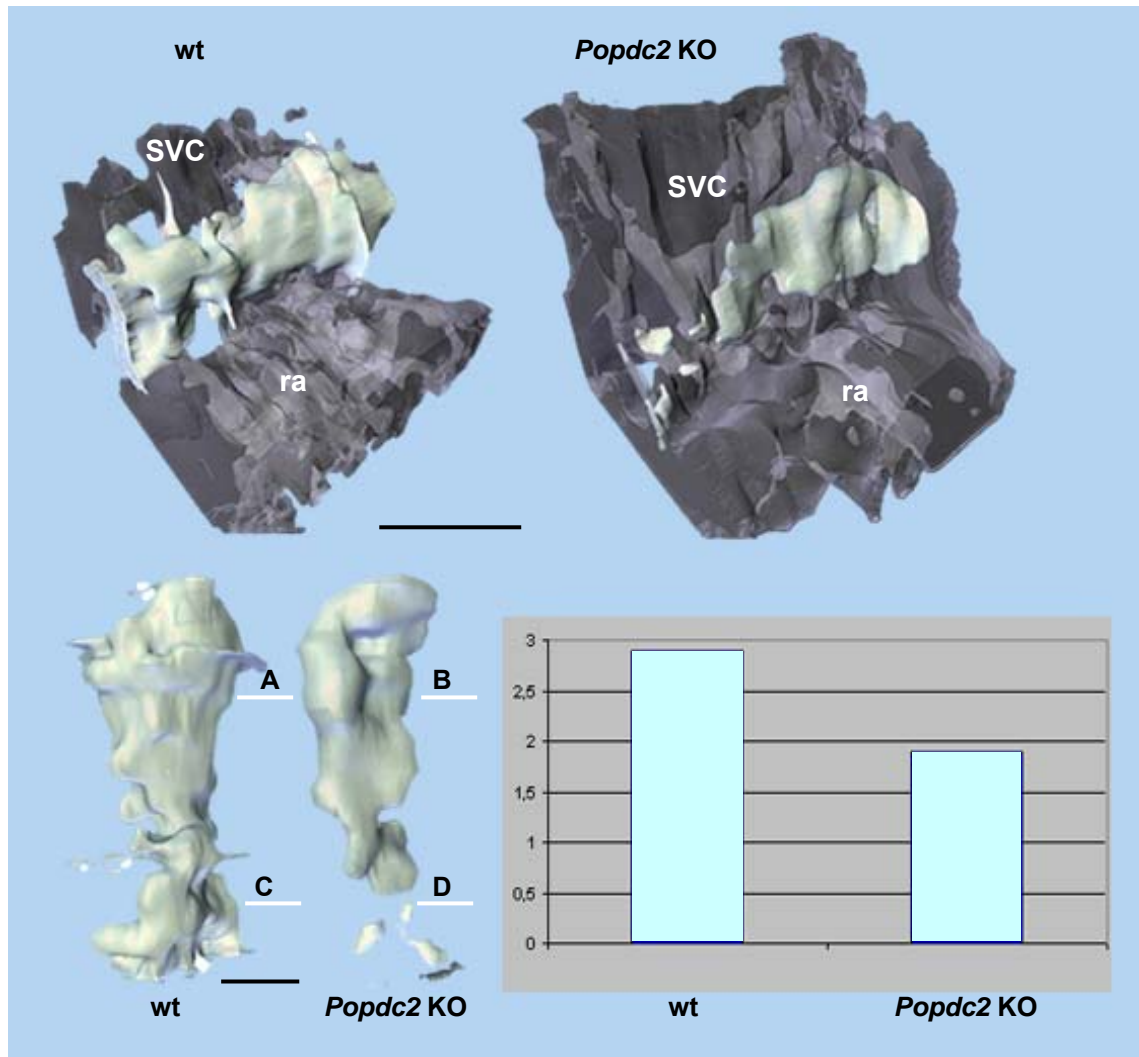


Figure 37. Three-dimensional reconstructions of an adult (3 months old) WT and KO atrial preparations with a dorsal lateral (top, whole preparation) and dorsal view (bottom, HCN4 cells only) on the SAN. Cryosection immunostaining for HCN4 positive cells. Green indicates HCN4 positive tissues and diagram represents their volumes in mm^3 . Scale bars (in black): $500\mu\text{m}$ in the top, $200\mu\text{m}$ in the bottom. ra, right atria; SVC, superior caval vein. A, B, C and D bars point out positions of the sections shown in the Fig.38. This experiment was performed together with J. Schlüter, Würzburg.

The volume reduction of the SAN tissue in the *Popdc2* KO is due to a loss of sinus node tissue in the inferior vena cava. Masson's Trichrome staining of the sections cut through the SAN demonstrated a loss of extracellular matrix in the superior domain of the *Popdc2* KO SAN (Fig. 38 A, B), whereas the inferior domain of *Popdc2* KO SAN displayed an increase (Fig. 38 C, D).

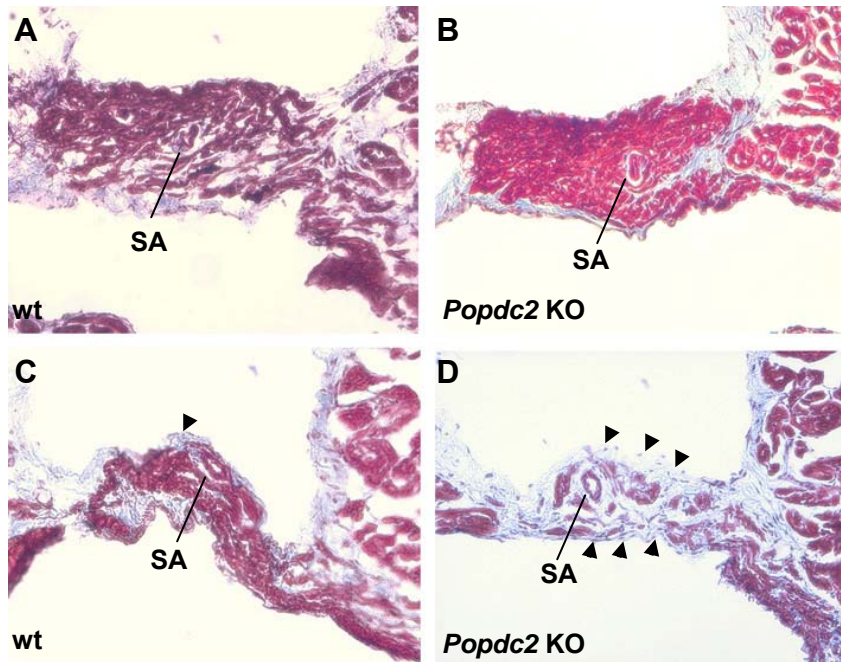


Figure 38. Structure of the WT and *Popdc2* KO SA nodes as revealed by the section Masson's Trichrome staining. Section through the WT (A, C) and *Popdc2* KO (B, D) SA nodes at levels shown in Fig. 37 (white bars). (B) Loss of extracellular matrix in *Popdc2* KO SAN as compared to the WT (A). Extensive fibrosis in the *Popdc2* KO SA nodes (D, arrowheads) as compared to the amount of the extracellular matrix in WT (C, arrowheads). SA, sinus node artery; ct, crista terminalis.

4.4 *Popdc2* promoter analysis

4.4.1 Transcriptional control of *Popdc2*

Genomic regions with important biological functions are usually conserved between different species. In this study a pre-computed alignment of the entire human and mouse genome (VISTA Browser; <http://pipeline.lbl.gov>) was used to identify any conserved sequences in 26kb of the *Popdc2* gene. As expected a high sequence conservation was observed in all four coding exons. Intronic sequences and 5' and 3' flanking sequences with significant conservation (70% of sequence conservation over 100bp) were also observed in the *Popdc2* gene (Fig. 39).

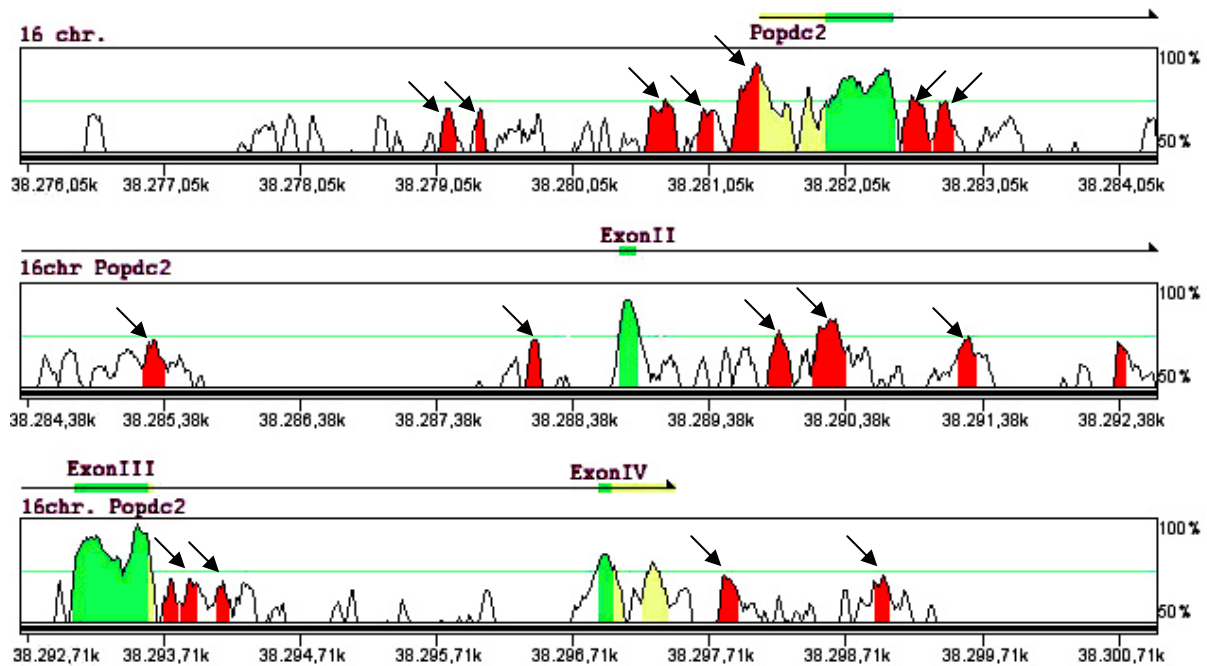


Figure 39. Inter-species comparison of the *Popdc2* coding and non coding sequence. 26kb of human and mouse sequence were aligned using the VISTA software. Red picks indicate at least 70% of sequence conservation over 100bp. Peaks with high sequence conservation aside from the coding region (pointed out by arrows) may reflect regions involved in transcriptional control. The position of the noncoding regions of *Popdc2* are indicated in yellow, whereas the exons are demarcated in green.

The 5' flanking sequence of the *Popdc2* gene was subjected to further analysis for its transcriptional control. 1750 bp of upstream sequence plus 550 bp of the 5' UTR was subcloned into pGL3, a vector that contains a luciferase reporter gene. This construct was transfected into primary cultures of chick cardiac myocytes and luciferase activity was measured. The 1750 bp sequence showed strong and specific luciferase activity in chick cardiac myocytes. Transfection of this sequence with a LacZ reporter gene resulted in a strong labelling of cardiac myocytes, whereas cardiac fibroblasts were devoid of any labelling. In order to map the functional domains within this sequence different deletions were generated and tested for luciferase activity in cardiac myocytes (Fig. 40). This approach resulted in the identification of three functional domains in the 5' flanking sequence of the *Popdc2* gene: an enhancer was identified between -1750 and approx. -1000, a strong negative regulatory element located between -517 and -418, and a promoter proximal element between -418 and -77 nt.

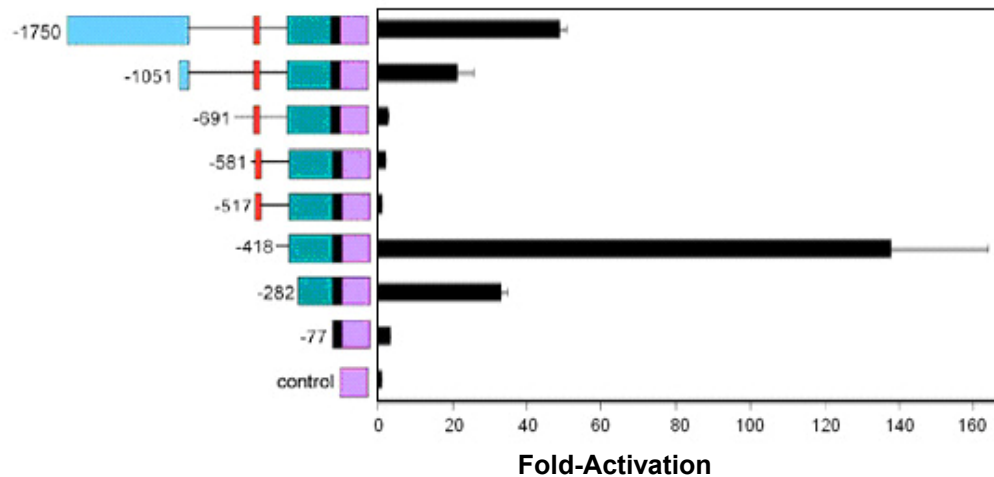


Figure 40. Deletion analysis of the 5' flanking sequence of the *Popdc2* gene. 1750 bp of 5' flanking sequence together with 550 bp of 5' UTR of the *Popdc2* cDNA (purple) was subcloned into the luciferase vector pGL3 and transfected it together with *Renilla* luciferase control plasmid into primary embryonic chick cardiac myocytes. Firefly luciferase activity was normalized to *Renilla* luciferase activity. Basal luciferase activity of the -77 bp basic promoter (black) was given a value of 1. The results of the deletion analysis indicates the presence of three functional domains in the 5' flanking sequence of the *Popdc2* gene: an enhancer (light blue) between -1750 and approx. -1000, a silencer element (labeled in red) between -517 and -418, and a promoter proximal element (labeled in green) which is located between -418 and -77 nt. Luciferase activity is depicted as fold-increased above the mean of empty pGL3 plasmid expression (control).

To learn about transcription factors, which might bind to the promoter proximal sequence Genomatix MatInspector (<http://www.genomatic.de/products/MatInspector/index.html>) software was utilized. With help of this software a large library of matrix descriptions for transcription factor binding sites was screened and two binding sites for GATA4 and SRF were predicted. In order to analyse these two sites for functional contribution to transcriptional activity they were mutagenized in the context of the -417/+550 bp construct as well as a shorter deletion construct (-217/+550) and both constructs were tested in chick cardiac myocytes. The SRF binding site (SRE) mutation resulted in a loss of 50 % of the luciferase activity obtained with the wild-type constructs (Fig. 41). Mutagenesis of the GATA binding site in addition to the SRE mutation using the -218/+550 construct lead to a further reduction of luciferase activity. This demonstrated the importance of these two binding sites for *Popdc2* promoter activity. However since transcriptional activity was not abolished completely by mutating both SRE and GATA4 binding sites, additional element(s) involved in transcriptional control of *Popdc2* basic promoter were predicted but are currently undefined.

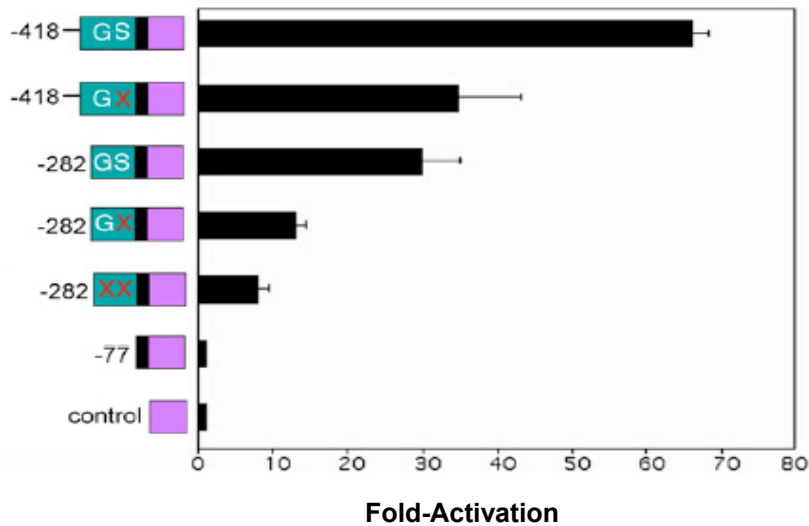


Figure 41. Mutagenesis of GATA4 (G) and SRF (S) binding sites. Putative binding sites were mutagenized (X) in the -418, or -282 DNA fragment of the *Popdc2* gene. Luciferase activity is depicted as fold-increased above the mean of empty pGL3 plasmid expression (control).

To corroborate the mutagenesis results we tested whether the SRE physically can bind SRF in vitro. We therefore performed a gel retardation assay (Fig. 42). In this experiment nuclear extracts of mouse hearts mixed with radioactively labelled double-stranded oligonucleotides containing the *Popdc2* SRE resulted in a band-shift. To demonstrate specificity, a competition experiment employing a 100-fold higher concentrated unlabeled SRE oligonucleotide resulted in loss of the band-shift. The band was also missing in case of a SRE mutant oligonucleotide (harbouring the same mutation as in the transcription assay). Finally, an antibody directed against mouse SRF was added to the band-shift reaction producing a supershift. Altogether these results prove that at least in vitro, SRF can bind the SRE in the promoter-proximal region of *Popdc2*.

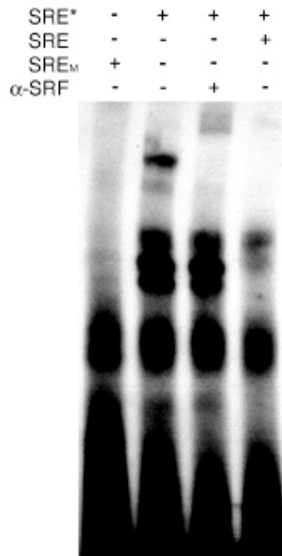


Figure 42. Gel retardation assay to determine binding of SRF to the CARg box identified in the *Popdc2* promoter. A nuclear extract of mouse embryonic heart was prepared and was incubated with a double-stranded wild type (SRE*) or mutant (SRE_M) oligonucleotide that was end-labelled by ³²P γ-ATP. As a control the nuclear extract was preincubated with a 100x concentrated unlabeled wild type oligo-nucleotide (SRE). Evidence for the identity of SRF was provided by adding an SRF antibody to the nuclear extract, which produced a supershift.

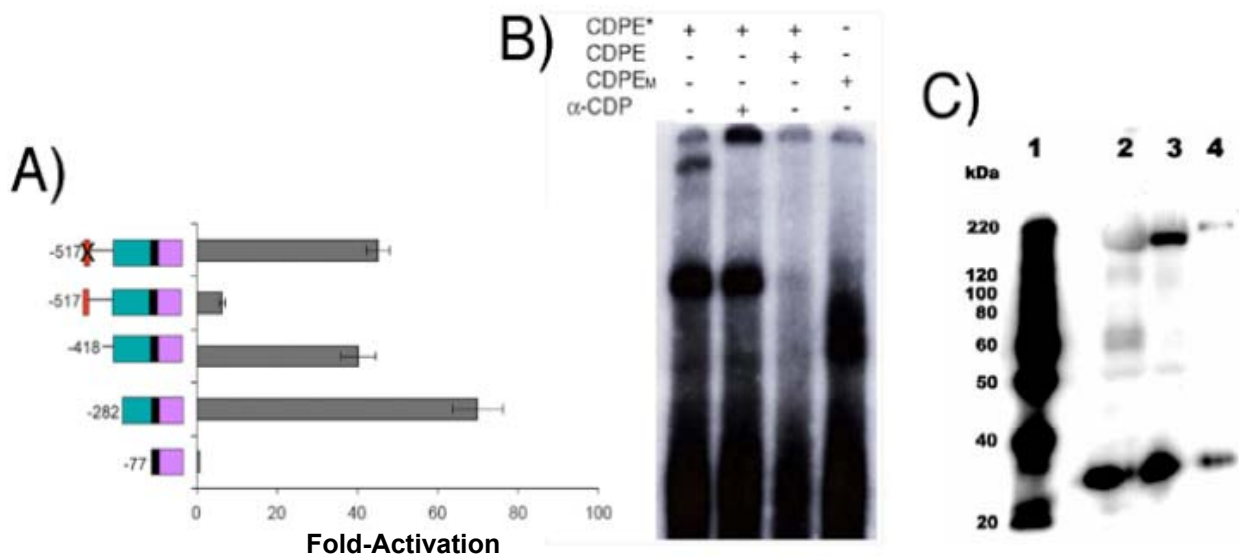


Figure 43. The CDP binding site functions as a silencer element in the *Popdc2* promoter (done by F. David, Studienarbeit). (A) Reporter gene analysis. (B) Gel retardation assay to demonstrate CDP binding. (C) Western blot analysis. (1) Molecular weight marker, (2-4) nuclear extracts of (2) 14.5 embryonic heart, (3) neonatal heart, (4) C2C12 cells.

As indicated by the deletion analysis a negative regulatory element is probably located between -517 and -418 in the *Popdc2* promoter. The database for predicted binding sites of known transcriptional repressors was screened. This resulted in the identification of a binding site for the transcriptional repressor CCAAT displacement protein (CDP). All three binding sites, for SRF, GATA and CDP transcription factors were also identified in similar location in the 5' flanking region of the *Popdc2* gene of

zebrafish and chick. This suggests that these sites are probably functionally conserved.

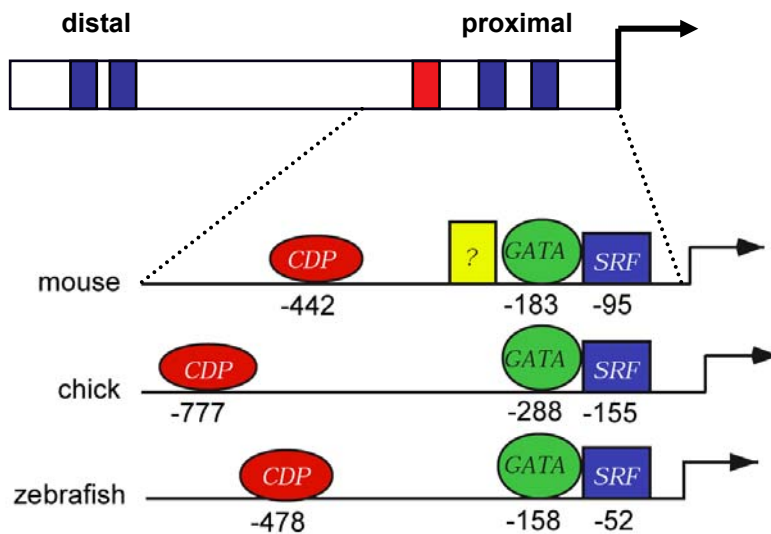


Figure 44. Popdc2 5' flanking region of the mouse, chick and zebrafish. All three species in the similar order contain in the proximal part of the sequence predicted binding sites for SRF, GATA and CDP transcription factors.

In order to investigate the functional activity of the putative CDP binding site, it was mutated using the -517/+550 deletion construct and used in transfection assays. Consistent with the previous results (Fig. 40) transfection of the -517/550 construct resulted in very low luciferase activity (Fig.43 A). In contrast, the -517 construct harbouring a mutated CDP binding site showed luciferase activity which was comparable to the -417/550 construct (Fig. 43 A), suggesting that the CDP binding site is a likely candidate for the silencer activity that was initially mapped. These results were corroborated by a gel retardation assay (Fig. 43 B). Binding of CDP to the labelled WT oligo was seen and a band-shift was obtained when an antibody against CDP was added. In this experiment two different complexes were formed by CDP. This is probably due to fact that CDP is posttranscriptionally modified by proteolysis. A Western blot analysis (Fig.43 C) demonstrated the presence of a major 200 kDal species, as well as several smaller immunoreactive protein bands that were especially prominent in the embryonic nuclear extract. This probably reflects proteolytical processing of CDP during embryogenesis. Remarkable, only in the case of the neonatal nuclear extract a strong 200 kDal signal was observed. This probably

might explain our inability to perform a gel retardation assay with the embryonic cardiac extract as well as using nuclear extract of C2C12 myoblasts.

4.4.2 The 1.7 kb promoter fragment is sufficient to recapitulate *Popdc2* gene expression in transgenic mouse embryos

Experiments with the 5' flanking sequence of the *Popdc2* gene demonstrated that 1.7 kb fragment has at least three regulatory domains, two of which bind positive transcriptional regulators among which we have identified SRF and a GATA4 binding site in the promoter proximal region. In addition a binding site for a transcriptional repressor, which has been tentatively identified as being CDP is present in the *Popdc2* promoter. These experiments thus far have however been performed by transient transfection in cultured chick embryonic cardiac myocytes, and thus we do not know whether the observed promoter activity is also seen in the in vivo context of a mouse embryo. In order to test to what extent this 1.7 kb fragment contributes to the transcriptional activity during mouse embryonic development, a transient transgenic expression was performed. This part of the project was done in collaboration with Prof. Dr. Brian Black from the Cardiovascular Research Institute at UCSF. 1.7 kb sequence was subcloned into an appropriate vector with a LacZ reporter gene and used for blastocyst injections. To our surprise the resulting LacZ staining pattern in the transgenic embryos resembled the LacZ expression in the *Popdc2* KO model (Fig. 45 A-F). This data suggests that the 1.7 kb of promoter region contains most transcriptional control elements needed for endogenous *Popdc2* expression during early mouse embryogenesis. After a short time of staining LacZ was readily seen in the myocardium. Overnight staining resulted in LacZ expression in the entire lateral plate mesoderm. In both cases, LacZ knock-in construct and transgenic 1.7 kb promoter construct, expression was also observed in branchial arches. The only difference between the LacZ knock-in and the transgenic construct was seen in case of the somites. In contrast to strong somite expression in case of the LacZ knock-in construct no expression was driven by the 1.7 kb transgene.

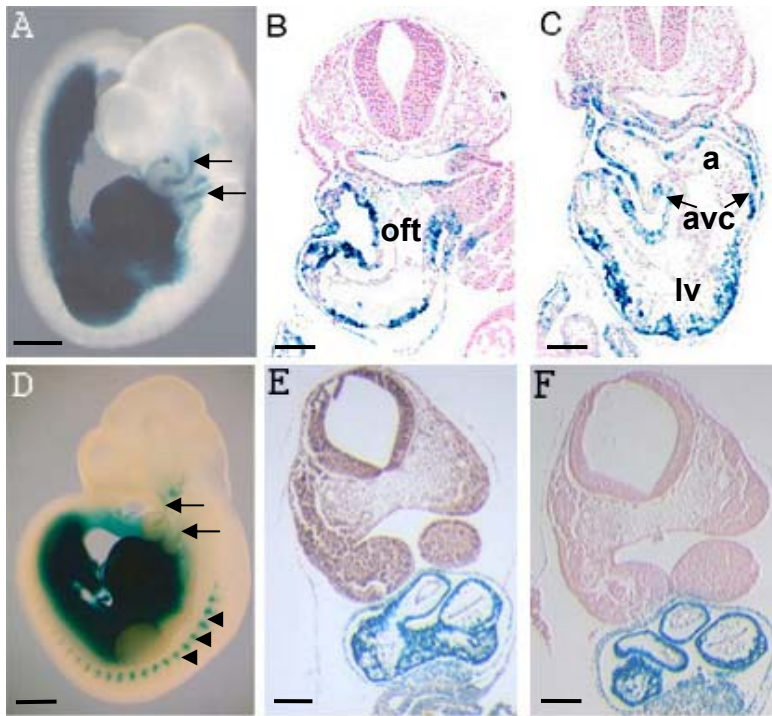


Figure 45. A 1.7kb fragment is sufficient to recapitulate *Popdc2* gene expression in transgenic mouse embryos. (A) Whole-mount LacZ labelling of E9.5 embryo revealing expression of the transgene in lateral plate mesoderm, heart and pericardium as well as of facial skeletal muscle precursors (arrows). (B-C) Transversal sections of the embryo shown in (A) reveal myocardial expression of the entire myocardium as well as the pericardium and the septum transversum. No expression is seen in the endocardium. (D) Whole-mount LacZ staining of *Popdc2* E10.5 KO mouse embryo. In addition to LacZ expression pattern described in (A) there is strong LacZ labelling of somites (arrowheads). a, atrium; lv, left ventricle; rv, right ventricle; v, ventricular chamber; oft, outflow tract. Scale bars: A and D, 500 μ m; B, C, E and F, 200 μ m.

The 1.7 kb fragment was mutagenized in the CDP binding site like in the -517/+550 deletion construct shown in the Fig. 43 A and tested for transgenic expression in the mouse embryo (Fig. 46 A). Surprisingly, no difference in the LacZ expression pattern was observed in comparison to the WT construct (Fig. 45 A).

The -418bp sequence, which in transfection assays demonstrated strong luciferase activity (Fig. 40), was also subcloned into a LacZ reporter vector and used for oocyte injections. LacZ expression was weak and found only in the heart (Fig. 46 B). However, other expression domains might have been missed due the overall weak activity of this fragment.

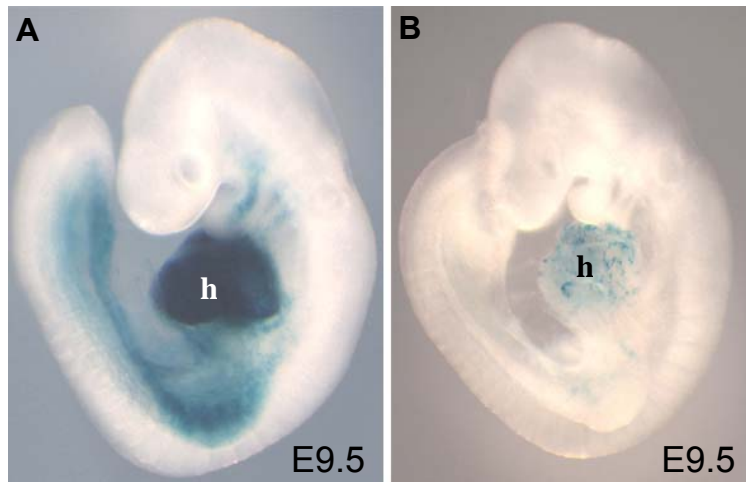


Figure 46. (A, B) Whole-mount LacZ labelling of E9.5 transgenic embryo (A) CDP mutation in a 1.7kb fragment does not change LacZ expression pattern and almost recapitulates ones of a *Popdc2-LacZ* allele in KO mouse (Fig. 45 A). (B) A -418bp fragment of the *Popdc2* gene 5' flanking sequence results in a weak LacZ expression in the heart. h, heart.

The WT 1.7kb fragment was also utilized for electroporation in early chick embryos. For this purpose the left pericardial coelom was microinjected with a LacZ reporter construct. In order to identify the transfected cells a GFP reporter construct was co-electroporated. The 1.7kb fragment of the mouse promoter region was sufficient to drive expression in the chicken heart (Fig. 47 A-C). Remarkably, in both experiments, electroporation and deletion analysis transfected into cultured cardiac myocytes, DNA sequences derived from the mouse were transcriptionally active in the chick. Which suggests a high evolutionary conservation of the *Popdc2* promoter region.

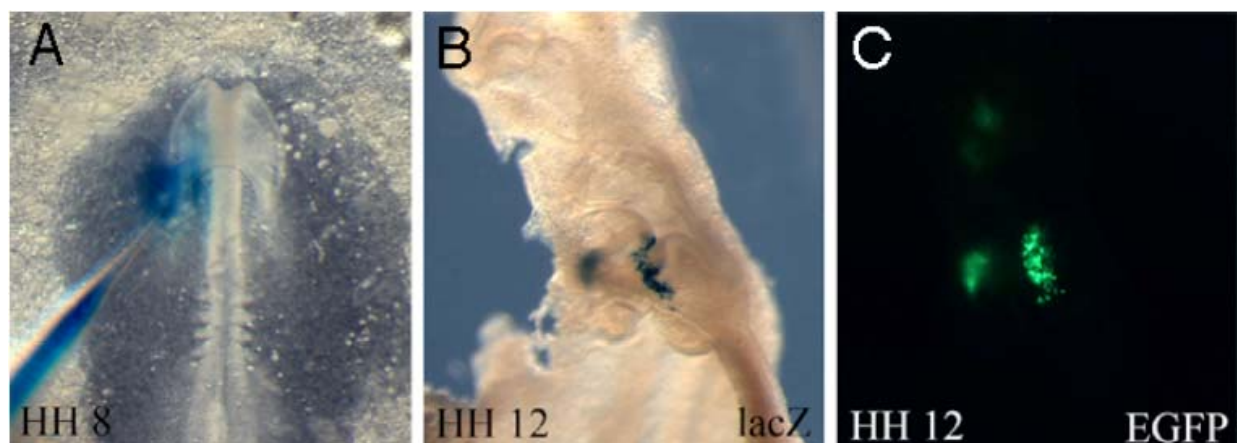


Figure 47. A 1.7kb DNA fragment is sufficient to drive expression in the myocardium of transgenic chick embryos (done by J. Schlütter). (A) Injection of DNA into the left pericardial coelom. (B) LacZ expression in the primitive ventricle. (C) GFP staining.

Taken together these data suggest that elements responsible for LacZ expression in the heart, lateral plate mesoderm and branchial arches at E9.5 are located in the Popdc2 promoter between nt -1 and -1750. The basic promoter, which displays strong transcriptional activity in cell culture experiments and contains SRF and GATA4 binding sites was not sufficient to confer strong LacZ activity *in vivo*. A CDP binding site located at nt -517, which also showed functional importance in cell culture did not affect gene expression in the E9.5 heart. However this construct might show altered expression patterns at later stages of development or in the postnatal animal. Full promoter activity requires an as yet poorly characterized enhancer, which is localized between -1000 and -1750. A deletion series has been produced recently and preliminary analysis points to an enhancer of about 100 bp length (A. Pompl and A. Froese, unpublished). However, further work is required to identify the essential binding sites in this sequence.

5. Discussion

5.1 *Popdc2* knockout mouse

In this work a knockout mouse for the *Popdc2* gene was generated. The expression pattern of the LacZ reporter was found to be identical to that of the endogenous *Popdc2* gene. Strong expression of the *Popdc2-LacZ* allele was present in the heart. Very strong β -gal activity was found in the different elements of the cardiac conduction system (CCS). Analysis of the CCS in the *Popdc2* knockout mouse revealed structural abnormalities in the sinus node. Moreover, the mutant animals developed in an age-dependent manner a stress-induced bradycardia. Thus, *Popdc2* mutant mice are a novel animal model for the sick sinus syndrome in humans, a condition which is a major indicator for the implantation of electronic pacemakers.

5.1.1 *Popdc2* gene inactivation

The main aim of this work was to generate and characterize a *Popdc2* knockout mouse model. For the generation of a *Popdc2* deficient mouse a targeting construct harbouring a LacZ reporter gene was placed into the *Popdc2* locus by homologous recombination in ES cells. The targeting construct designed for this purpose included two homologous arms, flanking a pgk-neo selection cassette and a LacZ reporter gene. Another cassette coding for thymidine kinase located downstream of the right arm was used for negative selection. After homologous recombination the coding sequence of the first exon of *Popdc2* was replaced by the sequence between the two homology arms of the targeting construct. Directly downstream of the *Popdc2* start codon the LacZ reporter gene having a FLAG-tag and a nuclear localization signal (NLS) was placed. CMV poly(A) signal located at the 3' end of the LacZ is required for efficient translation. To avoid any change in the regulation of the *Popdc2* gene the first intron as well as 5' untranslated (UTR) region were kept intact.

ES clones, which survived both positive and negative selection were further analysed. The DNA region, which includes both the endogenous 5' UTR and transgenic sequences, was PCR amplified and in frame sequences of all elements of interest (*Popdc2* start codon, FLAG-tag, NLS and β -gal start codon) were verified by sequencing. ES colonies, which also possessed appropriated size, shape and spacing were chosen for the morula aggregation step.

Nine chimeras were yielded by aggregation of the ES cells clones with the CD1 morulae. Two female chimeras were discarded. Male chimeras were crossed with C57-Bl6J female mice. Three male chimeras were infertile. There are few possible explanations for this observation. First of all it could happen due to insufficient contribution of the male ES cells to gonad formation in the chimeric mouse derived from the male morulae. In such case probability that developing germ cells will carry genetic information derived from the ES cells is very low. Second, it could happen when male ES cells have not fully overtaken the forming gonads developing from the female morulae. Such mice develop different forms of hermaphroditism and are not fertile.

One of the male chimeras was however fertile and the F1 generation derived from this mouse proved to carry the transgenic allele. Homozygous i.e. *Popdc2* KO mice resulted from intercrossing of heterozygous mice and made up 25% of all mice born which correlated well with the expected Mendelian rate and suggest that *Popdc2* has no critical role during development. Homozygous *Popdc2* null mice were alive and fertile. Northern blot analysis demonstrated absence of any aberrant transcript derived from the residual *Popdc2* gene in heart, bladder and skeletal muscles. Moreover histological analysis of several organs of newborn and adult mice did not reveal any obvious difference between homozygous and WT animals. Based on the fact that in many vertebrates and invertebrates the *Popdc* expression is conserved and that highly conserved genes usually play critical roles, it was expected that *Popdc2* KO mouse would display prominent disorders. Absence of any obvious phenotype probably is due to compensation of the absence of *Popdc2* function by the other two members of the *Popdc* gene family. This hypothesis is supported by the fact that all three genes have a similar structure and an overlapping pattern of expression (Andree et al., 2000) although RT-PCR analysis in *Popdc2* KO mice demonstrate no compensation of the *Popdc2* loss by increased expression of the *Popdc1* and *Popdc3*.

Some of the *Popdc2* KO mice similar to *Popdc1* null mutants, displayed by the age of 2 months a typical whistling sound when getting disturbed. However no pathological alterations were detected in the lungs, diaphragm and bronchi which could also be potentially involved in this phenomenon. Another explanation, which we can think of

to explain this phenotype, could be a neurological defect. However in contrast to *Popdc1*, *Popdc2-LacZ* expression and RT-PCR analysis revealed no expression in the brain or spinal cord.

Retarded ability of *Popdc1* KO mice to regenerate damaged skeletal muscles (Andree et al., 2002) is a phenotype which is likely to be present also in *Popdc2* KO mice. Both genes have a very similar expression pattern in skeletal muscle.

Preliminary anatomical and histological examinations revealed mild cardiac hypertrophy in *Popdc2* KO mice. Means heart/body weight ratios of *Popdc2* KO mice were significantly higher than that of WT mice. Moreover, the expression of hypertrophy markers such as ANF, GATA-4 and β -MHC were elevated. In contrast to *Popdc2* in the *Popdc1* null mutant no hypertrophy was detected under baseline conditions. Likewise RT-PCR analysis of GATA-4 and ANF in *Popdc1* KO mice demonstrated no increased expression in mutant hearts (Andree et al., 2002). The difference in *Popdc1* and *Popdc2* postnatal cardiac phenotypes probably is reflected by the different postnatal pattern of expression of these two genes. Expression of the *Popdc2* in the heart postnatally does not decline, whereas expression of *Popdc1* in ventricular tissue shows a rapid and dramatic decline in the early postnatal period (Andree et al., 2002).

5.1.2 Analysis of *Popdc2-LacZ* expression in development and postnatally and comparison with *Popdc1-LacZ* expression

Alignments of the mouse *Popdc2* and *Popdc1* protein sequences demonstrated high similarity (Andree et al., 2000). Both KO mice, *Popdc2* and *Popdc1* when getting disturbed displayed heavy breathing with a typical whistling sound. Also the expression pattern of both genes and the corresponding knock-in *LacZ* alleles are very similar.

As previously reported the *Popdc1-LacZ* gene was first detected at E7.5 in the mesoderm of the cardiac crescent (Andree et al., 2002). The first *Popdc2-LacZ* expression was already seen at E6.0 in the cells of the visceral layer of extra-embryonic mesoderm and at E7.0 in the allantois, embryonic mesoderm and in the node. At E7.5 *Popdc2-LacZ* and *Popdc2* (Andree et al., 2000) expression was observed in the cardiac crescent similar to that of the *Popdc1-LacZ* gene (Andree et al., 2002) and in the amnion.

At E10.5, both, *Popdc1-LacZ* and *Popdc2-LacZ* are expressed in cardiac myocytes of both atrial and ventricular chambers, as well as in somites, myotome and branchial arches. *Popdc2-LacZ* was also seen in dorsal mesocardium, ventral foregut, body wall, pericardium and transiently in the proepicardium. Interestingly, a recently published study of the chick revealed the absence of *Popdc1* protein in the proepicardium, epicardium, or the smooth muscle layer of the coronary vessels at any time point during development (Torlopp et al., 2006). Likewise *Popdc2* expression was found to be absent from proepicardium or epicardium (Breher et al. 2004). *Popdc1*, but not *Popdc2* at E10.5 was detected in a posterior domain within the limb. *Popdc2* but not *Popdc1* strongly labelled mesothelial cells lining the coelom and extraembryonic tissues. Both *Popdc2* and *Popdc1* beginning at E10.5 are detectable in the developing skeletal muscles, bladder and gut. At E11.5 *Popdc1-LacZ* became downregulated in the trabecular layer, but not in the compact layer myocardium.

At E12.5 prominent expression of the *Popdc2-LacZ* was observed in the coelomic wall as well as in skeletal muscle of the limbs and myotome. As revealed by section Lacz staining of the heart region, at this stage *Popdc2-LacZ* is seen in the myocardium of both compact and trabecular layers and pericardium but not in the epicardium. In contrast to *Popdc2*, *Popdc1* till E11.5 is expressed only in some restricted areas in the dorsal part of the ventricle. Beginning E12.5 *Popdc1* expression is also observed in the ventral half of the ventricles where it is confined to the subepicardial compact layer and absent from the trabeculated area (Andree et al., 2000). Sagittal section through the *Popdc2* embryo at E12.5 demonstrated expression in addition to the heart in skeletal muscle and in smooth muscle cells of the gut and bladder. Section in situ hybridization of *Popdc2* mRNA in this stage resulted in almost identical pattern of expression.

Later at dE13.5 *Popdc1* as revealed by whole mount staining, was found in the heart mainly in the compact layer myocardium and very weak in the trabecular myocardium (Andree et al., 2000). Similar to the *Popdc2-LacZ* expression at E12.5 and later, at E13.5 no *Popdc1-LacZ* expression was seen in the endocardium and pericardium (Andree et al., 2002). Like in the case of *Popdc2-LacZ* no expression of *Popdc1-LacZ* was found in coronary arteries, cardiac valves and the vasculature at this and all

other developmental and postnatal stages. Within the limbs at E13.5 *Popdc1-LacZ* was expressed in peridigital mesenchyme (Andree et al., 2002). Another *Popdc1-LacZ* activity at E13.5 was detected in the smooth muscle of the trachea and in the smooth muscle cells lining the digestive tract (Andree et al., 2002). In contrast to the *Popdc2*, *Popdc1* was also detected in the dorsal root ganglia, and the pancreas anlage (Andree et al., 2002). *Popdc2-LacZ* at E13.5 was identified in the addition to the heart in all skeletal muscles of the trunk and limbs, smooth muscle of the bladder and gut. Staining was also observed in the mesenteric vessels, umbilical vein and both umbilical cord arteries. In skeletal muscles not all cells were labelled by LacZ staining of the *Popdc2* transgene. Negative for LacZ staining are probably unfused myoblast and non-muscle cells. Another population of unstained cells, which were in the close contact with the muscle fibers, are presumably satellite cells.

Expression of the *Popdc1-LacZ* at E14.5 was not much different from *Popdc1-LacZ* expression at E13.5, and expression of the *Popdc2-LacZ* at E17.5 was not much different from *Popdc2-LacZ* expression at E12.5 and at E14.5 (at E14.5 data besides heart staining not shown). Both *Popdc1-LacZ* at E14.5 (A. Fleige, Diplomarbeit) and *Popdc2-LacZ* at dE17.5 were found in heart, skeletal muscle and in smooth muscle cells of the gut and bladder. *Popdc1-LacZ* was also expressed in the pancreas, brain and in the smooth muscle of the esophagus, trachea, bronchi and hypophysis (A. Fleige, Diplomarbeit). *Popdc2-LacZ* at E17.5 also was found to be expressed in the umbilical vein and both umbilical cord arteries.

Postnatally both *Popdc1-LacZ* and *Popdc2-LacZ* are expressed in the heart, skeletal muscle and in the smooth muscle of the digestive tract and bladder. In the brain, in addition to the hypophysis *Popdc1-LacZ* is seen in the hippocampus. *Popdc1-LacZ* activity is also detected in the smooth muscle of the bronchi, aorta and distal parts of the lungs (A. Fleige, Diplomarbeit). *Popdc2-LacZ* in newborns strongly labelled the proximal part of the pulmonary veins. Cells, which were labelled are derived from the secondary heart field and called pulmonary myocardium (Millino et al., 2000).

Expression of the *Popdc1-LacZ* at postnatal day 1 in the heart is in the entire myocardium, being weaker expressed in the atria than in the ventricles (Andree et al., 2002; A. Fleige, Diplomarbeit). Section of the d3, d8, d14 and 3 and 8 months old

hearts stained with LacZ demonstrated an age-dependent reduction of the *Popdc1-LacZ* activity (Andree et al., 2002; A. Fleige, Diplomarbeit). In contrast to *Popdc1*, no age-dependent decrease of the *Popdc2-LacZ* activity was noted. Postnatally, *Popdc2-LacZ* was strongly expressed in both atria and ventricles at all ages tested. Remarkably, in case of both *Popdc1-LacZ* and *Popdc2-LacZ* genes strong expression, which was higher than in working myocardium was observed in case of the adult CCS elements: SA node, AV node, His bundles and bundle branches (Andree et al., 2002; A. Fleige, Diplomarbeit).

As mentioned above both *Popdc1-LacZ* and *Popdc2-LacZ* were found in the digestive tract. Both *Popdc1-LacZ* and *Popdc2-LacZ* were detected in the colon smooth muscle and in the stomach. In contrast to the expression of *Popdc2-LacZ* in the pyloric epithelium *Popdc1-LacZ* in stomach was localized in the smooth muscle layers (A. Fleige, Diplomarbeit).

5.2 Role of *Popdc2* gene in the cardiac conduction system

First signs of a possible cardiovascular disorder in *Popdc2* KO mice were observed after subjecting the animals to physical load. WT and *Popdc2* KO mice were subjected to a swimming exercise and their behaviour was observed. After swimming WT mice moved around and cleaned themselves. In contrast, *Popdc2* KO mice did not move for approximately 10-15min and were heavily breathing. The general anatomical and histological analysis of the heart, diaphragm, lungs and bronchi did not reveal any differences in comparison to WT organs. Since this approach did not provide any explanation for the observed phenotype, we decided to learn more about cardiovascular phenotypes of *Popdc2* KO mice. ECG recorded during and after swimming revealed the presence of a sinus bradycardia in 8 month old *Popdc2* KO mice. Similar results were also obtained in mutant mice under mental stress (air-jet) and isoproterenol injection. In summary, mutant *Popdc2* mice have a stress-induced bradycardia. At present it is unclear why this phenotype develops only at later times of postnatal aging. The Popeye domain has been recently observed to constitute a cAMP-binding domain (unpublished, S. Breher, personal communications) via which it presumably mediates stress signals. In this context it is interesting that the predominant sinoatrial HCN channel isoform HCN4, is gated via cAMP. A cardiac-

specific null mutation for *Hcn4* results in a cardiac arrhythmia under resting conditions, however when these *Hcn4* KO hearts are stimulated with isoproterenol, in contrast to the *Popdc2* KO, they do not show any impairment in heart rate acceleration after beta adrenergic stimulation (Herrmann et. al., 2007). Thus in the *Hcn4* null mutant there is a defect in baseline cardiac activity, while in the *Popdc2* KO animals a stress induced bradycardia is present. Both proteins have a cAMP domain. It therefore will be interesting to learn more about the functional interaction between *Popdc2* and HCN4. In contrast to β -adrenergic stimulation, which apparently is defective in *Popdc2* mutant hearts, parasympathetic stimulation with carbachol did not show any differences between mutant and WT hearts. This results demonstrates specificity, however this finding is somewhat surprising since *Popdc* proteins are able to bind also cGMP, and thus both second messengers are able to bind to *Popdc* proteins, however only cAMP binding appears to be an essential function. Further work including generation of cAMP binding mutants will be an important approach to delineate the functional significance in this matter. Interesting results were also obtained in the experiments with zebrafish morphants. Knockdown of *Popdc1* and *Popdc2* in the SAN using morpholino based approach lead to sinus node dysfunction (unpublished, B. Kirchmaier, Franziska Guenther personal communication).

There are generally two known disorders which may lead to bradycardia: disorders of the SAN and disorders of the AVN. PQ intervals at a fixed heart rate of 600 bpm in 8 month old WT and *Popdc2* KO did not show any significant differences, even after isoproterenol stimulation. Since PQ interval reflects the time between the beginning of atrial depolarisation and the beginning of ventricular depolarisation, it means that no abnormal function in the AVN of the *Popdc2* KO was observed. In contrast the SAN of *Popdc2* KO mice is clearly unable to adapt to stress. In 8 month old *Popdc2* KO mice during the 30 min. resting period immediately after 6min of swimming revealed the presence of sinus pauses. On average 542 sinus pauses occurred in mutant hearts vs. 2 in control mice.

In experiments analyzing heart function under different conditions (physical exercise, mental stress and administration drugs influencing heart rhythmus) mice at three ages 3, 6 and 8 months were utilized. *Popdc2* KO mice at age 8 months were the most affected in all cases. Mice at age 3 months never showed any pathology and

mice at age 6 month displayed only slight alterations in cardiac contractility after imposing stress. The fact that the strongest phenotype was found by 8 month probably reflects an age-dependent process in the SAN. We think that *Popdc2* null mutant is a novel animal model for studying sick sinus syndrome. Taken together results obtained in experiments described above suggested more detailed analysis of the 8 months *Popdc2* KO SAN structure.

Sick sinus syndrome or sinus node dysfunction (SND) is a disorder, which characterized by various manifestations as recorded by ECG including sinus bradycardia, sinus arrest, sinoatrial block, and alternating patterns of bradycardia and tachycardia (Adán and Crown, 2000). Another feature of the SND is inappropriate responses of heart rate during exercise or stress (Benditt et al., 1995). SND is diagnosed in one of every 600 cardiac patients older than 65 years and may account for 50 percent or more of permanent implanted pacemakers in the United States (Rodriguez and Schocken, 1990). There are multiple factors which can cause SND. The most common case is a generative fibrosis of nodal tissue (Wahls, 1985).

Function of the SAN undergoes significant changes in the normal aging process not only in humans but in other mammals as well (Benditt et al., 1995; Alings and Bouman, 1993). These changes become apparent in a slowing of the intrinsic heart rate and increase in the SAN conduction time (Benditt et al., 1995; Alings and Bouman, 1993). One of the explanations of these changes could be alteration in the functions of ion channels and gap junctions. For example, expression of the $\text{Na}_v1.5$ and presence of the I_{NA} in the periphery of the SAN is critical for the transduction of the action potential to the surrounding atrial muscle. In the periphery of the rabbit SAN simultaneously with age-dependent slowing of the action potential upstroke (Alings and Bouman, 1993) there is a loss of I_{NA} in this region. This may serve as a explanation for the increase in SAN conduction time and SAN exit block (Zhang et al., 2007).

$\text{Na}_v1.5$ plays a pivotal role in the generation of action potential in the SAN and in the following propagation of the wave depolarization in the heart (Li et al., 2004). $\text{Na}_v1.5$ is encoded by *SCN5A* and is the subunits of the principal Na^+ channel found in the heart. Importance of the *SCN5A* became obvious after identifying mutations that are associated with cardiac dysfunctions including bradycardias (Tan et al., 2003). Like

other ion channels, $\text{Na}_v1.5$ is found in a multiprotein complex. Activity of the $\text{Na}_v1.5$ channel is regulated by the direct binding of the proteins: ankyrin, fibroblast growth factor homologous factor 1B, calmodulin, Nedd4-like ubiquitin-protein ligases and syntrophin proteins (Abriel and Kass, 2005). *Scn5a* null mutant mice are embryonically lethal. Heterozygous *Scn5a*^{+/-} mice display various heart dysfunctions like impaired atrioventricular conduction, delayed intramyocardial conduction, increased ventricular refractoriness, and ventricular tachycardia with characteristics of reentrant excitation (Papadatos et al., 2002). *Scn5a*^{+/-} mice develop the so called Lenègre and Lev's disease which is characterized by the age-related slowing of the atrial and ventricular conduction of the action potential. Age-related slowing of the impulse propagation was shown to be due to progressive myocardial rearrangement and fibrosis (Royer et al., 2005).

Age-dependent decrease of sodium and pacemaker currents is opposed by an increase in contribution of the L-type calcium current (Baruscotti and Robinson, 2007). Recently it was demonstrated that $\text{Ca}_v1.2$ channel protein decreases with aging and concomitant decrease of SAN activity (Jones et al., 2007). Baruscotti and Robinson (2007) have proposed that the observed age-dependent increase of the L-type calcium current, while expression of the $\text{Ca}_v1.2$ channel protein decreases is probably due to compensation by $\text{Ca}_v1.3$ type. This hypothesis is supported by the fact that $\text{Ca}_v1.3$ (Zhang et al., 2002) is not necessary during early heart development while absence of $\text{Ca}_v1.2$ is lethal.

Age dependent processes in the heart also include alterations in expression of the connexins, which affects its function. For example, in the guinea pig SAN region characterized by the absence of the Cx43 increases approx. 14 times during aging (Jones et al., 2004).

There are already few mouse models known representing sick sinus syndrome. One of them is the *klotho* KO mouse, which displays multiple age-related disorders. *Klotho* was found to be expressed in the SAN. Mice with a *klotho* null mutant gene develop normally until the age of 3 weeks, than gradually become inactive and die at 8-9 weeks of age. Under stress *klotho* KO mice manifest SAN dysfunctions (conduction block or arrest) which result in a high rate of premature death (Takeshita et al., 2004). When isolated, SAN preparations were subjected to β -adrenergic stimulation with isoproterenol, which normally exerts a positive chronotropic effect on the heart, *klotho*

KO mice responded less than WT mice (Takeshita et al., 2004). Parasympathetic stimulation with acetylcholine resulted in significantly greater negative chronotropic effect in *klotho* KO than in WT mice (Takeshita et al., 2004). Despite the presence of a very strong phenotype in the *klotho* KO mice no degenerative structural changes in SAN were identified (Takeshita et al., 2004). The different phenotype of the *klotho* null mutant makes it unlikely that *Popdc2* and *klotho* interact directly but most likely act in different pathways.

Another interesting animal model of the human sick sinus syndrome is the ankyrin B KO mouse. Mice heterozygous for the ankyrin-B gene (*Ank2*) display a similar arrhythmia as humans. Stimulation with catecholamines and/or physical load leads in these mice to sudden death (Mohler et al., 2003). In man loss-of-function variants in *ANK2* (encodes ankyrin-B) results in a dominantly-inherited cardiac arrhythmia, which is characterized by an increased risk for sudden cardiac death. Initially these disorders were referred to type 4 long QT syndromes but later they were categorized as sick sinus syndromes with bradycardia or “ankyrin-B syndromes” (Mohler et al., 2007; Mohler et al., 2003; Mohler et al., 2004).

The *Popdc2-LacZ*, as mentioned above is strongly expressed in the CCS. For the demonstration of the specific *Popdc2-LacZ* expression in the SAN, section cut perpendicular to and through the Crista terminalis was first stained with LacZ and subsequently for the CCS specific marker- AchE activity. Both patterns of staining labelled the same region and therefore *Popdc2* is expressed at high levels in SAN tissue. To demonstrate specificity of the *Popdc2-LacZ* expression in the SAN tissue, whole mount in situ hybridization was performed. LacZ staining of the whole mount interventricular wall preparation revealed *Popdc2-LacZ* expression in both His bundle branches and Purkinje cells.

Whole mount HCN4 staining of the 8 months *Popdc2* KO and WT atrial preparations revealed significant alterations in the SAN structure. A reduction in cell extensions and a significant reduction in the number of sinus node cells were found in the pacemaker center. Moreover, as revealed by 3-D reconstructions of 8 month old *Popdc2* KO and WT SA nodes, there was an approx. 30% reduction of the total SAN volume in *Popdc2* KO mice. Masson's Trichrome staining of sections at different

levels along the superior inferior axis of the SAN demonstrated that this loss was caused by the presence of extensive fibrosis in the inferior part of the *Popdc2* KO SAN. In the superior region on the other hand we noted a reduction in the number of non-muscle cells and an increased volume fraction of sinus node myocytes. At present it is unclear which of these alterations is responsible for the observed phenotype of an age-dependent development of a stress-induced bradycardia.

Loss of inferior SAN myocytes may be directly affecting stress adaptation since it has been shown that the pacemaker center shifts in its relative position under the influence of different physiological stimuli. Especially interesting in this regard is the finding that with adrenergic stimulation there is a pacemaker shift towards the inferior half of the node (Boyett et al., 2000).

These finding has however been made so far only in rabbits, while in other species there is also an opposite translocation observed i.e. shift to the superior side of the node. The molecular basis for pacemaker shifts is currently unexplained on the molecular level since the receptor density in different parts of the node was found in one study not to be related to this phenomenon (Kurogouchi et al., 2002), while others found a direct correlation between pacemaker center and receptor density (Beau et al., 1995).

Figure 48 graphically depicts the possible functional role of the *Popdc2* based on the predictions and results obtained so far. *Popdc2* is a transmembrane protein with C-terminus located in cytoplasm. In all three proteins *Popdc1*, *Popdc2* and *Popdc3* N-terminus N-glycosylation sites were predicted and in the case of *Popdc1* experimentally shown to be functional and extracellularly located (Knight et al. 2003). *Popdc2* protein is localized to the plasma membrane as a dimer with a dimerization motive as part of the Popeye domain located in the cytoplasm. Figure 48 shows that when epinephrine binds to its receptor, it associates with a heterotrimeric G protein, which ultimately results in the activation of adenylyl cyclase. and a rise in the cytoplasmic concentration of cAMP. We propose that cAMP binds among other proteins also to the Popeye domain of the three *Popdc* proteins. Binding of the cAMP probably changes the conformation of *Popdc* proteins. Associated proteins might alter their interaction or get activated. We have evidence that a downstream target of *Popdc* signalling is a potassium channel. This interaction might have a direct effect

on the membrane potential. Since the closure of potassium channels raises the resting potential, it is possible that the beta adrenergic-mediated frequency adaptation in sinus node cells may be regulated via potassium channels.

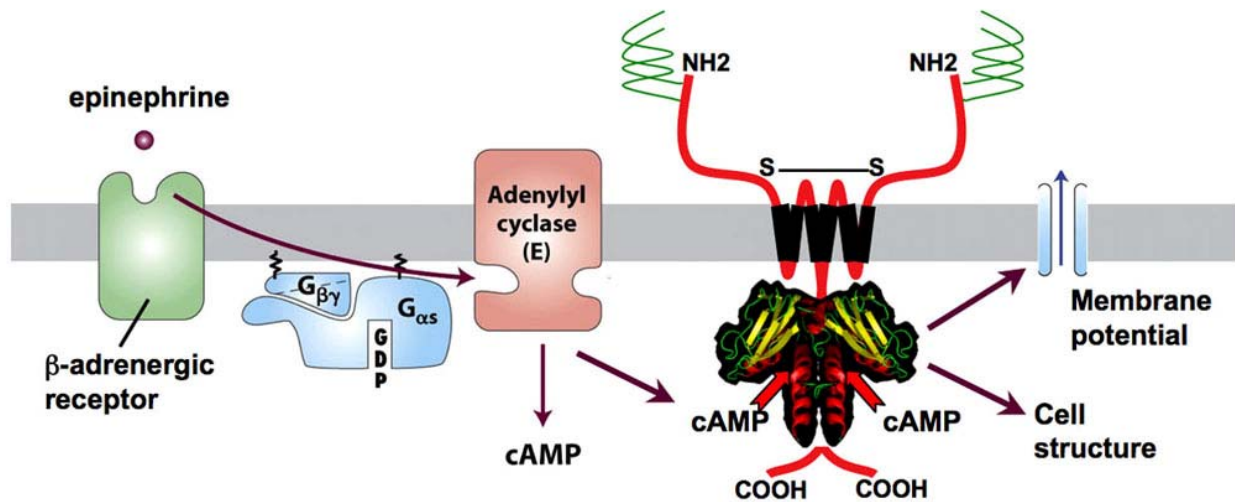


Figure 48. Schematic representation of the Popdc2 protein location, structure and possible function in CCS.

Further work is required to elucidate this phenomenon and to relate it to the here observed loss in the stress adaptation.

5.3 Molecular control of *Popdc2* expression

Another part of this work was devoted to the analysis of the *Popdc2* promoter. In this project 1750bp sequence of the *Popdc2* promoter was identified to contain conserved sequences and therefore further functionally analyzed. Using appropriate software multiple binding site for different transcription factors were predicted. Among these, binding sites for GATA4 and SRF transcription factors, which are known to activate many cardiac tissue-restricted genes, have been chosen for initial analysis. Site directed mutagenesis of GATA4 and SRF binding sites, which are located between -418 and -77 nt demonstrated functional importance of these two elements as was demonstrated by transfection of the corresponding constructs using a luciferase reporter gene into chick primary culture.

Another interesting candidate for regulation of the *Popdc2* expression is the transcriptional repressor CCAAT displacement protein (CDP). CDP factors are known to be expressed in muscle and heart (Andres et al., 1992) however its function in

these tissues is not clear until today. CDP has been shown to physically bind to the *Popdc2* promoter and suppress reporter gene activity in chick primary myocytes. Transfection of a CDP mutant revealed gain of promoter activity, suggesting that CDP might act as transcriptional repressor in the context of the *Popdc2* promoter. Indeed that is the property in the context of many other genes (Nepveu, 2001).

In order to test this concept in the *Popdc2* promoter we have generated a mouse that harboured a construct which lacked a functional CDP binding site. At the age of E9.5 the CDP mutant and wild type promoter resulted in identical expression patterns. Thus, CDP probably does not play an important role during the early phase of cardiac development. However this may be different at later stages of development, which so far have not been studied. CDP might be differentially expressed in the myocardium and especially be differentially expressed in working myocardium.

Transgenic mice harbouring a LacZ construct with the 1.7kb *Popdc2* promoter sequence displayed β -gal expression at E9.5 similar to that of the endogenous *Popdc2* promoter. The only difference between the transgenic construct and the endogenous pattern was the absence of LacZ staining in somites in case of the promoter construct. This suggests that the 1.7 kB promoter fragment contains the sequences important for expression in cardiac myocytes, facial muscles and mesothelial cells in the coelomic wall. However, the regulatory elements important for expression in somites are located elsewhere. There are many examples that expressions of genes that are coexpressed in cardiac and skeletal muscle are regulated by independent promoter regions. This for example holds true for the cardiac Troponin T promoter (Parmacek et al., 1994). In this regard it is highly significant that in the first intron a conserved sequence is present, which is a strong candidate for the skeletal muscle enhancer. Further work using transgenic lines will reveal which of the different conserved sequences that we have identified is important for regulating *Popdc2* during development but also in the adult and under pathophysiological conditions.

All transgenic mice in this project so far were analysed at E9.5 only, thus we do not know, which effect the different point mutations might have on the expression pattern

at later stages of development. Stable lines would be an appropriate solution for a more comprehensive expression study at different embryonic stages and postnatally. Further analysis is required to answer the question what elements of the *Popdc2* promoter are needed to resemble the endogenous expression pattern in the myocardium and in the CCS. Also how regulation of *Popdc2* expression in extracardiac tissue like stomach epithelium and skeletal and smooth muscle occurs should be determined.

Between -1750 and -1000nt according to the transfection data a region is located with significant enhancer activity. Within this region predicted binding sites for Mef2, Tbx, Hand and Nkx transcription factors are located. Mef2, Tbx, Hand and Nkx are all implicated heavily in cardiac gene regulations (Cripps and Olson, 2002). Which of these transcription factors are involved in the *Popdc2* gene regulation in the cardiac tissue has to be clarified.

Popdc2 KO mouse model described in this work in many respects is similar to the *Popdc1* KO mice previously produced in our lab. Both mouse models were extensively studied and revealed very interesting phenotypes. These phenotypes raised many questions which have still to be answered. However the most interesting question is about the phenotype of a mouse with inactivated all three *Popdc* genes. There is significant similarity between the *Popdc* genes sequences and *Popdc* proteins features. There is also significant redundancy between pattern of the *Popdc* genes expressions as well as *Popdc1* and *Popdc2* KO mice phenotypes. All these facts make us believe that such a triple KO mouse model will be very informative and will be an essential contribution to the study of the *Popdc* gene family.

6. References

Abriel H, Kass RS. (2005) Regulation of the voltage-gated cardiac sodium channel Nav1.5 by interacting proteins. *Trends Cardiovasc Med.* 15:35-40.

Adán V, Crown LA. (2003) Diagnosis and treatment of sick sinus syndrome. *Am Fam Physician.* 67:1725-32.

Alcolea S, Theveniau-Ruissy M, Jarry-Guichard T, Marics I, Tzouanacou E, Chauvin JP, Briand JP, Moorman AF, Lamers WH, Gros DB. (1999) Downregulation of connexin 45 gene products during mouse heart development. *Circ Res* 84:1365-1379.

Alings AM, Bouman LN. (1993) Electrophysiology of the ageing rabbit and cat sinoatrial node a comparative study. *Eur Heart J.* 14:1278-88.

Andree B, Hillemann T, Kessler-Icekson G, Schmitt-John T, Jockusch H, Arnold HH, Brand T. (2000) Isolation and characterization of the novel popeye gene family expressed in skeletal muscle and heart. *Dev Biol* 15:371-82.

Andree B, Fleige A, Arnold HH, Brand T. (2002) Mouse Pop1 is required for muscle regeneration in adult skeletal muscle. *Mol Cell Biol* 22:1504-12.

Arsenian S, Weinhold B, Oelgeschlager M, Ruther U, Nordheim A. (1998) Serum response factor is essential for mesoderm formation during mouse embryogenesis. *EMBO J* 17:6289-6299.

Baldini A. (2004) DiGeorge syndrome: an update. *Curr Opin Cardiol* 19:201-204.

Bamshad M, Lin RC, Law DJ, Watkins WC, Krakowiak PA, Moore ME, Franceschini P, Lala R, Holmes LB, Gebuhr TC, Bruneau BG, Schinzel A, Seidman JG, Seidman CE, Jorde LB. (1997) Mutations in human TBX3 alter limb, apocrine and genital development in ulnar-mammary syndrome. *Nat Genet* 16:311-5.

Barber TD, Barber MC, Tomescu O, Barr FG, Ruben S, Friedman TB. (2002) Identification of target genes regulated by PAX3 and PAX3-FKHR in embryogenesis and alveolar rhabdomyosarcoma. *Genomics* 79:278-84.

Baruscotti M, Robinson RB. (2007) Electrophysiology and pacemaker function of the developing sinoatrial node. *Am J Physiol Heart Circ Physiol*. 293:H2613-23

Basson CT, Bachinsky DR, Lin RC, Levi T, Elkins JA, Soultis J, Grayzel D, Kroumpouzou E, Traill TA, Leblanc-Straceski J, Renault B, Kucherlapati R, Seidman JG, Seidman CE. (1997) Mutations in human TBX5 [corrected] cause limb and cardiac malformation in Holt-Oram syndrome. *Nat Genet* 15:30-5.

Beau SL, Hand DE, Schuessler RB, Bromberg BI, Kwon B, Boineau JP, Saffitz JE. (1995) Relative densities of muscarinic cholinergic and beta-adrenergic receptors in the canine sinoatrial node and their relation to sites of pacemaker activity. *Circ Res*. 77:957-63.

Benditt DG, Sakaguchi S, Goldstein MA, Lurie KG, Gornick CC, Adler SW. (1995) Sinus node dysfunction: pathophysiology, clinical features, evaluation, and treatment. Zipes DP, Jalife J. *Cardiac electrophysiology. From cell to bedside*. 2nd ed. Philadelphia, PA: WB Saunders. 1215–1247

Biben C, Weber R, Kesteven S, Stanley E, McDonald L, Elliott DA, Barnett L, Koentgen F, Robb L, Feneley M, Harvey RP. (2000) Cardiac septal and valvular dysmorphogenesis in mice heterozygous for mutations in the homeobox gene *Nkx2-5*. *Circ Res*. 87:888-95.

Blaschke RJ, Hahurij ND, Kuijper S, Just S, Wisse LJ, Deissler K, Maxelon T, Anastassiadis K, Spitzer J, Hardt SE, Schöler H, Feitsma H, Rottbauer W, Blum M, Meijlink F, Rappold G, Gittenberger-de Groot AC. (2007) Targeted mutation reveals essential functions of the homeodomain transcription factor *Shox2* in sinoatrial and pacemaking development. *Circulation*. 115:1830-8.

-
- Blaschke RJ, Monaghan AP, Schiller S, Schechinger B, Rao E, Padilla-Nash H, Ried T, Rappold GA. (1998) SHOT, a SHOX-related homeobox gene, is implicated in craniofacial, brain, heart, and limb development. *Proc Natl Acad Sci U S A.* 95:2406-11.
- Bodmer R. (1993) The gene tinman is required for specification of the heart and visceral muscles in *Drosophila*. *Development.* 118:719-29.
- Boheler KR, Czyz J, Tweedie D, Yang HT, Anisimov SV, Wobus AM. (2002) Differentiation of pluripotent embryonic stem cells into cardiomyocytes. *Circ Res.* 91:189-201.
- Boyett MR, Honjo H, Kodama I. (2000) The sinoatrial node, a heterogeneous pacemaker structure. *Cardiovasc Res.* 47:658-87.
- Brand T. (2003) Heart development: molecular insights into cardiac specification and early morphogenesis. *Dev Biol.* 258:1-19.
- Brand T. (2005) The Popeye domain-containing gene family. *Cell Biochem Biophys.* 43:95-103.
- Breher SS, Mavridou E, Brenneis C, Froese A, Arnold HH, Brand T. (2004) Popeye domain containing gene 2 (*Popdc2*) is a myocyte-specific differentiation marker during chick heart development. *Dev Dyn* 229:695-702.
- Breitbart RE, Liang CS, Smoot LB, Laheru DA, Mahdavi V, Nadal-Ginard B. (1993) A fourth human MEF2 transcription factor, hMEF2D, is an early marker of the myogenic lineage. *Development* 118:1095-106.
- Bruneau BG, Logan M, Davis N, Levi T, Tabin CJ, Seidman JG, Seidman CE. (1999) Chamber-specific cardiac expression of *Tbx5* and heart defects in Holt-Oram syndrome. *Dev Biol.* 211:100-8.

Bruneau BG, Nemer G, Schmitt JP, Charron F, Robitaille L, Caron S, Conner DA, Gessler M, Nemer M, Seidman CE, Seidman JG. (2001) A murine model of Holt-Oram syndrome defines roles of the T-box transcription factor Tbx5 in cardiogenesis and disease. *Cell* 106:709-21.

Favaro, G. (1910) Contributi all'istologica umana e compararata du vasi pulmonari. *Int. Monatschr. Anat. Physiol.* 27:375.

Garcia-Martinez V, Schoenwolf GC. (1993) Primitive-streak origin of the cardiovascular system in avian embryos. *Dev Biol.* 159:706-19.

Chan-Thomas PS, Thompson RP, Robert B, Yacoub MH, Barton PJ. (1993) Expression of homeobox genes Msx-1 (Hox-7) and Msx-2 (Hox-8) during cardiac development in the chick. *Dev Dyn.* 197:203-16.

Chapman DL, Garvey N, Hancock S, Alexiou M, Agulnik SI, Gibson-Brown JJ, Cebra-Thomas J, Bollag RJ, Silver LM, Papaioannou VE. (1996) Expression of the T-box family genes, Tbx1-Tbx5, during early mouse development. *Dev Dyn.* 206:379-90.

Chapman SC, Collignon J, Schoenwolf GC, Lumsden A. (2001). Improved method for chick whole-embryo culture using a filter paper carrier. *Dev Dyn.* 220:284-9.

Chin MT, Maemura K, Fukumoto S, Jain MK, Layne MD, Watanabe M, Hsieh CM, Lee ME. (2000) Cardiovascular basic helix loop helix factor 1, a novel transcriptional repressor expressed preferentially in the developing and adult cardiovascular system. *J Biol Chem.* 275:6381-7.

Christoffels VM, Hoogaars WM, Tessari A, Clout DE, Moorman AF, Campione M. (2004) T-box transcription factor Tbx2 represses differentiation and formation of the cardiac chambers. *Dev Dyn.* 229:763-70.

Creemers EE, Sutherland LB, Oh J, Barbosa AC, Olson EN. (2006) Coactivation of MEF2 by the SAP domain proteins myocardin and MASTR. *Mol Cell.* 7;23:83-96.

Cripps RM, Olson EN. (2002) Control of cardiac development by an evolutionarily conserved transcriptional network. *Dev Biol.* 246:14-28.

Davenport TG, Jerome-Majewska LA, Papaioannou VE. (2003) Mammary gland, limb and yolk sac defects in mice lacking *Tbx3*, the gene mutated in human ulnar mammary syndrome. *Development.* 130:2263-73.

Davidson B, Levine M. (2003) Evolutionary origins of the vertebrate heart: Specification of the cardiac lineage in *Ciona intestinalis*. *Proc Natl Acad Sci U S A.* 100:11469-73.

DeHaan R. (1965) Morphogenesis of the vertebrate heart. In: DeHaan R, Ursprung H (eds) *Organogenesis*. Holt, Rinehart and Winston, New York, pp 377-419.

Delorme B, Dahl E, Jarry-Guichard T, Briand JP, Willecke K, Gros D, Theveniau-Ruissy M. (1997) Expression pattern of connexin gene products at the early developmental stages of the mouse cardiovascular system. *Circ Res.* 81:423-37.

Delorme B, Dahl E, Jarry-Guichard T, Marics I, Briand JP, Willecke K, Gros D, Theveniau-Ruissy M. (1995) Developmental regulation of connexin 40 gene expression in mouse heart correlates with the differentiation of the conduction system. *Dev Dyn.* 204:358-71.

DiAngelo JR, Vasavada TK, Cain W, Duncan MK. (2001) Production of monoclonal antibodies against chicken Pop1 (BVES). *Hybrid Hybridomics.* 20:377-81.

Ellis T, Gambardella L, Horcher M, Tschanz S, Capol J, Bertram P, Jochum W, Barrandon Y, Busslinger M. (2001) The transcriptional repressor CDP (*Cutl1*) is essential for epithelial cell differentiation of the lung and the hair follicle. *Genes Dev.* 15:2307-19.

Evans MJ, Kaufman MH. (1981) Establishment in culture of pluripotential cells from mouse embryos. *Nature.* 292:154-6.

-
- Fire A, Harrison SW, Dixon D. (1990) A modular set of lacZ fusion vectors for studying gene expression in *Caenorhabditis elegans*. *Gene*. 93:189-98.
- Firulli AB, McFadden DG, Lin Q, Srivastava D, Olson EN. (1998) Heart and extra-embryonic mesodermal defects in mouse embryos lacking the bHLH transcription factor Hand1. *Nat Genet*. 18:266-70.
- Fischer A, Schumacher N, Maier M, Sendtner M, Gessler M. (2004) The Notch target genes Hey1 and Hey2 are required for embryonic vascular development. *Genes Dev*. 18:901-11.
- Fischer A, Klattig J, Kneitz B, Diez H, Maier M, Holtmann B, Englert C, Gessler M. (2005) Hey basic helix-loop-helix transcription factors are repressors of GATA4 and GATA6 and restrict expression of the GATA target gene ANF in fetal hearts. *Mol Cell Biol*. 25:8960-70.
- Fishman MC, Chien KR. (1997) Fashioning the vertebrate heart: earliest embryonic decisions. *Development* 124:2099-2117.
- Gessler M, Knobloch KP, Helisch A, Amann K, Schumacher N, Rohde E, Fischer A, Leimeister C. (2002) Mouse gridlock: no aortic coarctation or deficiency, but fatal cardiac defects in Hey2 $-/-$ mice. *Curr Biol*. 12:1601-4.
- Gonzalez-Sanchez A, Bader D. (1990) In vitro analysis of cardiac progenitor cell differentiation. *Dev Biol* 139:197-209.
- Gourdie RG, Harris BS, Bond J, Justus C, Hewett KW, O'Brien TX, Thompson RP, Sedmera D. (2003) Development of the cardiac pacemaking and conduction system. *Birth Defects Res C Embryo Today*. 69:46-57.
- Gourdie RG, Wei Y, Kim D, Klatt SC, Mikawa T. (1998) Endothelin-induced conversion of embryonic heart muscle cells into impulse-conducting Purkinje fibers. *Proc Natl Acad Sci U S A*. 95:6815-8.

Gros D, Dupays L, Alcolea S, Meysen S, Miquerol L, Theveniau-Ruissy M. (2004) Genetically modified mice: tools to decode the functions of connexins in the heart-new models for cardiovascular research. *Cardiovasc Res.* 62:299-308.

Herrmann S, Stieber J, Stöckl G, Hofmann F, Ludwig A. (2007) HCN4 provides a 'depolarization reserve' and is not required for heart rate acceleration in mice. *EMBO* 26:4423-32.

Habets PE, Moorman AF, Clout DE, van Roon MA, Lingbeek M, van Lohuizen M, Campione M, Christoffels VM. (2002) Cooperative action of Tbx2 and Nkx2.5 inhibits ANF expression in the atrioventricular canal: implications for cardiac chamber formation. *Genes Dev.* 16:1234-46.

Hamburger V., Hamilton HL. (1951) A series of normal stages in the development of the chick embryo. *J Morph.* 88:49-92.

Harrelson Z, Kelly RG, Goldin SN, Gibson-Brown JJ, Bollag RJ, Silver LM, Papaioannou VE. (2004) Tbx2 is essential for patterning the atrioventricular canal and for morphogenesis of the outflow tract during heart development. *Development.* 131:5041-52.

Harvey RP. (1996) NK-2 homeobox genes and heart development. *Dev Biol.* 178:203-16.

Harvey RP, Lai D, Elliott D, Biben C, Solloway M, Prall O, Stennard F, Schindeler A, Groves N, Lavulo L, Hyun C, Yeoh T, Costa M, Furtado M, Kirk E. (2002) Homeodomain factor Nkx2-5 in heart development and disease. *Cold Spring Harb Symp Quant Biol.* 67:107-14.

Harvey RP. (2002) Patterning the vertebrate heart. *Nat Rev Genet.* 3:544-56.

Hescheler J, Fleischmann BK, Lentini S, Maltsev VA, Rohwedel J, Wobus AM, Addicks K. (1997) Embryonic stem cells: a model to study structural and functional properties in cardiomyogenesis. *Cardiovasc Res.* 36:149-62.

Hitz MP, Pandur P, Brand T, Kuhl M. (2002) Cardiac specific expression of *Xenopus* Popeye-1. *Mech Dev.* 115:123-6.

Holtzinger A, Evans T. *Gata5* and *Gata6* are functionally redundant in zebrafish for specification of cardiomyocytes. *Dev Biol.* 2007 Dec 15;312(2):613-22.

Hoogaars WM, Engel A, Brons JF, Verkerk AO, de Lange FJ, Wong LY, Bakker ML, Clout DE, Wakker V, Barnett P, Ravesloot JH, Moorman AF, Verheijck EE, Christoffels VM. (2007) *Tbx3* controls the sinoatrial node gene program and imposes pacemaker function on the atria. *Genes Dev.* 21:1098-112.

Hoogaars WM, Tessari A, Moorman AF, de Boer PA, Hagoort J, Soufan AT, Campione M, Christoffels VM. (2004) The transcriptional repressor *Tbx3* delineates the developing central conduction system of the heart. *Cardiovasc Res.* 62:489-99.

Jiang X, Rowitch DH, Soriano P, McMahon AP, Sucov HM. (2000) Fate of the mammalian cardiac neural crest. *Development.* 127:1607–1616.

Jerome LA, Papaioannou VE. (2001) DiGeorge syndrome phenotype in mice mutant for the T-box gene, *Tbx1*. *Nat Genet.* 27:286-91.

Jones SA, Boyett MR, Lancaster MK. (2007) Declining into failure: the age-dependent loss of the L-type calcium channel within the sinoatrial node. *Circulation.* 115:1183-90.

Jones SA, Lancaster MK, Boyett MR. (2004) Ageing-related changes of connexins and conduction within the sinoatrial node. *J Physiol.* 560:429-37.

Jones WK, Sanchez A, Robbins J. (1994) Murine pulmonary myocardium: developmental analysis of cardiac gene expression. *Dev Dyn.* 200:117-28.

Kasahara H, Wakimoto H, Liu M, Maguire CT, Converso KL, Shioi T, Huang WY, Manning WJ, Paul D, Lawitts J, Berul CI, Izumo S. (2001) Progressive atrioventricular conduction defects and heart failure in mice expressing a mutant Csx/Nkx2.5 homeoprotein. *J Clin Invest.* 108:189-201.

Kaufman MH. (2004) *The atlas of mouse development.* London: Oxford Academic press.

Kelly RG, Buckingham ME. (2002) The anterior heart-forming field: voyage to the arterial pole of the heart. *Trends Genet.* 18:210-6.

Kelly RG, Brown NA, Buckingham ME. (2001) The arterial pole of the mouse heart forms from Fgf10-expressing cells in pharyngeal mesoderm. *Dev Cell.* 1:435-40.

Knight RF, Bader DM, Backstrom JR. (2003) Membrane topology of Bves/Pop1A, a cell adhesion molecule that displays dynamic changes in cellular distribution during development. *J Biol Chem.* 278:32872-9.

Ko LJ, Engel JD. (1993) DNA-binding specificities of the GATA transcription factor family. *Mol Cell Biol.* 13:4011-22.

Kondo RP, Anderson RH, Kupersmidt S, Roden DM, Evans SM. (2003) Development of the cardiac conduction system as delineated by minK-lacZ. *J Cardiovasc Electrophysiol.* 14:383-91.

Kruithof BP, van den Hoff MJ, Wessels A, Moorman AF. (2003) Cardiac muscle cell formation after development of the linear heart tube. *Dev Dyn.* 227:1-13.

Kuo CT, Morrisey EE, Anandappa R, Sigrist K, Lu MM, Parmacek MS, Soudais C, Leiden JM. (1997) GATA4 transcription factor is required for ventral morphogenesis and heart tube formation. *Genes Dev.* 11:1048-60.

Kurogouchi F, Nakane T, Furukawa Y, Hirose M, Inada Y, Chiba S. Heterogeneous distribution of beta-adrenoceptors and muscarinic receptors in the sinoatrial node and right atrium of the dog. *Clin Exp Pharmacol Physiol*. 2002 Aug;29(8):666-72.

Ledford AW, Brantley JG, Kemeny G, Foreman TL, Quaggin SE, Igarashi P, Oberhaus SM, Rodova M, Calvet JP, Vanden Heuvel GB. (2002) Deregulated expression of the homeobox gene *Cux-1* in transgenic mice results in downregulation of p27(kip1) expression during nephrogenesis, glomerular abnormalities, and multiorgan hyperplasia. *Dev Biol*. 245:157-71.

Lewandoski M, Wassarman KM, Martin GR. (1997) *Zp3-cre*, a transgenic mouse line for the activation or inactivation of loxP-flanked target genes specifically in the female germ line. *Curr Biol*. 7:148-51.

Li QY, Newbury-Ecob RA, Terrett JA, Wilson DI, Curtis AR, Yi CH, Gebuhr T, Bullen PJ, Robson SC, Strachan T, Bonnet D, Lyonnet S, Young ID, Raeburn JA, Buckler AJ, Law DJ, Brook JD. (1997) Holt-Oram syndrome is caused by mutations in *TBX5*, a member of the Brachyury (T) gene family. *Nat Genet*. 15:21-9.

Li S, Moy L, Pittman N, Shue G, Aufiero B, Neufeld EJ, LeLeiko NS, Walsh MJ. (1999) Transcriptional repression of the cystic fibrosis transmembrane conductance regulator gene, mediated by CCAAT displacement protein/cut homolog, is associated with histone deacetylation. *J Biol Chem*. 274:7803-15.

Li RA, Tomaselli GF, Marban E. (2004) Sodium channels. In Zipes DP, Jalife J, eds. *Cardiac Electrophysiology: From Cell to Bedside*, Philadelphia, PA, Saunders. 1–9.

Lilly B, Galewsky S, Firulli AB, Schulz RA, Olson EN. (1994) D-MEF2: a MADS box transcription factor expressed in differentiating mesoderm and muscle cell lineages during *Drosophila* embryogenesis. *Proc Natl Acad Sci U S A*. 91:5662-6.

Lilly B, Zhao B, Ranganayakulu G, Paterson BM, Schulz RA, Olson EN. (1995) Requirement of MADS domain transcription factor D-MEF2 for muscle formation in *Drosophila*. *Science*. 267:688-93.

Lin Q, Schwarz J, Bucana C, Olson EN. (1997) Control of mouse cardiac morphogenesis and myogenesis by transcription factor MEF2C. *Science*. 276:1404-7.

Lin, S., Zhao, D. and Bownes, M (2002) 43rd Annual Drosophila Research Conference, San Diego, California.

Lints TJ, Parsons LM, Hartley L, Lyons I, Harvey RP. (1993) Nkx-2.5: a novel murine homeobox gene expressed in early heart progenitor cells and their myogenic descendants. *Development*. 119:419-31.

Luong MX, van der Meijden CM, Xing D, Hesselton R, Monuki ES, Jones SN, Lian JB, Stein JL, Stein GS, Neufeld EJ, van Wijnen AJ. (2002) Genetic ablation of the CDP/Cux protein C terminus results in hair cycle defects and reduced male fertility. *Mol Cell Biol*. 22:1424-37.

Mailly F, Berube G, Harada R, Mao PL, Phillips S, Nepveu A. (1996) The human cut homeodomain protein can repress gene expression by two distinct mechanisms: active repression and competition for binding site occupancy. *Mol Cell Biol*. 16:5346-57.

Maltsev VA, Rohwedel J, Hescheler J, Wobus AM. (1993) Embryonic stem cells differentiate in vitro into cardiomyocytes representing sinusnodal, atrial and ventricular cell types. *Mech Dev*. 44:41-50.

Merika M, Orkin SH. (1993) DNA-binding specificity of GATA family transcription factors. *Mol Cell Biol*. 13:3999-4010.

Miano JM, Ramanan N, Georger MA, de Mesy Bentley KL, Emerson RL, Balza RO Jr, Xiao Q, Weiler H, Ginty DD, Misra RP. (2004) Restricted inactivation of serum response factor to the cardiovascular system. *Proc Natl Acad Sci U S A*. 101:17132-7.

Millino C, Sarinella F, Tiveron C, Villa A, Sartore S, Ausoni S. (2000) Cardiac and smooth muscle cell contribution to the formation of the murine pulmonary veins. *Dev Dyn.* 218(3):414-25.

Mohler PJ, Le Scouarnec S, Denjoy I, Lowe JS, Guicheney P, Caron L, Driskell IM, Schott JJ, Norris K, Leenhardt A, Kim RB, Escande D, Roden DM. (2007) Defining the cellular phenotype of "ankyrin-B syndrome" variants: human ANK2 variants associated with clinical phenotypes display a spectrum of activities in cardiomyocytes. *Circulation.* 115:432-41

Mohler PJ, Schott JJ, Gramolini AO, Dilly KW, Guatimosim S, duBell WH, Song LS, Haurogné K, Kyndt F, Ali ME, Rogers TB, Lederer WJ, Escande D, Le Marec H, Bennett V. (2003) Ankyrin-B mutation causes type 4 long-QT cardiac arrhythmia and sudden cardiac death. *Nature.* 421:634-9.

Mohler PJ, Splawski I, Napolitano C, Bottelli G, Sharpe L, Timothy K, Priori SG, Keating MT, Bennett V. (2004) A cardiac arrhythmia syndrome caused by loss of ankyrin-B function. *Proc Natl Acad Sci U S A.* 101:9137-42.

Molkentin JD, Lin Q, Duncan SA, Olson EN. (1997) Requirement of the transcription factor GATA4 for heart tube formation and ventral morphogenesis. *Genes Dev.* 11:1061-72.

Molkentin JD. (2000) The zinc finger-containing transcription factors GATA-4, -5, and -6. Ubiquitously expressed regulators of tissue-specific gene expression. *J Biol Chem.* 275:38949-52.

Moon NS, Berube G, Nepveu A. (2000) CCAAT displacement activity involves CUT repeats 1 and 2, not the CUT homeodomain. *J Biol Chem.* 275:31325-34.

Moorman AF, Houweling AC, de Boer PA, Christoffels VM. (2001) Sensitive nonradioactive detection of mRNA in tissue sections: novel application of the whole-mount in situ hybridization protocol. *J Histochem Cytochem.* 49:1-8.

Morrisey EE, Tang Z, Sigrist K, Lu MM, Jiang F, Ip HS, Parmacek MS. (1998) GATA6 regulates HNF4 and is required for differentiation of visceral endoderm in the mouse embryo. *Genes Dev.* 12:3579-90.

Moskowitz IP, Pizard A, Patel VV, Bruneau BG, Kim JB, Kupersmidt S, Roden D, Berul CI, Seidman CE, Seidman JG. (2004) The T-Box transcription factor Tbx5 is required for the patterning and maturation of the murine cardiac conduction system. *Development.* 131:4107-16.

Mu H, Ohashi R, Lin P, Yao Q, Chen C. (2005) Cellular and molecular mechanisms of coronary vessel development. *Vasc Med.* 10:37-44.

Nepveu A. (2001) Role of the multifunctional CDP/Cut/Cux homeodomain transcription factor in regulating differentiation, cell growth and development. *Gene* 270:1-15.

Neufeld EJ, Skalnik DG, Lievens PM, Orkin SH. (1992) Human CCAAT displacement protein is homologous to the *Drosophila* homeoprotein, cut. *Nat Genet* 1:50-5.

Niu Z, Yu W, Zhang SX, Barron M, Belaguli NS, Schneider MD, Parmacek M, Nordheim A, Schwartz RJ. (2005) Conditional mutagenesis of the murine serum response factor gene blocks cardiogenesis and the transcription of downstream gene targets. *J Biol Chem* 280:32531-8.

Norman C, Runswick M, Pollock R, Treisman R. (1988) Isolation and properties of cDNA clones encoding SRF, a transcription factor that binds to the c-fos serum response element. *Cell* 55:989-1003.

Olson EN, Perry M, Schulz RA. (1995) Regulation of muscle differentiation by the MEF2 family of MADS box transcription factors. *Dev Biol* 172:2-14.

Olson EN, Arnold HH, Rigby PW, Wold BJ. (1996). Know your neighbors: three phenotypes in null mutants of the myogenic bHLH gene MRF4. *Cell* 85:1-4.

Osler ME, Chang MS, Bader DM. (2005) Bves modulates epithelial integrity through an interaction at the tight junction. *J Cell Sci* 118:4667-78.

Papadatos GA, Wallerstein PM, Head CE, Ratcliff R, Brady PA, Benndorf K, Saumarez RC, Trezise AE, Huang CL, Vandenberg JI, Colledge WH, Grace AA. (2002) Slowed conduction and ventricular tachycardia after targeted disruption of the cardiac sodium channel gene *Scn5a*. *Proc Natl Acad Sci U S A*. 99:6210-5.

Parmacek MS, Ip HS, Jung F, Shen T, Martin JF, Vora AJ, Olson EN, Leiden JM. (1994) A novel myogenic regulatory circuit controls slow/cardiac troponin C gene transcription in skeletal muscle. *Mol Cell Biol*. 14:1870-85.

Pennisi DJ, Rentschler S, Gourdie RG, Fishman GI, Mikawa T. (2002) Induction and patterning of the cardiac conduction system. *Int J Dev Biol* 46:765-75.

Plageman TF Jr, Yutzey KE. (2004) Differential expression and function of *Tbx5* and *Tbx20* in cardiac development. *J Biol Chem*. 279:19026-34.

Plageman TF Jr, Yutzey KE. (2005) T-box genes and heart development: putting the "T" in heart. *Dev Dyn*. 232:11-20.

Plageman TF Jr, Yutzey KE. (2006) Microarray analysis of *Tbx5*-induced genes expressed in the developing heart. *Dev Dyn*. 235:2868-80.

Rao E, Weiss B, Fukami M, Rump A, Niesler B, Mertz A, Muroya K, Binder G, Kirsch S, Winkelmann M, Nordsiek G, Heinrich U, Breuning MH, Ranke MB, Rosenthal A, Ogata T, Rappold GA. (1997) Pseudoautosomal deletions encompassing a novel homeobox gene cause growth failure in idiopathic short stature and Turner syndrome. *Nat Genet*. 16:54-63.

Rauschel, F. (1836) "De Arteriarum et Venarum Structura." (monograph) Breslau.

Reese DE, Zavaljevski M, Streiff NL, Bader D. (1999) *bves*: A novel gene expressed during coronary blood vessel development. *Dev Biol*. 209:159-71.

Rentschler S, Zander J, Meyers K, France D, Levine R, Porter G, Rivkees SA, Morley GE, Fishman GI. (2002) Neuregulin-1 promotes formation of the murine cardiac conduction system. *Proc Natl Acad Sci U S A.* 99:10464-9.

Ripley, AN. (2004) Bves function in epithelial movement during development. (Dissertation) Vanderbilt University, Nashville, TN.

Ripley AN, Osler ME, Wright CV, Bader D. (2006) Xbves is a regulator of epithelial movement during early *Xenopus laevis* development. *Proc Natl Acad Sci U S A.* 103:614-9.

Rodriguez RD, Schocken DD. (1990) Update on sick sinus syndrome, a cardiac disorder of aging. *Geriatrics.* 45(1):26-30, 33-6.

Rosenqulst, G.C., and DeHaan, R.L. (1966). Migration of precardiac cells in the chick embryo: a radioautographic study. *Carnegie Inst Washington, Contrib. Embryol.* 38, 111-121.

Rovescalli AC, Asoh S, Nirenberg M. (1996) Cloning and characterization of four murine homeobox genes. *Proc Natl Acad Sci U S A.* 93:10691-6.

Royer A, van Veen TA, Le Bouter S, Marionneau C, Griol-Charhbili V, Léoni AL, Steenman M, van Rijen HV, Demolombe S, Goddard CA, Richer C, Escoubet B, Jarry-Guichard T, Colledge WH, Gros D, de Bakker JM, Grace AA, Escande D, Charpentier F. (2005) Mouse model of SCN5A-linked hereditary Lenègre's disease: age-related conduction slowing and myocardial fibrosis. *Circulation.* 111:1738-46.

Rutenberg JB, Fischer A, Jia H, Gessler M, Zhong TP, Mercola M. (2006) Developmental patterning of the cardiac atrioventricular canal by Notch and Hairy-related transcription factors. *Development.* 133:4381-90.

Sanger F, Nicklen S, Coulson AR. (1977) DNA sequencing with chain-terminating inhibitors. *Proc Natl Acad Sci U S A.* 74:5463-7.

-
- Santaguida M, Nepveu A. (2005) Differential regulation of CDP/Cux p110 by cyclin A/Cdk2 and cyclin A/Cdk1. *J Biol Chem.* 280:32712-21.
- Schott JJ, Benson DW, Basson CT, Pease W, Silberbach GM, Moak JP, Maron BJ, Seidman CE, Seidman JG. (1998) Congenital heart disease caused by mutations in the transcription factor NKX2-5. *Science.* 281:108-11.
- Schultheiss TM, Xydas S, Lassar AB. (1995) Induction of avian cardiac myogenesis by anterior endoderm. *Development.* 121:4203-14.
- Schwartz RJ, Olson EN. (1999) Building the heart piece by piece: modularity of cis-elements regulating Nkx2-5 transcription. *Development.* 126:4187-92.
- Sepulveda JL, Vlahopoulos S, Iyer D, Belaguli N, Schwartz RJ. (2002) Combinatorial expression of GATA4, Nkx2-5, and serum response factor directs early cardiac gene activity. *J Biol Chem.* 277:25775-82.
- Showell C, Binder O, Conlon FL. (2004) T-box genes in early embryogenesis. *Dev Dyn.* 229:201-18.
- Shore P, Sharrocks AD. (1995) The MADS-box family of transcription factors. *Eur J Biochem.* 229:1-13.
- Sinclair AM, Lee JA, Goldstein A, Xing D, Liu S, Ju R, Tucker PW, Neufeld EJ, Scheuermann RH. (2001) Lymphoid apoptosis and myeloid hyperplasia in CCAAT displacement protein mutant mice. *Blood.* 98:3658-67.
- Singh MK, Christoffels VM, Dias JM, Trowe MO, Petry M, Schuster-Gossler K, Burger A, Ericson J, Kispert A. (2005) Tbx20 is essential for cardiac chamber differentiation and repression of Tbx2. *Development.* 132:2697-707.
- Smith DM, Grasty RC, Theodosiou NA, Tabin CJ, Nascone-Yoder NM. (2000) Evolutionary relationships between the amphibian, avian, and mammalian stomachs. *Evol Dev.* 2:348-59.

Srivastava D, Thomas T, Lin Q, Kirby ML, Brown D, Olson EN. (1997) Regulation of cardiac mesodermal and neural crest development by the bHLH transcription factor, dHAND. *Nat Genet.* 16:154-60.

Steidl C, Leimeister C, Klamt B, Maier M, Nanda I, Dixon M, Clarke R, Schmid M, Gessler M. (2000) Characterization of the human and mouse HEY1, HEY2, and HEYL genes: cloning, mapping, and mutation screening of a new bHLH gene family. *Genomics.* 66:195-203.

Stennard FA, Costa MW, Elliott DA, Rankin S, Haast SJ, Lai D, McDonald LP, Niederreither K, Dolle P, Bruneau BG, Zorn AM, Harvey RP. (2003) Cardiac T-box factor Tbx20 directly interacts with Nkx2-5, GATA4, and GATA5 in regulation of gene expression in the developing heart. *Dev Biol.* 262:206-24.

Sun Q, Chen G, Streb JW, Long X, Yang Y, Stoeckert CJ Jr, Miano JM. (2006) Defining the mammalian CArGome. *Genome Res.* 16:197-207.

Takebayashi-Suzuki K, Pauliks LB, Eltsefon Y, Mikawa T. (2001) Purkinje fibers of the avian heart express a myogenic transcription factor program distinct from cardiac and skeletal muscle. *Dev Biol.* 234:390-401.

Takeshita K, Fujimori T, Kurotaki Y, Honjo H, Tsujikawa H, Yasui K, Lee JK, Kamiya K, Kitaichi K, Yamamoto K, Ito M, Kondo T, Iino S, Inden Y, Hirai M, Murohara T, Kodama I, Nabeshima Y. (2004) Sinoatrial node dysfunction and early unexpected death of mice with a defect of klotho gene expression. *Circulation.* 13;109:1776-82.

Tan HL, Bezzina CR, Smits JP, Verkerk AO, Wilde AA. (2003) Genetic control of sodium channel function. *Cardiovasc Res.* 57:961-73.

Thomas T, Kurihara H, Yamagishi H, Kurihara Y, Yazaki Y, Olson EN, Srivastava D. (1998) A signaling cascade involving endothelin-1, dHAND and msx1 regulates development of neural-crest-derived branchial arch mesenchyme. *Development.* 125:3005-14.

- Tilley LP. (1977) Feline cardiac arrhythmias. *Vet Clin North Am.* 7:274
- Torlopp A, Breher SS, Schlüter J, Brand T. (2006) Comparative analysis of mRNA and protein expression of Popdc1 (Bves) during early development in the chick embryo. *Dev Dyn.* 235:691-700.
- Treisman R. (1994) Ternary complex factors: growth factor regulated transcriptional activators. *Curr Opin Genet Dev.* 4:96-101.
- Truscott M, Raynal L, Premdas P, Goulet B, Leduy L, Berube G, Nepveu A. (2003) CDP/Cux stimulates transcription from the DNA polymerase alpha gene promoter. *Mol Cell Biol.* 23:3013-28.
- Vasavada TK, DiAngelo JR, Duncan MK. (2004) Developmental expression of Pop1/Bves. *J Histochem Cytochem.* 52:371-7.
- Viragh S, Challice CE. (1982) The development of the conduction system in the mouse embryo heart. *Dev Biol.* 89:25-40.
- Wada AM, Smith TK, Osler ME, Reese DE, Bader DM. (2003) Epicardial/Mesothelial cell line retains vasculogenic potential of embryonic epicardium. *Circ Res.* 92:525-31.
- Wahls SA. Sick sinus syndrome. (1985) *Am Fam Physician.* 31:117-24.
- Wang D, Chang PS, Wang Z, Sutherland L, Richardson JA, Small E, Krieg PA, Olson EN. (2001) Activation of cardiac gene expression by myocardin, a transcriptional cofactor for serum response factor. *Cell.* 105:851-62.
- Wobus AM, Holzhausen H, Jakel P, Schoneich J. (1984). Characterization of a pluripotent stem cell line derived from a mouse embryo. *Exp Cell Res.* 152:212-9.
- Wobus AM, Guan K, Yang H-T, Boheler KR. (2002). Embryonic stem cells as a model to study cardiac, skeletal muscle, and vascular smooth muscle cell differentiation. *Methods Mol Biol.* 185:127–156.

- Yamada M, Revelli JP, Eichele G, Barron M, Schwartz RJ. (2000) Expression of chick Tbx-2, Tbx-3, and Tbx-5 genes during early heart development: evidence for BMP2 induction of Tbx2. *Dev Biol.* 228:95-105.
- Yasui K, Liu W, Opthof T, Kada K, Lee JK, Kamiya K, Kodama I. (2001). I(f) current and spontaneous activity in mouse embryonic ventricular myocytes. *Circ Res.* 88:536-42.
- Yelon D, Ticho B, Halpern ME, Ruvinsky I, Ho RK, Silver LM, Stainier DY. (2000) The bHLH transcription factor hand2 plays parallel roles in zebrafish heart and pectoral fin development. *Development.* 127:2573-82.
- Yutzey KE, Kirby ML. (2002) Wherefore heart thou? Embryonic origins of cardiogenic mesoderm. *Dev Dyn.* 223:307-20.
- Zaffran S, Frasch M. (2002) Early signals in cardiac development. *Circ Res.* 91:457-69.
- Zhang Z, Xu Y, Song H, Rodriguez J, Tuteja D, Namkung Y, Shin HS, Chiamvimonvat N. (2002) Functional Roles of Ca(v)1.3 (alpha(1D)) calcium channel in sinoatrial nodes: insight gained using gene-targeted null mutant mice. *Circ Res.* 90:981-7.
- Zhang H, Zhao Y, Lei M, Dobrzynski H, Liu JH, Holden AV, Boyett MR. (2007) Computational evaluation of the roles of Na⁺ current, iNa, and cell death in cardiac pacemaking and driving. *Am J Physiol Heart Circ Physiol.* 292:H165-74
- Zhong TP, Childs S, Leu JP, Fishman MC. (2001) Gridlock signalling pathway fashions the first embryonic artery. *Nature.* 414:216-20.
- Xin M, Davis CA, Molkenstein JD, Lien CL, Duncan SA, Richardson JA, Olson EN. (2006) A threshold of GATA4 and GATA6 expression is required for cardiovascular development. *Proc Natl Acad Sci U S A.* 103:11189-94.

7. Supplement

7.1 Abbreviations

AchE	Acetylcholinesterase
Approx.	Approximately
BLAST	Basic Local Alignment Search Tool
bp	Base pairs
Bpm	Beats per minute
BSA	Bovine Serum Albumin
β -gal	β -galactosidase
cDNA	complementary DNA
cAMP	cyclic adenosine monophosphate
CMV	Cytomegalovirus
d	day(s)
DAB	3,3'-diaminobenzidine
dATP	2'-deoxyadenosine 5'-triphosphate
dCTP	2'-deoxycytidine 5'-triphosphate
dE	embryonic day
DMEM	Dulbecco's modified eagle's medium
DMSO	Dimethylsulfoxid
DNA	desoxiribonucleic acid
dNTP	Deoxy-Nukleosid-Triphosphat
ds	double stranded
dTTP	2'-deoxythymidine 5'-triphosphate
DTT	Dithiotreitol
EB	Embryonic Bodies
E. coli	Escherichia coli
ECG	Electrocardiogram
ECL	Enhanced Chemiluminescence
EDTA	Ethylene Diamine Tetra Acetate
EGFP	Enhanced Green Fluorescent Protein
ES	Embryonic Stem Cells
FCS	Foetal Calf Serum

g	Gramm
h	Hour
H ₂ O bidest.	Double distilled water
H ₂ O ₂	Hydrogen peroxide
hom	Homozygous
HR	Heart rate
HRP	Horse Radish Peroxidase
kb	Kilobase(s)
KO	Knockout
l	Liter
LB	Luria Bertami
M/mM	Molar/millimolar
min	Minute
mg	Milligramm
ml	Milliliter
m/μm	meter/micro meter
M _r	Molecular weight
μCi	micro Curie
μF	microfarad
ng	Nanogramm
NLS	Nuclear Localization Signal
nm	Nanometer
nt	Nucleotide(s)
NTP	Nukleosid-Triphosphat
OD	Optical Density
PAGE	Polyacrylamide Gel Electrophoresis
PBS	Phosphate Buffered Saline
PCR	Polymerase Chain Reaction
PFA	Paraformaldehyde
PMSF	Phenylmethylsulphonyl Fluoride
RNA	Ribonucleic acid
RNase	Ribonuclease
rpm	Rotations per minute
RT	Room temperature

RT-PCR	Reverse Transcription Polymerase Chain Reaction
SDS	Sodium Dodecyl Sulphate
TBE	Tris-Borate-EDTA buffer
TBS	Tris Buffered Saline
TBST	TBS with Tween
Tween 20	Polyoxyethylen-Sorbitan Monolaurat
V	Volt
v/v	Volume to volume
U	Unit(s)
UTP	Uridine 5'-triphosphate
UTR	Untranslated region
WT	Wild type

7.2 Publications

Froese, A. and Brand T. Expression pattern of *Popdc2* during mouse embryogenesis and in the adult. *Dev dyn*. Manuscript in print. Eine der Abbildungen aus diesem Manuskript wurde als Cover (Titelphoto) für die Zeitschrift *Developmental Dynamics* März 2008 ausgewählt.

Breher, SS., Mavridou, E., Brenneis, C., **Froese, A.**, Arnold, HH. and Brand T. Popeye domain containing gene 2 (*Popdc2*) is a myocyte-specific differentiation marker during chick heart development. *Dev Dyn*. 2004 Mar;229(3):695-702.

Froese, A., Schlueter, J., Breher, S, Kirchmaier, B, Günthner, F, Torlopp, A, Waldeyer, C., Kirchhof, P., Vauti F., Arnold, H-H. and Brand, T. The *Popdc2* null mutant mouse has a stress-induced bradycardia. In preparation.

7.3 Presentations

Alexander Froese, Maren Meysing, and Thomas Brand. Characterization of the promoter – proximal elements of the murine Popeye2 (Pop2) gene. (Poster) Deutsche Gesellschaft für Zellbiologie. Annual Meeting. March 26-29, 2003. Bonn.

Alexander Froese, and Thomas Brand. (Poster) EU-FP6 Symposium 'Heart Repair', Amsterdam, NL, 19.-21.01.2006

Alexander Froese, Jan Schlüter, Christoph Waldeyer, Larissa Fabritz, Stephanie Breher, Bettina Kirchmaier, Sonja Katharina Liebig, Sandra Laakmann, Paulus Kirchhof, Joachim Neumann, Franz Vauti, Hans-Henning Arnold, & Thomas Brand. Popdc1 and Popdc2 null mutant mice display a stress induced cardiac conduction defect. (Poster) 5th Dutch-German Joint Meeting of Molecular Cardiology Groups. February 8-10. 2007. Würzburg

8. Zusammenfassung

Im Vordergrund dieser Arbeit stand die Generierung und Analyse der *Popdc2* Knockout Maus. Die Expression des *Popdc2-LacZ* Konstruktes war vorwiegend im Herz, der Blase, sowie in der glatten und Skelett Muskulatur detektierbar/sichtbar.

Der Herzrhythmus 8 Monate alter *Popdc2* Mutanten und WT Nachkommen wurde anhand von Elektrokardiogrammen (EKGs) untersucht. Bei dieser Analyse wurden die Mäuse verschiedenen Stresssituationen ausgesetzt, d.h. Injektion von Isoproterenol, mentaler bzw. physikal. Stress. Die Aufzeichnung der EKG-Kurve erfolgte direkt nach der Stressinduktion über eine Zeitspanne von 6 Minuten. Es konnte gezeigt werden, dass die Mäuse eine ausgeprägte Sinus Bradykardie entwickelten.

Anhand histologischer Schnitte 8 Monate alter *Popdc2* KO SAN Mäuse konnten strukturelle Veränderungen im Vergleich zum WT aufgedeckt werden. Auf der Grundlage serieller Schnitte, gefärbt mit HCN4 Antikörper, wurden 3D-Rekonstruktionen erzeugt. Dabei stellte sich heraus, dass das Volumen des SAN in *Popdc2* Mutante um 30% gegenüber dem Wildtyp verringert ist.

Auf Grund der hier vorgestellten Daten scheint die *Popdc2* KO Maus ein nützliches Tiermodell im Hinblick auf menschl. Sinus-Erkrankungen zu sein.

Der zweite Teil der Arbeit beschäftigt sich mit der *Popdc2* Promotor Analyse. In Promotorregion konnten drei Bindungsstellen für Transkriptionsfaktoren charakterisiert werden. Um weitere Faktoren, die eine Rolle bei der *Popdc2* Genregulation spielen könnten, zu identifizieren sind weiterführende Studien unerlässlich.

PERSÖNLICHE DATEN

Name: Alexander Froese
Geburtsdatum: 29.04.1973
Geburtsort: Dushanbe (Tadjikistan)
Familiensand: Verheiratet, 2 Kinder
Staatsangehörigkeit: Israeli

AKADEMISCHER WERDEGANG

- 2001 – 2007 Doktorand an der Universität Braunschweig, Abteilung Zell- und Molekularbiologie (bis 2005) und an der Universität Würzburg, Lehrstuhl für Zell- und Entwicklungsbiologie.
Doctoral Thesis: *“The Popeye domain containing gene 2 (Popdc2). Generation and functional characterization of a null mutant in mice and promoter analysis”.*
(Doktorvater: Prof. Dr. rer. nat. Thomas Brand)
- 1998 – 2000: Diplomarbeit an der Tel-Aviv University, Sackler School of Medicine, Dept. of Pathology, Abschluss: M.Sc
Master Thesis: *“Identification of new genes potentially involved in the development of cardiac hypertrophy”.*
(Betreuer: Dr. Eli Golomb)
- 1995 – 1997: Biologie-Studium an der Tel Aviv University, Faculty of Life Science, Abschluss: B.A
- 1991 – 1993: Medizin-Studium an der School of Medicine, Dushanbe, (Tadjikistan)

FORT- UND WEITERBILDUNG

- April 25-29, 2004 Workshop on Phenotyping New Mouse Models for Heart, Lung, Blood and Sleep Disorders. The Jackson Laboratory, Bar Harbor, Maine, USA.